ANALYSIS OF MIXING LAYER HEIGHTS INFERRED FROM RADIOSONDE, WIND PROFILER, AIRBORNE LIDAR, AIRBORNE MICROWAVE TEMPERATURE PROFILER, AND IN-SITU AIRCRAFT DATA DURING THE TEXAS 2000 AIR QUALITY STUDY IN HOUSTON, TX

A Thesis

by

CHRISTINA LYNN SMITH

Submitted to the Office of Graduate Studies of
Texas A&M University
in partial fulfillment of the requirements for the degree of

MASTER OF SCIENCE

May 2005

Major Subject: Atmospheric Sciences

ANALYSIS OF MIXING LAYER HEIGHTS INFERRED FROM RADIOSONDE, WIND PROFILER, AIRBORNE LIDAR, AIRBORNE MICROWAVE TEMPERATURE PROFILER, AND IN-SITU AIRCRAFT DATA DURING THE TEXAS 2000 AIR QUALITY STUDY IN HOUSTON, TX

A Thesis

by

CHRISTINA LYNN SMITH

Submitted to the Office of Graduate Studies of
Texas A&M University
in partial fulfillment of the requirements for the degree of

MASTER OF SCIENCE

Approved as to style and content by:

John W. Nielsen-Gammon (Chair of Committee)	Luis A. Cifuentes (Member)
Donald R. Collins (Member)	Richard E. Orville (Head of Department)

May 2005

Major Subject: Atmospheric Sciences

ABSTRACT

Analysis of Mixing Layer Heights Inferred from Radiosonde, Wind Profiler, Airborne Lidar, Airborne Microwave Temperature Profiler, and In-Situ Aircraft Data during the Texas 2000 Air Quality Study in Houston, TX. (May 2005)

Christina Lynn Smith, B.S., Ohio University

Chair of Advisory Committee: Dr. John Nielsen-Gammon

The mixing layer (ML) heights inferred from radiosondes, wind profilers, airborne lidar, airborne microwave temperature profiler (MTP), and in-situ aircraft data were compared during the Texas 2000 Air Quality Study in the Houston area. The comparisons and resulting good agreement between the separate instruments allowed for the spatial and temporal evolution of the ML height distribution to be determined across the Houston area on September 1, 2000.

A benchmark method was created for determining ML heights from radiosonde data. The ML heights determined using this method were compared to ML heights determined using wind profiler data. The airborne lidar and MTP heights were also compared to the wind profiler heights. This was the first time the MTP was used for estimating ML heights. Because of this, the MTP heights were also compared to the ML heights determined by in-situ aircraft data.

There was good agreement between the ML estimates when the instruments were co-located. The comparisons between the benchmark method and the wind profilers were independent of the quality of the profiler heights. The statistics for lidar and the wind profilers were better for the inland profiler comparisons. Even so, the results for

coastal profilers were similar to the other comparisons. The results between the MTP and the wind profilers were comparable with the results found between the other instruments, and better, in that the statistics were similar for the both the inland and coastal profilers. The results between the MTP and in-situ aircraft data provided additional support for the use of MTP for determining ML heights.

The combination of the inland and coastal wind profilers with the airborne instruments provided adequate information for the spatial and temporal evolution of the ML height to be determined across the Houston area on September 1, 2000. By analyzing the ML height distribution, major features were evident. These features included the shallow ML heights associated with the marine air from Galveston Bay and the Gulf of Mexico, and the sharp gradient of increasing ML heights north of Houston associated with the variation in the inversion depth found on this day.

ACKNOWLEDGMENTS

First and foremost, I want to sincerely thank my advisor, Dr. John Nielsen-Gammon. This thesis would not have been possible without your support, both academic and financial. Thank you for your patience and assistance as I worked on my research and developed as a graduate student. I am very appreciative of the time you dedicated to me and my work. I would also like thank the professors at Texas A&M for your expertise and assistance both in and outside of the classroom, to which I owe much of my knowledge and understanding of science. Especially, I would like to thank my other committee members, Dr. Don Collins and Dr. Luis Cifuentes for your time and assistance.

I want to acknowledge Wayne Angevine, Christoph Senff, and MJ Mahoney for offering their knowledge and allowing me to use their data. I would like to thank the Texas Air Research Center and the Environmental Protection Agency for funding my research.

I want to thank my wonderful parents, Sally and Jerry Smith for your endless support throughout my academic career, especially my time at Texas A&M. Thank you for encouraging me in all that I do and reminding me that my options are endless. Also thanks to my sisters, Becky and Kindra; my brother, Joe; my niece, Zoé; and nephew, Mitch. I am very appreciative of your phone calls and keeping me close to home.

A giant thanks to my fiancé, Jeff Powell. I am especially thankful for your friendship and willingness to spend a few years in Texas. Thank you for your countless

hours of listening and proofreading. Your company, support, and intellect have made my work at Texas A&M bearable.

I am very thankful for my fellow graduate students at Texas A&M who have become not only lifelong friends, but family. The wonderful people I met here are too many to list, but I especially want to thank, Dan Hawblitzal, Kurt Buffalo, Abby Walter, and Kevin Walter for accepting me as your friend and giving me support both educationally and emotionally. I would like to thank James Tobin for your statistical help. Thank you to everyone who has made my stay in Aggieland a wonderful experience. Finally, I would like to thank Pat Price for your devotion regardless the situation.

TABLE OF CONTENTS

Page

ABSTRACT iii

ACKNOWLEDGMENTS v

TABLE OF CONTENTS vii

LIST OF FIGURES ix

LIST OF TABLES xi

CHAPTER

I INTRODUCTION 1

a. Planetary Boundary Layer 1
b. Mixing Layer Height 3

II BACKGROUND 9

III INSTRUMENTS 12

IV INSTRUMENT INTERCOMPARISONS 14

a. Radiosonde 14
1. Background 14
2. Method 19
3. Results 29
4. Discussion 33
b. Wind Profiler 37
1. Background 37
2. Method 39
3. Results 42
4. Discussion 47
c. Airborne Lidar 49
1. Background 49
2. Method 57
3. Results 59
4. Discussion 63

CHAPTER Page

d. Airborne MTP 65
1. Background 65
2. Method 66
3. Results 69
4. Discussion 75
e. In-Situ Aircraft Data 77
1. Background 77
2. Method 79
3. Results 81
4. Discussion 85
f. Overall Comparisons 86

V ML HEIGHT DISTRIBUTION – SEPTEMBER 1, 2000 90

a. Method 90
b. Results 98
c. Discussion 109

VI CONCLUSION 113

REFERENCES 116

VITA 119

LIST OF FIGURES

FIGURE		Page
1	The diurnal evolution of the PBL modified from Stull, 1988.....	1
2	The Houston area with wind profiler and radiosonde sites.	13
3	Skew-T chart for WH on 8/30/00 at 2245 UTC.	20
4	Skew-T chart for HDT on 8/25/00 at 2300 UTC.	23
5	Skew-T chart for HDT on 8/27/00 at 1700 UTC.	25
6	Skew-T chart for WH on 8/26/00 at 1640 UTC.	26
7a	Box and Whiskers plots of q Mid Method heights compared to the other method heights.	31
7b	Box and Whiskers plots of high quality q Mid Method heights compared to the other method heights	32
8	Scatter plot of q Mid Method and the other method ML heights.....	33
9	Box and Whiskers plots of the comparisons between the benchmark method and the wind profiler ML heights separated by the different quality flag of the wind profiler	43
10	Scatter plot of benchmark method and wind profiler ML heights ...	46
11	Box and Whiskers Plots of the comparisons between the lidar ML heights and the wind profiler ML heights separated by the different quality flag of the wind profiler	61
12	Scatter plot of wind profiler and lidar ML heights.....	63
13	Standard Deviation between the MTP algorithm ML heights and wind profiler ML heights for all the sites combined	70
14	Box and Whiskers Plots of the comparisons between the MTP algorithm 27 ML heights and the wind profiler ML heights separated by the different quality flag of the wind profiler.....	72

FIGURE Page

15 Scatter plot of wind profiler and MTP algorithm 27 ML heights 74

16 Scatter plot of MTP algorithm 27 and Electra aircraft ML heights for all distances between estimates 84

17 Evolution of ML heights as a function of time on 9/01/00 inferred by wind profilers at the Wharton (WH), Liberty (LB), Houston Southwest (HSW), Ellington (EL), and LaMarque (LM) sites..... 93

18 Skew-T of WH radiosonde data at 1100 UTC 95

19 Skew-T of WH radiosonde data at 2251 UTC 96

20 Average trend of the evolution of ML heights as a function of time on 9/01/00 inferred by wind profilers at the Wharton (WH), Liberty (LB), Houston Southwest (HSW), Ellington (EL), and LaMarque (LM) sites 97

21 The ML height distribution at 1600 UTC around the city of Houston 99

22 The ML height distribution at 1700 UTC around the city of Houston 100

23 The ML height distribution at 1800 UTC around the city of Houston 101

24 The ML height distribution at 1900 UTC around the city of Houston 102

25 The ML height distribution at 2000 UTC around the city of Houston 103

27 The ML height distribution at 2100 UTC around the city of Houston 104

28 A vertical cross-section of potential temperature as a function of latitude at -95.17° longitude between 1730 UTC and 1800 UTC on September 1, 2000 107

LIST OF TABLES

TABLE		Page
1a	Comparison of ML height estimates determined by the q Mid Method with the T Base Method and T Mid Method	30
1b	Comparison of ML height estimates determined by the q Mid Method with the q Base Method	30
2	Comparison of ML height estimates determined by the q Mid Method with the T Lapse Rate Method and the Θ Increase Method	30
3a	Comparison between all the wind profiler ML heights and benchmark method ML heights separated by the quality flag of the benchmark method	42
3b	Comparison between the high quality wind profiler ML heights and benchmark method ML heights separated by the quality flag of the benchmark method	42
4a	Comparison between all the wind profiler ML heights and the ML heights determined by the different components of the benchmark method separated by the quality flag of the radiosonde methods	45
4b	Comparison between the high quality wind profiler ML heights and the ML heights determined by the different components of the benchmark method separated by the quality flag of the radiosonde methods	45
5	Comparison of the difference in ML height estimates between the wind profilers and airborne lidar	60
6	Comparison of the difference in ML height estimates between the wind profilers and MTP algorithm 27	71
7	Comparison of the difference in ML height estimates between the wind profilers and MTP algorithm 27 without estimates from 8/30/00 after 2100 UTC	74

TABLE Page

8a Comparison of the difference in ML height estimates between the Electra and MTP algorithm 27 for all distances between instruments 83

8b Comparison of the difference in ML height estimates between the Electra and MTP algorithm 27 for distances of 16.38km and 10km between instruments. 83

CHAPTER I

INTRODUCTION

a. Planetary Boundary Layer

The planetary boundary layer (PBL) is in the lowest part of the troposphere where the air is influenced by the earth's surface and responds to surface forcings such as frictional drag, evapotranspiration, heat transfer, pollutant emission, and topography (Cooper and Eichinger 1994). Above the PBL is the free atmosphere where the effects of friction from the earth's surface are negligible and the motion of air can be treated as an ideal fluid (Glickman 2000). Within the PBL, several identifiable layers can exist which depend on the state of the atmosphere and local conditions. These layers are displayed in Figure 1 and include the surface layer, mixing layer (ML), entrainment zone, stable layer, residual layer, and capping inversion.

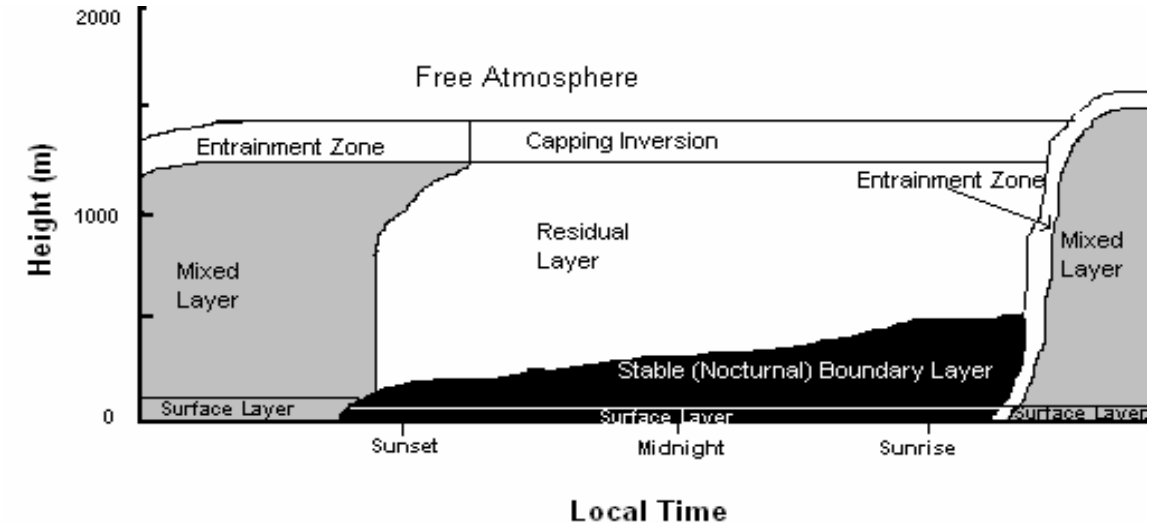

Fig. 1: The diurnal evolution of the PBL modified from Stull, 1988.

This thesis follows the style of the *Journal of Applied Meteorology.*

The surface layer is the layer of the atmosphere in contact with the earth's surface and is where the generation of mechanical turbulence by strong winds or wind shear is greater than the generation of buoyant turbulence associated with large thermals (Glickman 2000). The surface layer is always present, but the state of the atmosphere and time of the day determine the layer above the surface layer. During daytime convective conditions, an ML is above the surface layer and is characterized by turbulence created from forced or free convection that actively mixes such quantities as aerosols, potential temperature, and wind speed (Stull 1988). On warm sunny days, the surface forcings are dominated by the solar heating of the earth's surface and convective thermals are the main cause of development of the well-mixed PBL, which is often called the convective boundary layer (Marsik et al. 1995). At the top of the ML there exists a stable layer called the entrainment zone that is not well-mixed, and within which turbulence intensity decreases upwards (Seibert et al. 2000). This layer is an interface between the ML and the free atmosphere and is often called an inversion layer because there is a temperature increase with height. Above the entrainment zone, in the free atmosphere, the temperature usually decreases with height and the atmosphere becomes less stable.

During nighttime or newly stable conditions, a residual layer occurs above the surface layer in the middle of the PBL where weak sporadic turbulence takes place. This is the area that contains the initially uniformly-mixed potential temperature and pollutants from the ML of the previous day. With nighttime conditions of a radiatively cooled surface, the bottom of the residual layer is transformed into a stable boundary

layer. The stable boundary layer forms when air is cooled by the colder surface of the earth, creating a layer with stable stratification. Above the residual layer is a capping inversion layer, a statically stable layer that separates the residual layer and surface characteristics from the free atmosphere.

The actual diurnal cycle and characteristics of the PBL for a particular location depend on the geography and environmental features of that location. The PBL over coastal environments is highly influenced by marine air and is often called the marine boundary layer. The marine boundary layer is typically only several hundred meters deep without significant variations throughout the course of a day (Senff et al. 2002). In a study concerning the PBL height in Houston, TX, Senff et al. (2002) found that the daytime PBL height increased with increasing distance from the Galveston Bay coastal shoreline. Locations farther away from the coast experienced deeper mixing layers because the marine air was either gradually modified as it was advected inland, or because the local inland mixed layer had grown to larger depths.

b. Mixing Layer Height

Knowledge of the structure and characteristics of the PBL is important to fully understand profiles of momentum, heat, and moisture in the lower atmosphere and to characterize the transport and diffusion of pollutants. Within the PBL, the ML is of particular importance because the ML depth determines the volume in which daytime pollution is primarily concentrated. The ML height is defined by the American Meteorological Society as the location of a capping temperature inversion or statically stable layer of air and often associated with, or measured by, a sharp increase of

potential temperature with height, a sharp decrease of water-vapor mixing ratio, a sharp decrease in turbulence intensity, a sharp decrease in pollution concentration, a change of wind speed to geostrophic, a minimum of turbulent heat flux, and a maximum of signal intensity from remote sensors (Glickman 2000).

The development, temporal evolution, and spatial distribution of the ML height depends on many factors including variations in surface albedo, surface moisture, synoptic conditions, local circulation patterns, cloud cover, horizontal advection, land use, and the urban heat island effect (Seibert et al. 2000; Marsik et al. 1995; Dayan et al. 1988). Therefore, the ML height at a particular time and place is influenced by geographical location and environmental conditions. In particular, the ML height depends on the atmosphere's ability to mix or maintain vertical motion through convectively driven turbulence by buoyancy and mechanically induced turbulence by wind shear. In stable conditions, an ML is not necessarily present because turbulence tends to be weaker and sporadic leading to conditions that range from well-mixed to little mixing (Seibert et al. 2000). In an unstable atmosphere, the transition in turbulence intensity between the ML and the entrainment zone and the magnitude of the stability of the entrainment zone are important features that influence the method for determining the ML height.

The turbulence in the ML is usually convectively driven by such sources as heat transfer from a warm ground surface or radiative cooling from the top of clouds (Stull 1988). A well-mixed layer can develop where mixing ratios and potential temperature are nearly constant with height to the entrainment zone. The entrainment zone is marked

by the entrainment of dry, less turbulent air which allows the top of ML to be identified with a sharp moisture decrease and coincident temperature increase. Using radiosonde data, an ideal Skew-T will have a ML identified by a temperature profile that decreases with height along a dry adiabat and a dewpoint profile that remains at a constant mixing ratio value with height. In the real atmosphere, however, mixing ratios will decrease slightly with height. This is because moisture is added from below by surface evaporation, and dry air is added from above as it is entrained from the free atmosphere (Stull 1988).

The terminology of elevated inversion layer and stable layer is commonly used to describe the layer above the ML and in the entrainment zone. These two terms are mostly used interchangeably; however, they have been differentiated in past research when a specific difference is known for a particular area. For example, Baxter (1991) made a distinction between the two definitions so that the ML height information in the California coastal region could be interpreted. For Baxter (1991), the base of the inversion layer was the first point where the temperature lapse rate was less than isothermal and the base of the stable layer was the first point where the temperature lapse rate was less than dry adiabatic. Of the two definitions, the base of the inversion layer was found better correlated with pollutant-defined ML heights obtained from aircraft data. For this paper, the term "inversion layer" will be used to describe the ML height and refers to the layer above the ML regardless of its stratification.

The location of the ML height has been identified by both the base of the inversion layer (Dayan et al. 2002; Kalthoff et al. 1998; Martin et al. 1988; Kaimal et al.

1982) and the midpoint of the inversion layer (Stull 1988; Kaimal et al. 1982). Commonly, the base of the inversion layer was used because it was easily identified from lapse rate data and potential temperature profiles, and was based on the fact that the turbulent mixing extends to the bottom of the elevated inversion (Dayan et al. 2002; Martin et al. 1988; Kaimal et al. 1982). In these cases, it was assumed that the base of the inversion layer acted like a lid on pollutants mixed from the ground.

In the real atmosphere, thermals can overshoot the ML and cause mixing to extend past the base of the inversion. The pollutants that are well-mixed below the base of the inversion can exist in the entrainment zone where their concentrations decrease rapidly with height. This makes the base of the inversion less of a lid on the pollutants, and more of a beginning point for rapid decrease (Olsson et al. 1974). For air quality studies, the height of the inversion base usually underestimated the volume of air affected by a pollutant, and the ML height was found within the entrainment zone (Hooper and Eloranta 1986; Olsson et al. 1974). A better definition for the ML height in these cases was the altitude where half of the air had characteristics of the free atmosphere on a horizontal average which was determined as the midpoint between the base and top of the entrainment zone (Stull 1988).

Methods for determining the ML heights depend upon the types of observations available. Different instruments used for inferring the ML height have different strengths and are often only appropriate under certain conditions. Even under optimal conditions, ML height estimates differ because each instrument requires the use of a different variable or method as to which feature best defines the depth of ML for that

instrument. Thus, no single instrument is adequate by itself to fully determine the ML height of an area of interest.

There have been several techniques used in past research to determine the ML height. Techniques have included the use of rawinsonde, radiosonde, wind profiler, lidar, sodar, and measurements of aerosol concentrations and other in-situ data. For this research, the focus was the daytime ML heights inferred from radiosonde, wind profiler, airborne lidar, airborne microwave temperature profiler (MTP), and in-situ aircraft data.

Radiosonde systems measure profiles of temperature, pressure, and relative humidity as they ascend through the atmosphere and send these measurements to ground receivers. The ML height estimates determined from radiosonde systems depend on the atmospheric constituent used for the analysis. Wind profilers measure vertical variations in the refractive index, and lidar systems observe the distribution of particulate matter in the ML. MTP systems measure the thermal emissions and absorption from oxygen molecules in the atmosphere. In-situ instruments on aircraft often make measurements of temperature, humidity, wind speed, wind direction, and concentrations of various species from which the ML height can be determined.

The goal of this research is to quantify the relationship between the different techniques for estimating the daytime ML height using radiosondes, wind profilers, airborne lidar, airborne MTP, and in-situ aircraft data; and to provide a comprehensive depiction of ML height in the Houston area as a function of both space and time. Characterizing the spatial and temporal variation of the ML depth is important for determining air pollution concentrations near the ground. Determining the evolution of

the ML depth is also needed for air pollution modeling. Air pollution models are used to determine the appropriate control strategies and to assist the forecasting of pollution episodes. Reliable ML depths are needed to improve model performance.

The first part of this paper will describe comparisons between estimates from the separate instruments that were co-located in space and time. The sections include: the creation of a benchmark method to determine the ML height from radiosonde data; the comparisons between ML height estimates using the benchmark method and the wind profiler data; the comparisons between ML height estimates using the airborne lidar data and the wind profiler data; the comparisons between ML height estimates using the airborne MTP data and the wind profiler data; and the comparisons between ML height estimates using the airborne MTP data and the in-situ aircraft data. The second part of this paper will display and analyze the horizontal distribution of ML height across the Houston area as a function of space and time on September 1, 2000 of the Texas 2000 Air Quality Study.

CHAPTER II

BACKGROUND

The study area for this research is the Houston area, which is labeled as being one of the worst air quality cities in the United States due to high ozone concentrations. The Houston area has a highly variable ML height distribution because of its large metropolitan area and proximity to the Gulf of Mexico. The urban heat island effect is known to enhance ML depth, whereas the marine PBL is typically only several hundred meters deep without significant variations throughout the course of a day. Senff et al. (2002) studied the evolution of the ML height in the Houston area using airborne lidar and found the ML height to have a strong dependence on the advection of marine air. When the flow was onshore, the ML height increased with increasing distance from the Galveston Bay coastline, and locations farther away from the coast experienced deeper mixing layers.

The spatial and temporal variations of the ML in complex terrain have been analyzed and presented in several studies. Of these, few studies have focused on the complex terrain in coastal environments. Dayan et al. (1988) found the factors influencing spatial variations in the ML heights are mainly the topography and the distance from the shoreline and, to a lesser extent, synoptic weather systems. McElroy and Smith (1991) found the ML evolution to be related to the sea breeze, with differences in the ML thickness of hundreds of meters within only a few kilometers.

Along with determining the horizontal ML height distribution, the performance of separate instruments has been compared in past research. Estimates of the PBL structure and the ML height from different instruments show relative differences mostly less than 10% when the ML is well-mixed and the inversion capping the PBL is strong and has a well-defined base (Seibert et al. 2000). The results of individual studies are sensitive to the choice of instruments and the conclusions are not always consistent. Generally, the discrepancies between separate instruments are blamed on the physical limitations of the different instrument systems, the assumptions used with each system as to which variable most accurately defines the height of the ML, and the spatial inhomogeneity of the PBL structure across the region of study (Cohn and Angevine 2000; Seibert et al. 2000; White et al. 1999; Marsik et al. 1995; Cooper and Eichinger 1994; Van Pul et al. 1994; Kaimal et al.1982; Coulter 1979). In studies when the ML top was not as well-defined or in cloudy conditions, separate instruments were found to measure ML heights with greater variability (Seibert et al. 2000; White et al. 1999; Grimsdell and Angevine 1998; Marsik et al. 1995; Angevine et al. 1994).

In past research, the estimates of ML height by different instruments were mostly in good agreement and considered to have a high correlation between different measurements. This may be misleading, due to the fact the separate instruments measure the same changes in atmospheric phenomena as they occur, which masks biases due to the different definitions of the ML height by separate instruments. Few studies have focused on the comparison between several instruments that are co-located in space and time. Doing this helps reduce measurement limitations by relating a measurement

by one instrument in one location to a measurement by a different instrument in a different location.

The results from one area of study are not always transferable to another area of study because the individual factors influencing the ML height vary from place to place. Most research that compares ML height measurements from separate instruments has been conducted in urban areas away from coastal environments. Even though Senff et al. 2002 found ML heights inferred from radiosondes, wind profilers, and airborne lidar data to be in good agreement in the Houston area, there was not a direct comparison between instruments. Direct ML height comparisons between different instruments in coastal urban areas are important for determining the relationships between these instruments and mapping the ML height in such locations as Houston.

CHAPTER III

INSTRUMENTS

The ML heights used in this paper were determined from data collected around the Houston area during the Texas 2000 air quality study by five boundary layer profilers, three radiosonde sites, an airborne lidar, an airborne MTP, and in-situ temperature and dewpoint measurements collected by instruments aboard the NCAR L-188C Electra aircraft. The positions of the wind profilers and radiosonde sites are displayed in Figure 2. Acronyms for the site locations are: WH- Wharton (radiosonde and wind profiler), EL- Ellington (wind profiler), HDT- Houston Downtown (radiosonde), LM- LaMarque (wind profiler) and Houston Southeast (radiosonde), LB- Liberty (wind profiler), and HSW- Houston Southwest (radiosonde). The lidar, MTP, and Electra are all airborne and had varying flight paths around the Houston area during various days of the study.

The comparison to determine a benchmark method from the radiosonde data was for a selected time period during the Texas 2000 Air Quality study consisting of high ozone days from August 25, 2000 to September 1, 2000. The longer time period for the comparisons between the ML height estimates, determined using the benchmark method and the wind profiler data, was from August 17, 2000 to September 19, 2000. The time period for the comparisons between the ML height estimates, determined using the airborne lidar data and the wind profiler data, consisted of the following days: August 25th, 26th, 28th, 29th, 30th, and 31st and September 1st, 6th, and 7th. Similarly, the time

period for the comparisons between the ML height estimates, determined using the airborne MTP data and the wind profiler data, consisted of the following days: August 23rd, 25th, 27th, 28th, and 30th and September 1st, 3rd, and 6th. The time period for the comparisons between the ML height estimates, determined using the airborne MTP data and the in-situ aircraft data, was a subset of the days for MTP and wind profiler comparisons and consisted of: August 25th, 27th, 28th, and 30th, and September 1st.

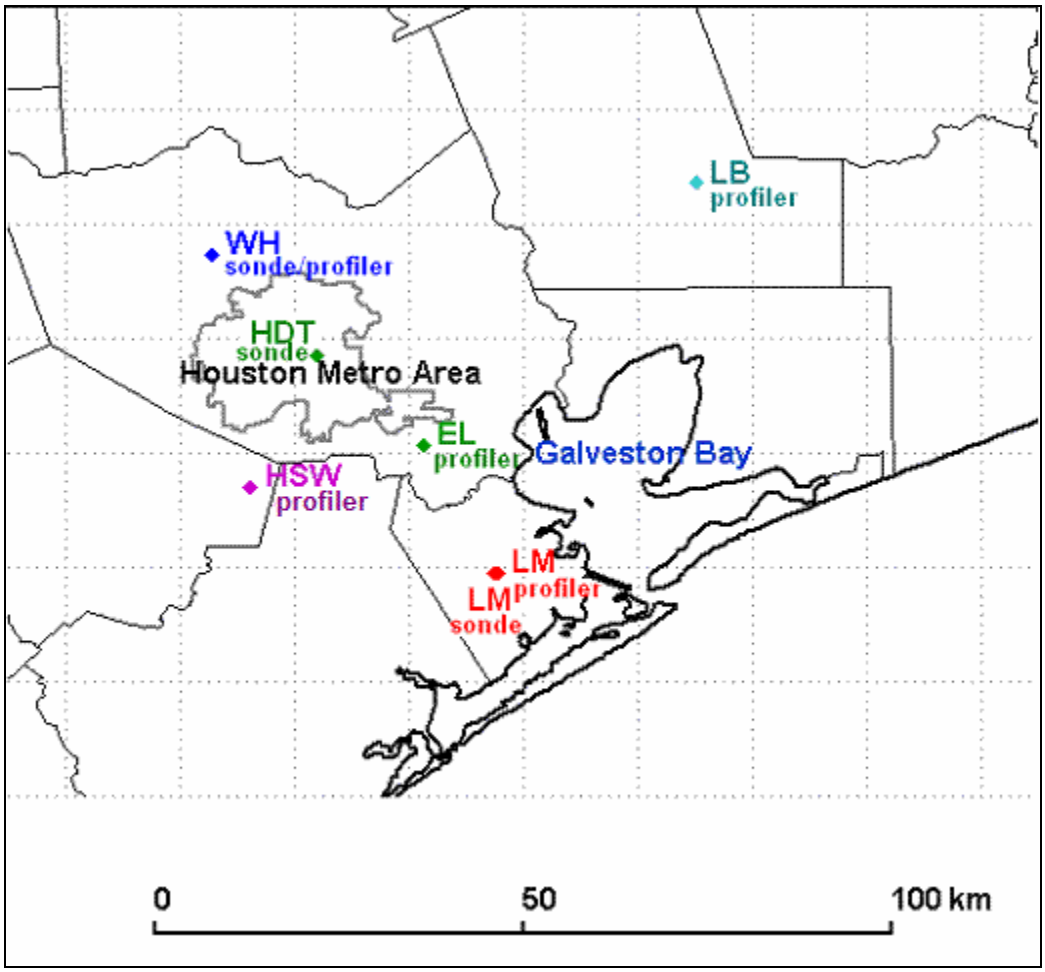

Fig. 2: The Houston area with wind profiler and radiosonde sites. Instruments of the same color represent co-location for comparisons.

CHAPTER IV

INSTRUMENT INTERCOMPARISONS

a. Radiosonde

1. BACKGROUND

Radiosonde systems obtain profiles of temperature, pressure, and relative humidity as they ascend through the atmosphere and send these measurements to a ground receiver. ML height estimates can be determined using radiosonde data by analyzing the vertical stability of the atmosphere. For a particular time and place, these estimates depend on the atmospheric constituent and technique used for the analysis. The choice of constituent and technique has varied in past research, and is dependent on the nature of the study and the local characteristics of the atmosphere.

During convective conditions, the ML can generally be considered an unstable region above which is the entrainment zone, which can be considered a stable region. The intense vertical mixing in an unstable atmosphere allows the ML height to be determined by conservative variables such as virtual potential temperature, potential temperature, and mixing ratio, which can be determined from sounding data. Of these variables, analysis of the virtual potential temperature can provide sufficient information for determining the ML height in ideal situations. This is because virtual potential temperature is a variable often used as a measure of buoyancy, which is one of the primary driving forces for turbulence in the PBL (Stull 1988). In the ML, virtual potential temperature is nearly constant with height so that in past research, the ML

height has been associated with the increase in virtual potential temperature (Dupont et al. 1999; Angevine et al. 1994).

Virtual potential temperature is a function of potential temperature and mixing ratio which means that if the potential temperature and mixing ratio are well-mixed, the virtual potential temperature will be well-mixed as well. In a well-mixed boundary layer, the potential temperature is nearly constant with height and at the top of the ML, in the inversion layer, the potential temperature is found to increase sharply with altitude. Because of these properties, the potential temperature is often used as the main variable to determine the ML height. Similar to virtual potential temperature, the ML height has been associated with the increase in potential temperature (Martin et al. 1988; Hooper and Eloranta 1986).

There have been more detailed methods that use potential temperature to determine the ML height. Around the city of Atlanta, Georgia, Marsik et al. (1995) determined the mixing heights from rawinsonde data by using the method described in Heffter (1980). In this method, the potential temperature profiles were computed for each sounding. The profiles were then analyzed for the existence of a critical inversion, which was assumed to mark the top of the mixed layer. A critical inversion was defined as the lowest inversion where the potential temperature lapse rate was greater than 5°C/km and the inversion layer was greater than 2 degrees. The height of the ML was that point in the inversion layer at which the temperature was 2 degrees above the temperature in the inversion base. This method was used because it recognized the likelihood of mixing to overshoot the base of the critical inversion (Marsik et al. 1995).

Similarly, the top of the mixed layer was defined by Garret (1981) from rawinsonde data to be the point at which the observed lapse rate became less negative than 80% of the dry adiabatic lapse rate which allowed an increase in potential temperature of about 2°C/km.

Determining the ML from mixing ratio data is often used in combination with the potential temperature (Beyrich and Gorsdorf 1995; Cooper and Eichinger 1994; Stull 1988) or separately when the potential temperature data is ambiguous (Senff et al. 2002). In a well-mixed layer, moisture is a conserved quantity and mixing ratio values are nearly constant with height. The location of the significant decrease in the mixing ratio found at the inversion base can be used to identify the ML height (Senff et al. 2002; Cooper and Eichinger 1994; Stull 1988).

The ML height can also be identified using the atmospheric temperature profiles. Techniques that use temperature are similar to techniques that use potential temperature in that a temperature profile that has a dry adiabatic lapse rate is equivalent to a well-mixed potential temperature profile. Likewise, a temperature profile that does not have a dry adiabatic lapse rate is equivalent to a potential temperature profile that is not well-mixed. Therefore, the ML height can be determined as the point where the temperature becomes less than dry adiabatic or there is a significant temperature increase with height (Baxter 1991; Kalthoff et al. 1988; Coulter 1979).

Calculation of the ML height using radiosonde data is commonly used in computer models and for comparisons with ML heights estimated by other methods. The bulk Richardson number methods calculate the ML height and depend on the level used for the near-surface temperature and wind, the parameterization of shear production

of turbulence in the surface layer, and the consideration of an excess surface temperature under convective conditions (Seibert et al. 2000). Grimsdell and Angevine (1998) used a bulk Richardson method to compare computed ML heights from radiosonde data to measured wind profiler ML heights. The bulk Richardson method overestimated the ML heights, due to the nature of the Richardson number calculation where the input values did not accurately represent the measurement spacing and the strength of turbulence.

When there is not available information on the conserved variables in the atmosphere for a desired time, objective methods have been used during convective conditions to estimate the ML height. The "parcel method" consists of using the most recent radiosonde data and following the dry adiabat from the surface with the measured or expected maximum temperature up to its intersection with the temperature profile (Seibert et al. 2000). This method determines the ML height as the equilibrium level of a hypothetical rising parcel of air. Refinements to this method differ in how the temperature of the air parcel is found and the thermodynamic variable used to define the equilibrium level (Seibert et al. 2000).

The method by Holzworth (1964) and refinements to this method have been used in several studies (Van Pul et al 1994; Holzworth 1967; Miller 1967; Garrett 1981). Generally, the Holzworth method was used to forecast ML heights at times when radiosonde soundings were not available (usually in the afternoon), and was based on the concept that heating of the surface during the daytime results in vertical mixing that allows the development of a dry adiabatic lapse rate. In the simple form, this method consists of extending a dry adiabat from the maximum surface temperature to its

intersection with the most recent temperature profile (usually in the morning), and neglecting temperature advection. Refinements to the Holzworth method depend on the location and nature of the study.

Estimating the ML height based on methods that use only the most recent sounding and the observed maximum temperature can result in errors. In the real atmosphere, there can be buoyant thermals which cause entrainment into the ML and allow the ML to grow deeper. Without considering these thermals, the resulting ML height would be underestimated. Also, at the surface there is often a superadiabatic layer which would cause the ML height to be at a lower value than otherwise estimated. This would cause the ML height to be overestimated. The ML heights estimated from parcel methods are not as accurate as the ML heights estimated by the vertical profiles of conserved variables. Therefore, discretion needs to be used when applying one of these methods.

The vertical profiles of conserved variables can provide a fairly accurate ML height estimate; however, errors can occur when using radiosonde data. Radiosondes provide a snapshot of the state of the atmosphere as they ascend, leading to a ML height represented by a point measurement in space and time. These point measurements can lead to errors and misleading results, because they are not representative of the entire PBL (Seibert et al. 2000; Marsik et al. 1995; Cooper and Eichinger 1994; Kaimal et al. 1982). This is especially true when a radiosonde passes through an individual thermal, updraft, or downdraft that is exceptionally strong, yielding higher or lower estimates of

the ML height than a different instrument whose estimate is averaged temporally and spatially (Senff et al. 2002; Cohn and Angevine 2000; Marsik et al. 1995).

2. METHOD

The data received from radiosondes employed between 1300 UTC and 2400 UTC (corresponding to 7:00 AM and 6:00 PM LST) were considered for analysis. The vertical resolution for the radiosonde data was approximately 10m. For each sounding, the ML height was determined by six different methods based on previous research. Four of the methods were subjective, obtaining the height directly from inspection of the Skew-T temperature and dewpoint profiles, and two of the methods were objective, employing the lapse rate and potential temperature data (Marsik et al. 1995; Baxter 1991; Garrett 1981; Heffter 1980). The heights estimated by each method were analyzed qualitatively and assigned quality flags.

The subjective methods are the T Base Method, T Mid Method, q Mid Method and q Base Method; and the objective methods are the T Lapse Rate Method and Θ Increase Method. An example of heights determined by these methods is displayed in Figure 3.

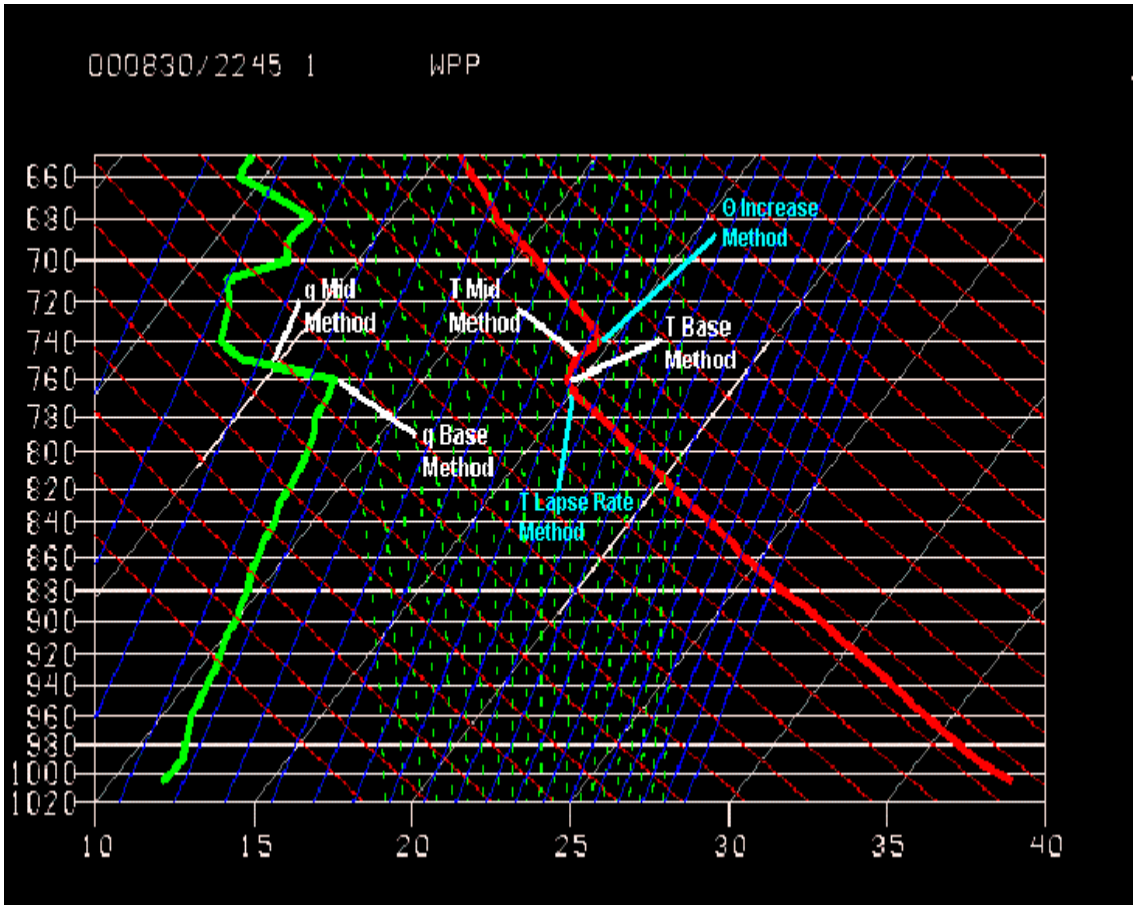

Fig. 3: Skew-T chart for WH on 8/30/00 at 2245 UTC. High quality ML heights determined from radiosonde data. White colors are subjective methods and light blue colors are objective methods.

For the T Base Method, the entire temperature profile was analyzed to locate an ML. In an ideal Skew-T, the temperature profile had a well-mixed layer where the temperature decreased with height along a dry adiabat. If the temperature profile did not have a well-mixed layer, the ML was taken as the layer where the temperature decrease was nearly dry adiabatic. The ML height was then defined as the base of the inversion layer above the ML where the temperature had a sharp increase with height or when the lapse rate was less than dry adiabatic. An ML height estimate was considered

high quality and assigned a high quality flag when the temperature profile was well-mixed and had a distinct inversion base (Figure 3).

For the T Mid Method, the ML height was the point halfway between the base and the top of the inversion layer in the temperature profile. The base of the inversion layer was as defined in the T Base Method, and the top was the point in the temperature profile where the lapse rate changed from being less than moist adiabatic to greater than moist adiabatic. This criterion was applied to identify the top of the inversion layer because, in the free atmosphere, the temperature does not decrease dry adiabatically as it does in the ML. The ML height estimate was considered highly confident and assigned a high quality flag, when the temperature profile was well-mixed and had a distinct inversion top and base (Figure 3).

For the q Base Method, the entire dewpoint profile was analyzed to locate an ML. In an ideal Skew-T, the dewpoint profile had a well-mixed layer where the mixing ratio was constant with height. If the dewpoint profile did not have a well-mixed layer, the ML was taken as the layer where the mixing ratio was nearly constant. The ML height was then defined as the point in the dewpoint profile where there was a significant decrease in mixing ratio above the ML. An ML height estimate was considered highly confident and assigned a high quality flag when the decrease in moisture was obvious (Figure 3).

For the q Mid Method, the ML height was the point halfway between the points where the dewpoint decreased significantly with height and increased slightly or decreased less drastically with height. This criterion was used to identify the top of the

inversion layer because in the free atmosphere the air is much drier and moisture is not conserved as it is in the ML. An ML height estimate was considered highly confident and assigned a high quality flag when the dewpoint profile was nearly constant and the ML height estimate was obvious (Figure 3).

When an ML height estimate was not easily identified from the Skew-T plot, the estimated height was subjectively assigned a low quality flag depending on its ambiguity and proximity to the estimates by the other methods. This usually occurred when there was deviation from dry adiabatic in the temperature profile, or the mixing ratio was not constant with height in dewpoint profile.

Figure 4 displays a Skew-T that had variable temperature and dewpoint profiles. Below the height labeled as the T Base Method ML height, there were deviations in the temperature profile near 980mb and 920mb where the lapse rate was less than dry adiabatic. The ML was considered as a whole and the ML height was determined to be at 880mb where there was an obvious temperature increase. Likewise, below the height labeled as the q Base Method ML height, there was a decrease in the mixing ratio at 960mb. Because the decrease was not significant and the ML was considered as a whole, the ML height was determined to be at 920mb where the decrease in moisture was better defined. The uncertainty in the dewpoint and temperature profiles resulted in ambiguity in the ML height estimates. Therefore, low quality flags were assigned to these estimates to represent uncertainty.

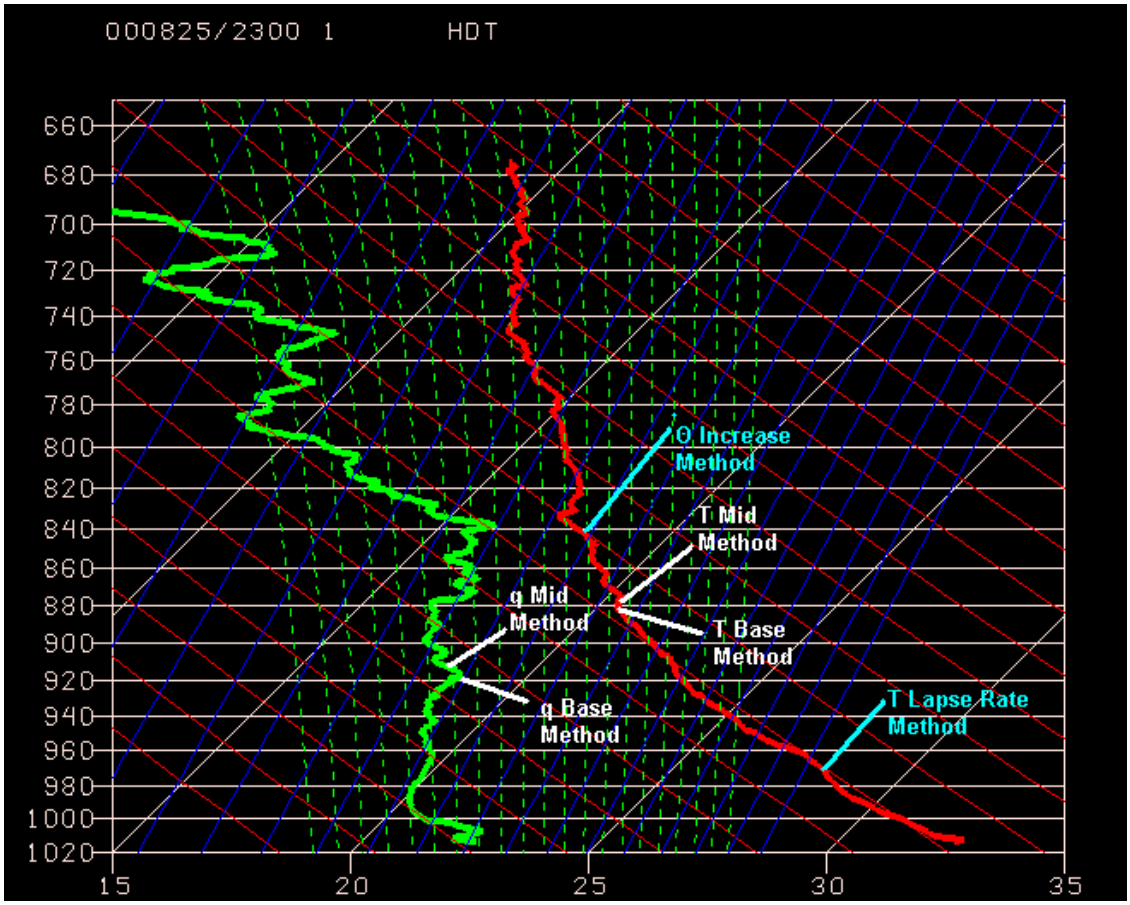

Fig. 4: Skew-T chart for HDT on 8/25/00 at 2300 UTC. ML heights determined from radiosonde data. White colors are subjective methods and light blue colors are objective methods. T Base, T Mid, q Base, q Mid, and Θ Increase Methods are all assigned low quality flags and T Lapse Rate Method is assigned a high quality flag.

When the T Base Method was assigned a low quality flag, the T Mid Method was also assigned a low quality flag (Figure 4). Likewise, when the q Base Method was assigned a low quality flag, the q Mid Method was also assigned a low quality flag (Figure 4). This was because the T Mid Method is based on the T base Method, and the q Mid Method is based on the q Base Method. Low quality flags were also assigned to the T Mid Method and q Mid Method when the top of the inversion in the temperature profile was not obvious, or the dewpoint profile did not have a slight increase in

moisture after it significantly decreased (Figure 5). In these cases, 32mb was subtracted from the pressure level of the inversion base in the temperature profile, or the pressure level of the significant decrease in the dewpoint profile; and the resulting ML depth was at the point either 16mb less than the inversion base, or 16mb less than the significant moisture decrease. By considering the typical inversion layer depth, the value of 32mb was chosen arbitrarily to represent the higher end of the observations. An example of this was applied in cases when the radiosonde went through a cloud.

Figure 5 shows a Skew-T that has temperature and dewpoint profiles from which the base and top of the inversion layer could not be determined. Both profiles were fairly well-mixed up to 880mb, at which point there was a decrease in moisture and the temperature lapse rate was less than dry adiabatic. However, the temperature and dewpoint profiles joined at this level and remained together until the 860mb level. Because of this, the ML height determined by the T Base Method and q Base Method was not at 880mb, but above 860mb where the profiles separated. The uncertainty when the temperature and dewpoint profiles were joined caused ambiguity in T Base Method and q Base Method estimates and the selected ML heights to be assigned low quality flags.

The top of the inversion was also ambiguous in both the temperature and dewpoint profiles in Figure 5. Because the top of the inversion could not be determined, the T Mid Method ML height was found by subtracting 16mb from the pressure level determined by T Base Method. Likewise, the ML height determined by the q Mid

Method was found by subtracting 16mb from the pressure level determined by the q Base Method.

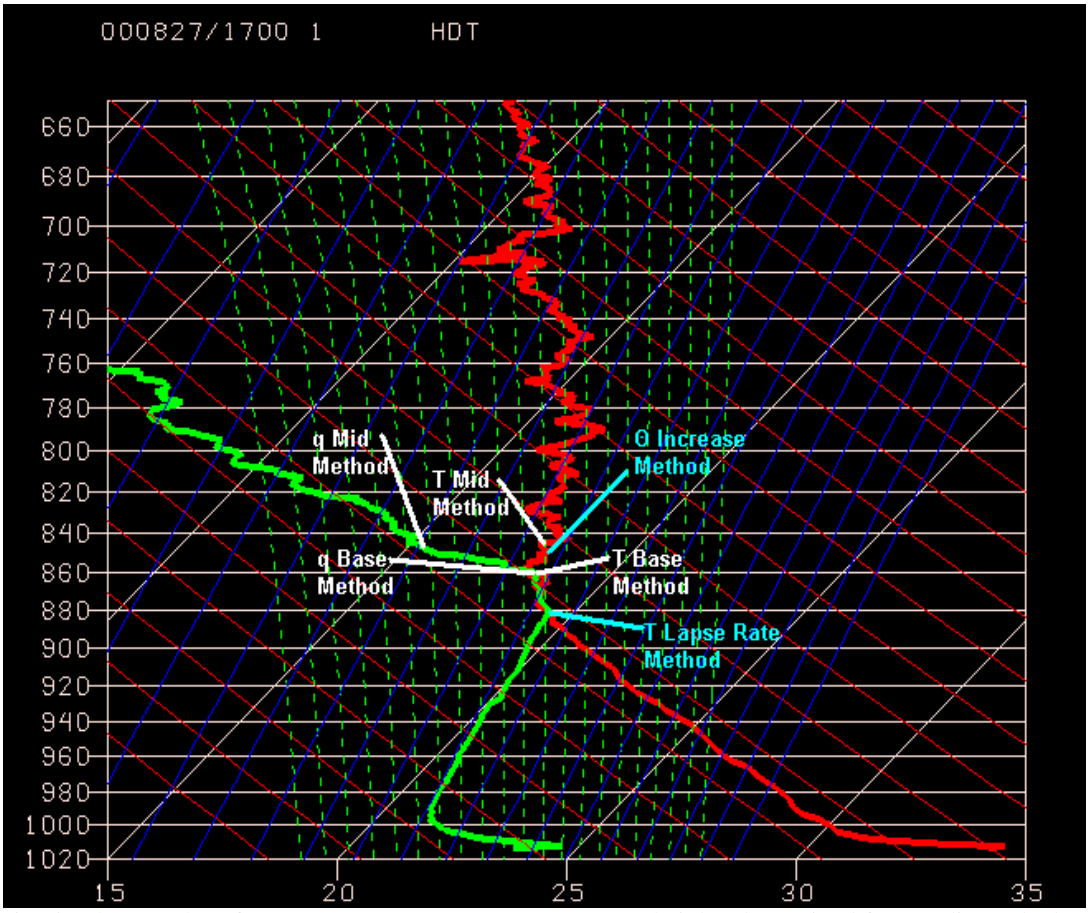

Fig. 5: Skew-T chart for HDT on 8/27/00 at 1700 UTC. ML heights determined from radiosonde data. White colors are subjective methods and light blue colors are objective methods. T Base, T Mid, q Base, q Mid, and Θ Increase Methods are all assigned low quality flags and T Lapse Rate Method is assigned a high quality flag.

For the T Lapse Rate Method, the ML height was the point above 10mb from the surface where the lapse rate calculated over10mb levels was less than -8 °C/km on a 30mb average (Marsik et al. 1995). A ML height estimate was considered highly confident when the first point that the lapse rate was less than -8 °C/km, was less than -8 °C/km over a 30mb average. In this case, the estimated height was assigned a high

quality flag (Figure 3, Figure 4, Figure 5). A low quality flag was assigned when the estimated height was ambiguous, and usually occurred when the first point that the lapse rate was less than -8 °C/km was not less than -8 °C/km over a 30mb average. Figure 6 is an example of a situation where the lapse rate was less than -8 °C/km but not over a 30mb average. In this case, the temperature profile had a slight superadiabatic layer, from approximately 940mb to 920mb, which caused the lapse rate to be less than -8 °C/km at approximately 920mb, but not over a 30mb average. Because of this, the selected ML height at 900mb was assigned a low quality flag.

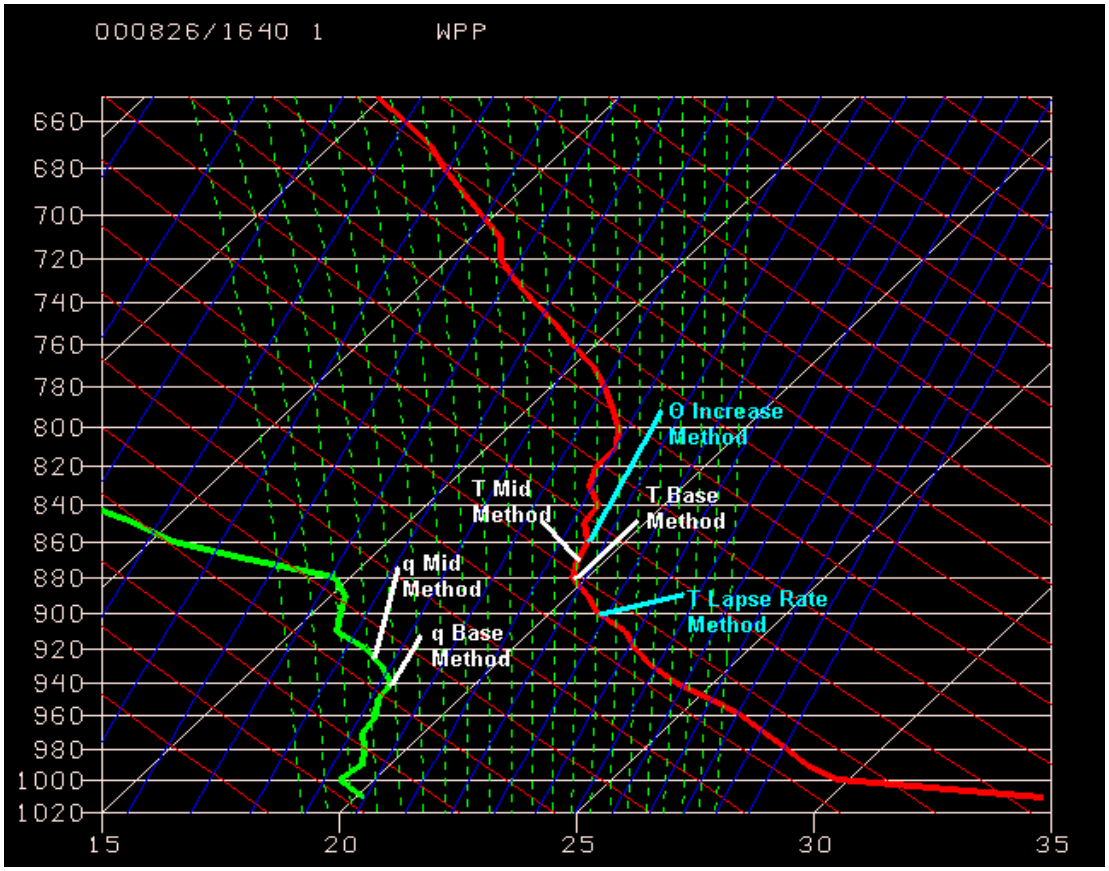

Fig. 6: Skew-T chart for WH on 8/26/00 at 1640 UTC. ML heights determined from radiosonde data. White colors are subjective methods and light blue colors are objective methods. T Base, T Mid, and T Lapse Rate Methods are all assigned low quality flags and q Base, q Mid, and Θ Increase Methods are all assigned high quality flags.

For the Θ Increase Method, the ML height was the point where the potential temperature was at least 2 degrees greater than the potential temperature in the ML (Heffter 1980, Marsik et al. 1995). The potential temperature was evaluated at 10mb levels. A well-mixed layer had nearly constant potential temperature values with height. If the ML was not well-mixed, the ML height was taken as the point where the potential temperature was at least 2 degrees greater than the average potential temperature of the ML. An ML height estimate was considered highly confident and assigned a high quality flag when the ML was well-mixed and an increase of 2 degrees or more was at an obvious level (Figure 3, Figure 6). A low quality flag was assigned when the estimated height was 2 degrees warmer than the average potential temperature in the ML, but not 2 degrees warmer than the potential temperature at a particular pressure level within the ML. This caused the estimated ML height to be ambiguous, and usually happened in cases when there was not a well-mixed ML and potential temperature was variable over a large area (Figure 4, Figure 5).

Figure 4 shows an ML height estimated by the Θ Increase Method where an obvious ML was not evident in potential temperature data. Because of this, the values below 900mb were taken as the ML. The values slightly increased with height so that the point where the potential temperature was 2 degrees warmer than the average potential temperature in the ML was not 2 degrees warmer than the potential temperature at particular pressure levels within the ML. This caused the ML height to be ambiguous and was assigned a low quality flag. Figure 5 shows an ML height estimated by the Θ Increase Method where the potential temperature was nearly constant in the ML;

however, near the top of the ML, the values slightly increased and there was not a strong inversion. The point where the potential temperature was 2 degrees warmer than the average potential temperature in the ML was not 2 degrees warmer than the potential temperature at particular levels within the ML. This was different than Figure 3 and Figure 6 because a stronger inversion was evident in the potential temperature data for these figures. The point where the potential temperature was 2 degrees warmer than the ML was clearly located at the selected ML height, and the potential temperature value was 2 degrees warmer than all the pressure levels within the ML.

One goal of this paper was to create a benchmark method for determining the ML height from radiosonde data for comparison of ML height estimates determined by other instruments. For the purposes of this study in relation to air quality, the first part of the benchmark method was based on the q Mid Method. This was because the height of the midpoint of the transition layer in the dewpoint profile was most analogous to the height that passive tracers were mixed. Determining the second part of the benchmark method was based on comparing the five other methods with the q Mid Method to ascertain the next best method to use when ML heights determined by the q Mid Method were ambiguous.

Results were found by statistical analysis performed on the differences between the heights in the form of bias, standard deviation, and root mean square error (RMSE). This was done for a variety of situations including comparisons of all the heights from the different methods, regardless of the quality flag and comparisons focusing on the separate quality flags. The combination of the q Mid Method and the next best method

was considered as the full benchmark method, and was used as the optimal method for determining the ML height from radiosonde data.

3. RESULTS

The results of the comparisons to determine the Benchmark Method are displayed in Table 1a, Table 1b, Table 2, Figure 7a, Figure 7b, and Figure 8. The bias and standard deviation were found by taking the difference in heights so that the q Mid Method heights were subtracted from the other radiosonde method heights. The table is broken down into sections to show the comparisons of the quality flags for both methods.

Overall, the subjective methods had lower bias and standard deviation values than the objective methods. Of the objective methods, the Θ Increase Method had the largest values and measured higher ML heights by more than 300m compared to high quality q Mid Method heights. In general, the statistics for the objective methods were similar depending on the quality flag of the q Mid Method.

For the subjective methods the statistics were nearly the same for all the comparisons with the q Base Method. The bias for the T Base Method and T Mid Method was nearly equal in value but opposite in sign for the comparison using all the heights from both methods. Between these two methods, the T Base Method had lower standard deviation values for most comparisons. For the case when the high quality q Mid Method heights were compared to these two methods, the T Base Method had much more negative values. These values were similar to the same comparison with the q Base Method.

Table 1a: Comparison of ML height estimates determined by the q Mid Method with the T Base Method and T Mid Method.

	T Base Method				T Mid Method			
Other Method	All	High Flag	High Flag	All	All	High Flag	High Flag	All
q Mid Method	All	High Flag	All	High Flag	All	High Flag	All	High Flag
Standard Deviation	0.21	0.08	0.18	0.20	0.27	0.08	0.15	0.34
Bias	-0.05	-0.12	-0.06	-0.06	0.06	0.00	0.00	0.10
Sample Size	50	13	31	19	50	8	17	19

Table 1b: Comparison of ML height estimates determined by the q Mid Method with the q Base Method.

	Q Base Method			
Other Method	All	High Flag	High Flag	All
q Mid Method	All	High Flag	All	High Flag
Standard Deviation	0.06	0.05	0.06	0.05
Bias	-0.11	-0.11	-0.11	-0.11
Sample Size	50	19	32	19

Table 2: Comparison of ML height estimates determined by the q Mid Method with the T Lapse Rate Method and the Θ Increase Method.

	T Lapse Rate Method				Θ Increase Method			
Other Method	All	High Flag	High Flag	All	All	High Flag	High Flag	All
Method 4	All	High Flag	All	High Flag	All	High Flag	All	High Flag
Standard Deviation	0.30	0.15	0.29	0.20	0.31	0.22	0.27	0.23
Bias	-0.12	-0.08	-0.14	-0.07	0.36	0.25	0.32	0.25
Sample Size	50	16	45	19	50	14	30	19

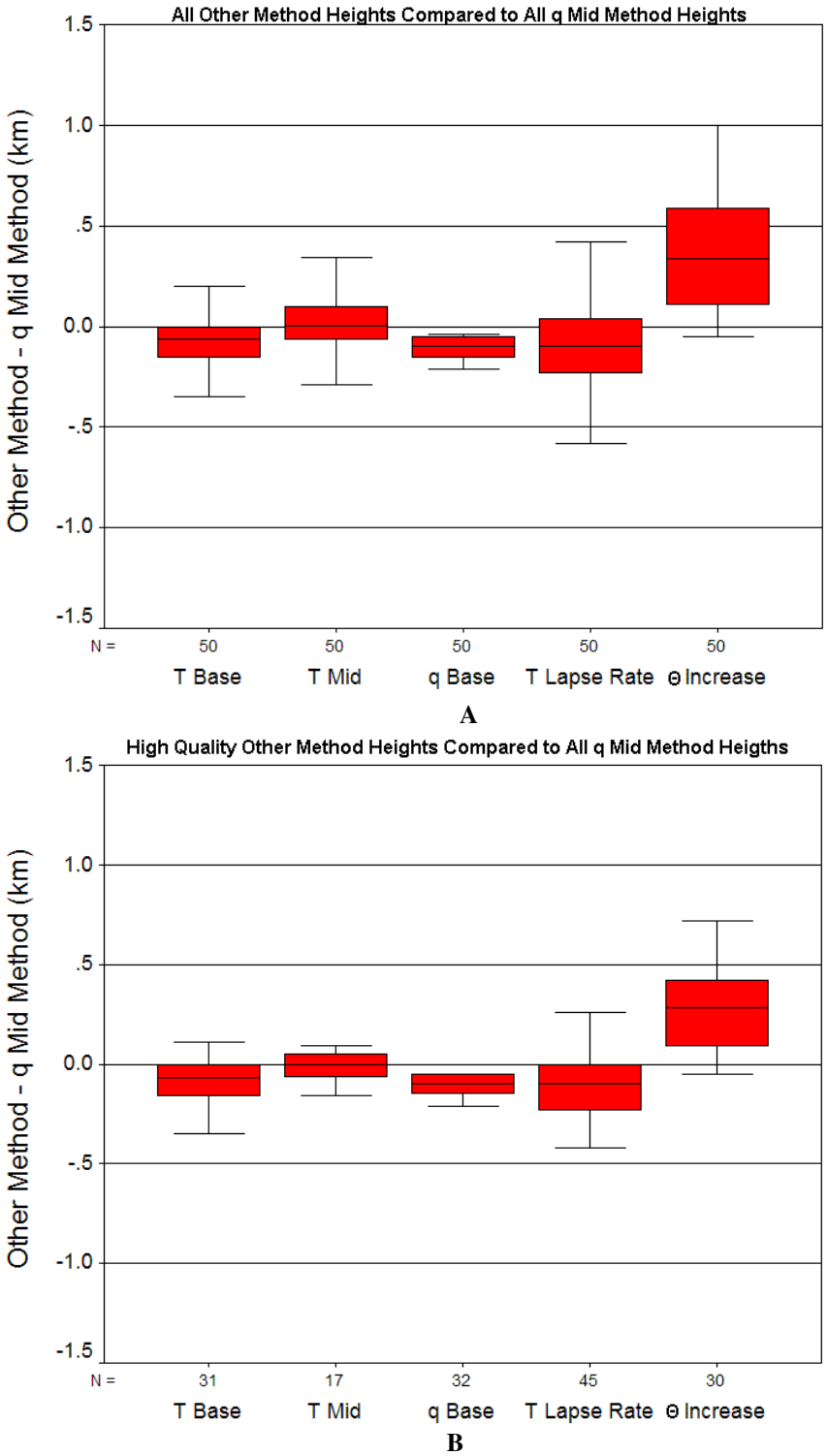

Fig. 7a: Box and Whiskers plots of q Mid Method heights compared to the other method heights. A: All heights from other methods. B: High quality heights from other methods. N represents number of heights available for the comparisons and the solid black lines represent the median.

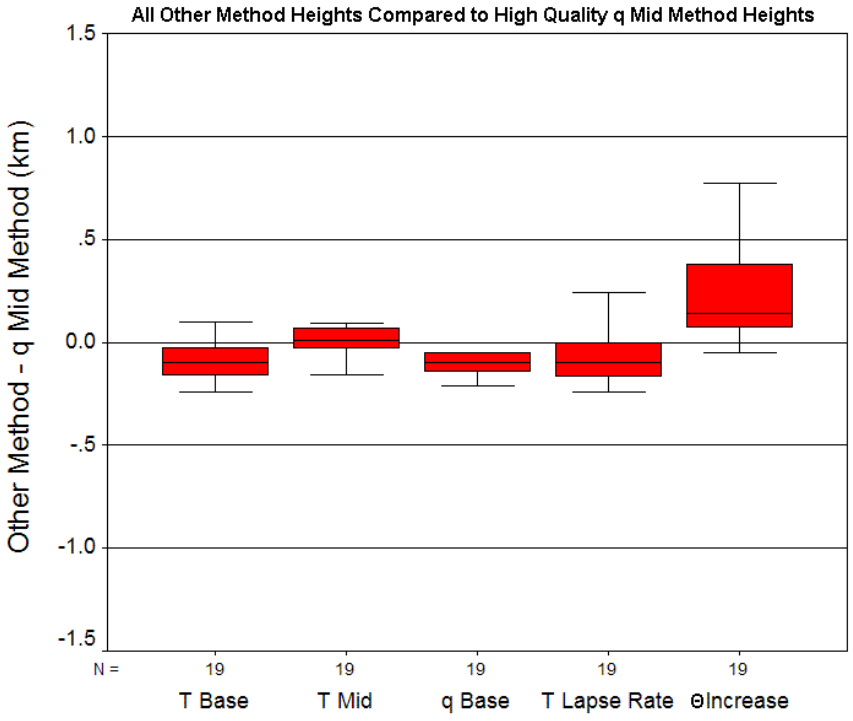

C

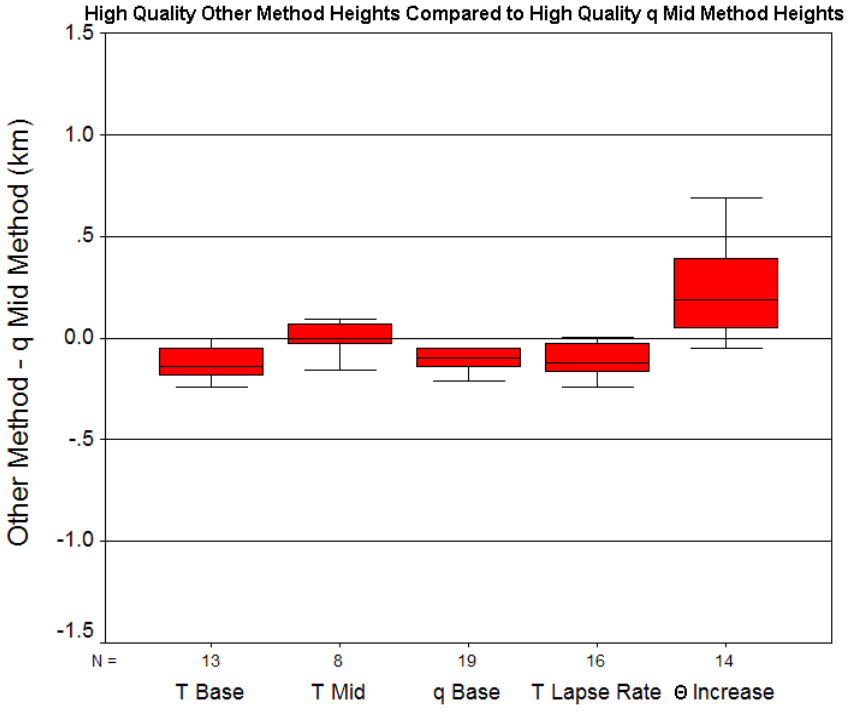

D

Fig. 7b: Box and Whiskers plots of high quality q Mid Method heights compared to the other method heights. C: All heights from other methods. D: High quality heights from other methods. N represents number of heights available for the comparisons and the solid black lines represent the median.

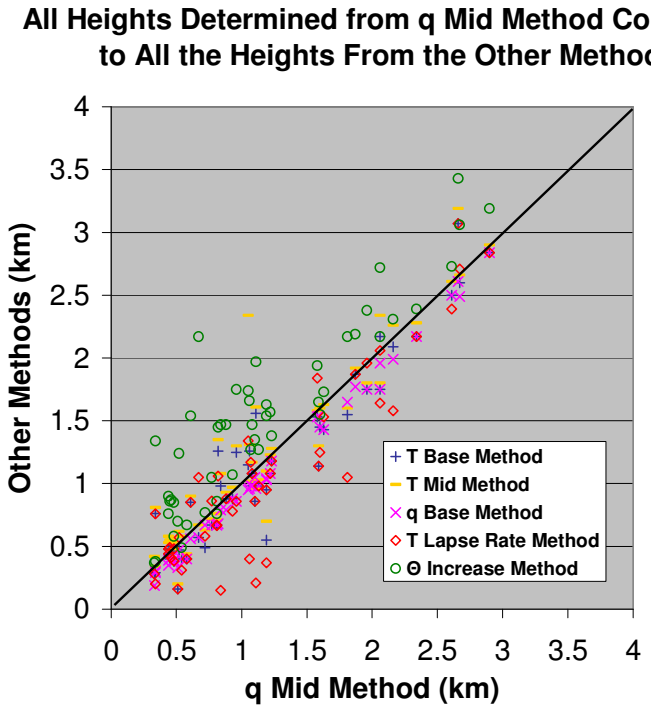

Fig. 8: Scatter plot of q Mid Method and the other method ML heights.

4. DISCUSSION

Overall, the statistics for the subjective methods were better than the statistics for the objective methods. The ML heights determined by the subjected methods consisted of direct analysis of temperature and dewpoint profiles. Generally, these profiles were coincident so that when the ML experienced such features as a cloud (Figure 5) or a strong inversion capping the ML (Figure 3), the ML heights determined by the other subjective methods were similar to the ML heights determined by the q Mid Method.

The largest bias values were found for the Θ Increase Method. The ML heights estimated by the Θ Increase Method were normally more than 200m higher than ML heights estimated by the q Mid Method heights. The results were consistent over a range of heights (Figure 8) which gives support that estimating the ML as the point 2 degrees

higher than the potential temperature in the ML was an overestimation. In the cases when the inversion layer was more distinct allowing the potential temperature to increase over a shallower layer, the estimated ML height was better located with the q Mid Method height (Figure 3). When the inversion layer was deeper and less stably stratified, the potential temperature increase usually occurred at much higher heights compared to the q Mid Method (Figure 6).

The bias for the T Lapse Rate Method was negative for all the comparisons. Generally, the T Lapse Rate Method heights were also lower than the heights determined by the T Base Method. This means that the temperature lapse rate was less than dry adiabatic below the base of the inversion. The bias was larger for the comparisons with all the heights and can be attributed to a few outliers where the T Lapse Rate heights were more than 100m higher than the q Mid Method heights (Figure 8). These outliers can be explained by cases when the lapse rate was less than -8 °C/km over a 30mb average; but by visual inspection of the temperature profile, this feature was only a temporary deviation, and on the whole, the ML extends to a higher altitude (Figure 4). Such features can be caused by the radiosonde passing through a buoyant plume or thermal. Other than these outliers, the estimated ML heights from the T Lapse Rate method were within 80m lower than the q Mid Method heights and fairly consistent over a range of ML heights (Figure 8). Because the T Lapse Rate Method was essentially measuring the base of the inversion layer, this method was considered the better method out of the two objective methods used in this study.

The q Base Method had the lowest standard deviation values. For all comparisons, these values were within 10m regardless of the quality flag, and the bias was the same for all the comparisons. This means that difference between the base and midpoint of the moisture transition layer averaged 110m regardless of the nature of the dewpoint profile.

Overall, the bias was lowest for the T Base Method and T Mid Method. This was especially true for the high quality T Mid Method comparisons, which had a zero bias. When the ML was well-mixed and a strong inversion was present, the change in temperature and moisture was coincident and the ML was determined to be at the same height by both the T Mid Method and q Mid Method. Likewise, when the high quality T Base Method heights were compared to the high quality q Mid Method heights, the bias was within 10m of the bias found between the q Base Method and the q Mid Method. This also shows that for a well-mixed layer, the base of the inversion in the temperature profiles is co-located to the base of the inversion in the dewpoint profiles.

The bias was less negative for the q Base Method than the T Base Method by 50m for the comparison of all heights regardless of quality flag. This means that the average point where the dewpoint decreased sharply with height, was below the average point where the temperature increased sharply with height, or became less than dry adiabatic. These two methods were compared directly and the statistics found were independent of quality flag, radiosonde location, and time of day.

For this paper, the reason for the lower q Base Method heights than T Base Methods heights was undetermined. One possible explanation was the response time of

the instruments. This possibility was considered to see if the relative humidity sensor was slower than the temperature sensor; however it was disregarded because the high quality heights comparisons by both methods had bias values within 10m of each other. If the reason the T Base Method heights were higher than the q Base Method heights was an instrument issue, a systematic difference in heights would have occurred for this comparison as well. More research is needed to determine other possible explanations which deal with the dynamics of the atmosphere

On the whole, the T Base Method and the T Mid Method had the lowest bias and standard deviation values. Specifically, for the comparison with the high quality q Mid Method heights, the T Base Method had a lower standard deviation and a bias closer to zero. Because the second part of the benchmark method was based on determining which method to use when ML heights determined by the q Mid Method were ambiguous, the T Base Method was determined as the next best method.

This benchmark method consisted of using the ML height determined by the q Mid Method when the height was assigned a high quality flag; using the ML height from T Base Method when the ML height determined by the q Mid Method was assigned a low quality flag, and the ML height determined by T Base Method was assigned a high quality flag; and using the ML height determined by q Mid Method when the ML heights determined by both the q Mid Method and the T Base Method were assigned low quality flags. Therefore, this new method combined the mid point of the moisture transition layer with the base of the temperature inversion using the mid point of the moisture transition layer as the preferred height.

b. Wind Profiler

1. BACKGROUND

Wind profilers are stationary instruments that provide nearly continuous measurements of the ML. Wind profiler systems measure vertical variations in the refractive index and are used to determine the evolution of the ML height by tracking the peak in signal-to-noise ratio (SNR). An increase to a peak value is evident at the entrainment zone followed by a decrease to free atmospheric values.

Errors can result, and the ML can be difficult to determine when peaks in the refractive index are caused by enhancements of reflectivity that occur in regions other than at the top of the ML. This can be caused by such things as turbulence within or above the PBL, clouds, precipitation, insects, birds, and ground clutter (White et al. 1999). Also, the lowest gate of a wind profiler system is usually not below 100m. Depending on the instrument, this can create problems when trying to resolve the SBL in detail or detecting turbulence structures in the lower PBL (Seibert et al. 2000; Marsik et al. 1995). Marsik et al. (1995) found wind profilers to have difficulty detecting turbulence structures in the lowest 400-600m of the PBL.

There has been past research that focused on the use of wind profilers for determining the ML height, including comparisons of the ML heights estimated by wind profilers with radiosondes or other instruments. Although in most cases there was good agreement, wind profiler ML height estimates were generally higher than the ML estimates by the other instruments. The reason for higher wind profiler ML estimates was related to the nature of the study.

Angevine et al. (1994) and Grimsdell and Angevine (1998) both focused on the relationship between wind profilers and radiosondes and found a good agreement between these two instruments with a slight bias representing higher wind profiler ML heights. In Champaign – Urbana, Illinois, Grimsdell and Angevine (1998) found this good agreement as a correlation coefficient of 0.88 for 150 estimated heights with slightly higher heights estimated from the wind profiler data. In Alabama, Angevine et al. (1994) also found the wind profiler estimates to be slightly higher than the radiosonde estimates. However, in this study, a good agreement between ML estimates from both instruments was limited to cases when the convective boundary layer top was very well defined and the inversion height remained constant after noon. When the convective boundary layer top was not as well defined, both instruments measured ML heights with greater variability. In both cases, the wind profiler was determined as the more reliable instrument for estimating the ML height.

Wind Profilers have produced higher estimates than other instruments, such as ground-based lidar and sodar. Both Marsik et al. (1995) and Beyrich and Gorsdorf (1995) found that wind profiler estimates were higher during conditions when a shallow ML was present. Marsik et al. (1995) measured the ML heights around the city of Atlanta by wind profilers, a rawinsonde system, and two ground-based lidars. The comparisons between all the instruments showed that there was often considerable spread in the estimates. The spread was greatest during the early morning hours with a peak standard deviation among estimates of nearly 800m at 0800 EDT. This was blamed on the fact the wind profiler overestimated the ML when it was below 200m,

which was below its minimal level of detection. The spread was greatly reduced by midday, with an average standard deviation of approximately 300m at 1200 EDT. After this time, estimates deviated once again, with average standard deviations increasing to between 400 and 450 m.

Beyrich and Gorsdorf (1995) compared the ML height values determined by sodar and wind profilers in Germany during convective conditions. The agreement was quite good, with only a small bias of less than 10m. The root mean square difference for 59 samples was 38m, which was less than the wind profiler vertical resolution, and the correlation coefficient was 0.97. The largest absolute differences observed were between 80m and 100m, which occurred during the times of rapid ML growth. A slight tendency towards higher ML height values from the wind profiler existed for very shallow convective PBL; this was blamed on the uncertainties in profiler measurements due to ground clutter.

2. METHOD

To make comparisons with the benchmark method, ML heights were obtained from wind profiler data for the closest time following each radiosonde deployment at the nearest site possible (Figure 1). The wind profiler PBL heights were given as heights AGL (above ground level) and were adjusted to heights above sea level by adding 37m to the WH heights, 10m to the EL, and 6m to the LM heights. For the WH comparison, the WH site consisted of both a wind profiler and radiosonde so that the ML height estimates from these two instruments were compared and considered exactly co-located. For the LM comparison, the LM wind profiler and HSE radiosonde were not exactly co-

located, but were within 65m of each other so the ML height estimates from these two instruments were compared and also considered co-located. For the EL comparison, the EL wind profiler was the closest wind profiler to the HDT radiosonde, but was located 18km away. The ML height estimates from these two instruments were compared but not considered co-located.

The wind profiler data was supplied at half hour intervals by Wayne Angevine. He determined the ML heights subjectively by using the refractive index structure parameter and finding the local maximum in the backscattered profiles. The vertical resolution was approximately 10m. The heights were assigned quality flags so that good heights were given flag 1, marginal heights were given flag 2, and bad heights were given either a flag 3 or flag 9999. The ML heights labeled as bad were not used for the comparison, while the flag 2 ML heights were considered ambiguous and low quality.

The benchmark method was assigned quality control flags based on what part of the method was used to determine the ML height. The ML height was considered high quality and assigned a quality control flag 1 when the q Mid Method height was assigned a high quality flag and the mid point of the moisture transition layer was taken as the ML height. The ML height was considered lower quality and assigned a quality control flag 2 when the q Mid Method height was assigned a low quality flag, the T Base Method height was assigned a high quality flag, and the base of the temperature inversion was taken as the ML height. The ML height was considered the lowest quality and assigned a quality control flag 3 when both the q Mid Method and the T Base Method heights

were assigned low quality flags and the mid point of the moisture transition layer was taken as the ML height.

The results of the comparisons between the radiosondes and the wind profiles were found by statistical analysis performed on the differences between the heights determined by these two instruments in the form of bias, standard deviation, and RMSE. This was done for a variety of situations including comparisons of all the heights from both instruments, regardless of the quality flag and comparisons focusing on the separate quality flags.

The statistics for the high quality flag comparisons were then evaluated to determine their significance for application in other situations. This was done using a two-tailed, one-sample t test performed on the difference in heights between the wind profiler and the benchmark method at a significance level of 0.05. The null hypothesis was a statement that the wind profiler and the benchmark method determined the ML to be at the same height so that the bias was equal to zero. The alternate hypothesis was a statement that the two instruments determined the ML to be at different heights so that the bias was nonzero. The corresponding p-value was also calculated to determine the probability of rejecting the null hypothesis when it was actually true. For a significance level of 0.05, the null hypothesis was not rejected when the calculated t statistical value was between -1.96 and 1.96 ($-1.96 \leq t \leq 1.96$) and the p-value was greater than 0.05. A p-value close to 1.00 represented high confidence in the null hypothesis while p-value close to 0.00 represented low confidence in the null hypothesis.

3. RESULTS

The comparison between the benchmark method ML heights and the wind profiler ML heights is displayed in Table 3a, Table 3b and Figure 9. The bias, standard deviation, and RMSE were found by taking the difference in heights so that the wind profiler heights were subtracted from the benchmark method heights. The table is broken down into sections to show the comparisons of the quality flags for both instruments.

Table 3a: Comparison between all the wind profiler ML heights and benchmark method ML heights separated by the quality flag of the benchmark method.

	All Profiler Heights and All Sonde Heights				All Profiler Heights and High Quality Sonde Heights			
Site	EL	LM	WH	WH& LM	EL	LM	WH	WH& LM
Standard Deviation	0.47	0.27	0.22	0.25	0.42	0.20	0.25	0.24
Bias	0.04	-0.07	-0.04	-0.06	-0.19	0.08	-0.05	-0.01
RMSE	0.47	0.28	0.23	0.26	0.46	0.21	0.25	0.24
Sample Size	31	22	17	39	11	6	12	18

Table 3b: Comparison between the high quality wind profiler ML heights and benchmark method ML heights separated by the quality flag of the benchmark method.

	High Quality Profiler Heights and All Sonde Heights				High Quality Profiler Heights and High Quality Sonde Heights			
Site	EL	LM	WH	WH& LM	EL	LM	WH	WH& LM
Standard Deviation	0.33	0.26	0.23	0.25	0.40	0.11	0.24	0.21
Bias	-0.08	-0.08	-0.02	-0.06	-0.26	0.00	-0.02	-0.01
RMSE	0.34	0.27	0.23	0.25	0.48	0.11	0.24	0.21
Sample Size	18	17	13	30	6	5	10	15

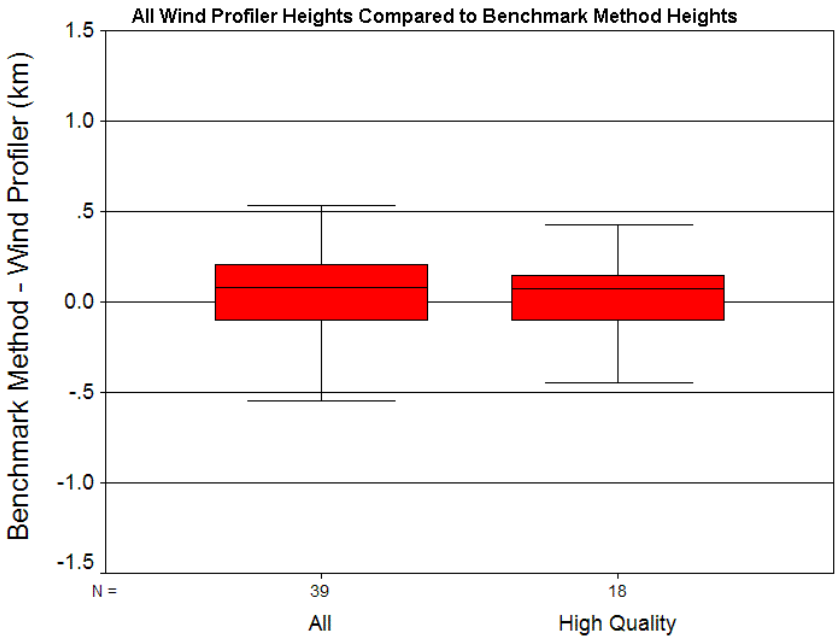

A

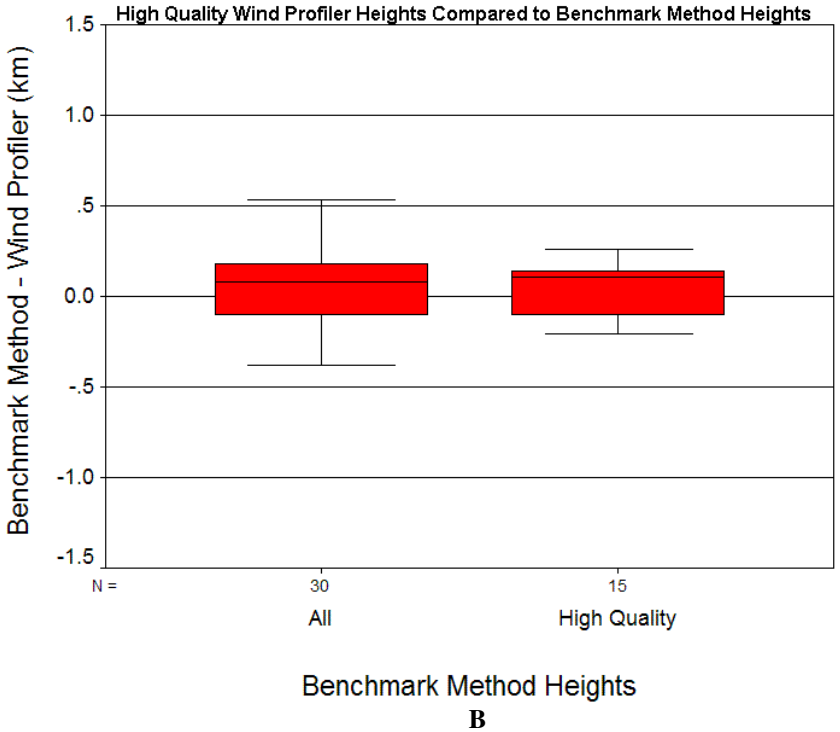

B

Fig. 9: Box and Whiskers plots of the comparisons between the benchmark method and the wind profiler ML heights separated by the different quality flag of the wind profiler.
A: All wind profiler heights compared to benchmark method heights. B: High quality wind profiler height compared to benchmark method heights. N represents number of heights available for the comparisons and the solid black lines represent the median.

Overall, the wind profiler heights were in good agreement with the benchmark method heights with a bias less than 100m in all cases, except for the EL comparisons using only high quality benchmark method heights. The standard deviation and RMSE values were also highest for the EL comparisons. The LM and WH comparisons had lower standard deviation and RMSE values, and were more comparable to each other. Because of this, the EL comparison was removed from the data set, and the LM and WH were combined to produce a larger dataset. These results are displayed in the fourth column for each comparison category in Table 3a and Table 3b and labeled as the WH&LM comparison.

The statistics were similar for the combined WH&LM comparison for all quality flag cases. The standard deviation was slightly better for the comparisons using only high quality flag heights from both instruments, and the bias was 50m less for the comparisons using only the high quality benchmark method heights. Because of this dependence on the quality flag of the benchmark method, the heights determined by the separate components of the benchmark method (T Base Method and q Mid Method) were compared to the wind profiler heights and displayed in Table 4a and Table 4b. Overall, the standard deviation values were less and bias was greater for the T Base Method compared to the q Mid Method.

Table 4a: Comparison between all the wind profiler ML heights and the ML heights determined by the different components of the benchmark method separated by the quality flag of the radiosonde methods.

	All Profiler Heights and All Sonde Heights			All Profiler Heights and High Quality Sonde Heights		
Site	Benchmark Method	T Base Method	q Mid Method	Benchmark Method	TBase Method	q Mid Method
Standard Deviation	0.25	0.25	0.29	0.24	0.14	0.24
Bias	-0.06	-0.06	-0.03	-0.01	-0.13	-0.01
RMSE	0.26	0.25	0.29	0.24	0.19	0.24
Sample Size	39	39	39	18	21	18

Table 4b: Comparison between the high quality wind profiler ML heights and the ML heights determined by the different components of the benchmark method separated by the quality flag of the radiosonde methods.

	High Quality Profiler Heights and All Sonde Heights			High Quality Profiler Heights and High Quality Sonde Heights		
Site	Benchmark Method	T Base Method	q Mid Method	Benchmark Method	T Base Method	q Mid Method
Standard Deviation	0.25	0.24	0.27	0.21	0.13	0.21
Bias	-0.06	-0.05	-0.06	-0.01	-0.11	-0.01
RMSE	0.25	0.25	0.27	0.21	0.17	0..21
Sample Size	30	30	30	15	17	15

The comparisons between the wind profilers and the benchmark method were consistent over a range of heights; this is represented in Figure 10. For shallow mixing layers below 1km, there was a slight bias towards the wind profiler determining higher heights. When the ML was deeper, there was more of a separation between estimates from the two instruments determining the ML at different heights. There were only a few cases when the instruments measured ML heights that were more than 500m

different, but for most of the cases, the ML heights were within a few tens of meters of each other.

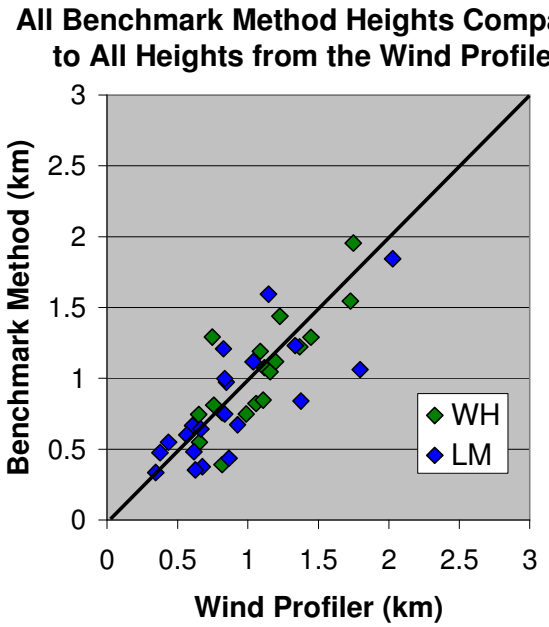

Fig. 10: Scatter plot of benchmark method and wind profiler ML heights.

The t statistic determined for the high quality flag WH and LM comparisons combined was 0.217 with a p-value of 0.831. The t statistic for the high quality flag WH comparison was 0.243 with a p-value of 0.814 and the t statistic for the high quality flag LM comparison was -0.049 with a p-value of 0.964. For all the comparisons, the t statistic was between -1.96 and 1.96 and the p-value was much greater than 0.00. Therefore, the null hypothesis was not rejected and the ML height estimated by both instruments was determined as not significantly different.

4. DISCUSSION

Overall, the ML heights estimated by the wind profiler data were in good agreement with the benchmark method ML heights. The largest discrepancies were found for the EL comparisons. This can be blamed on the distance between the radiosonde and wind profiler, and the effects of the sea breeze on the ML heights for the different locations. The EL wind profiler was located approximately 20km closer to the coast than the HDT radiosonde, which means that comparisons at the time of a sea breeze might cause the EL wind profiler to experience the influences of the marine air before the HDT radiosonde. There were two cases in the afternoon when this was possible, because the ML height estimated from the benchmark method was more than 1km higher than the ML height estimated from the wind profiler data.

More support for this is the fact that the comparisons for the LM and WH sites had lower values and were more comparable to each other. At the WH site the instruments were co-located and the LM wind profiler and radiosonde were not exactly co-located, but within a few meters of each other. The better statistics for the co-located estimates quantify the importance of comparing instruments that are co-located or within a distance that represents the same PBL.

Evaluation of the LM and WH comparison together illustrated that the results were mainly dependant on the quality flag of the benchmark method heights. When only the high quality benchmark method heights were used, the bias between the two instruments was less than 10m. In all cases, the bias was negative, indicating the ML heights estimated from the wind profiler data were higher than the ML heights estimated

from the benchmark method. This was consistent with past research that also found good agreement between these two instruments and the wind profiler heights to be slightly higher than those determined from radiosonde data (Grimsdell and Angevine 1998; Angevine et al. 1994).

For the comparisons between the wind profiler heights and the heights determined by the separate components of the benchmark method, the standard deviation was smallest for the T Base Method heights. This shows that the wind profiler heights were keying on the temperature variations caused by active turbulence, rather than the passive tracer mixing caused by turbulence that occurred over a time period of about an hour. The bias was largest for the high quality T Base Method heights which means that the active turbulence, from which the wind profiler heights are determined, on average extends above the base of the temperature inversion.

The comparisons between the wind profilers and the benchmark method were consistent over a range of heights. There was only a slight bias towards the wind profiler determining higher heights when both instruments measured the ML to be below 1km, and more of a separation between the estimates when the ML was deeper. The reason for the separation can be attributed to the physical limitations of both instruments. Because of the lowest gate, wind profiler systems often have problems resolving the lower PBL in detail. Radiosondes provided point measurements which may not have been completely representative of the entire PBL. The radiosondes may have traveled through individual plumes, which caused them to produce higher ML heights, and can

explain the outliers for deeper ML when the benchmark method determined higher ML heights than the wind profilers.

Other causes for the separation of ML heights by the two instruments (especially when the ML was deeper) may be due to the wind profilers measuring enhancements of reflectivity in regions other than at the top of the ML because of such things as turbulence, clouds, precipitation, insects, birds, and ground clutter. This might have caused the wind profilers to provide ML height estimates that were not representative of the top of the ML. Even so, in most cases the two instruments measured ML heights that were within a reasonable distance of each other.

c. Airborne Lidar

1. BACKGROUND

Measurements made by the airborne lidar are a function of both time and space, which allows for the determination of the horizontal distribution of ML height. Lidar systems observe the distribution of actual particulate matter in the ML. The ML height is determined by finding a maximum gradient in the lidar backscatter signal associated with the decrease in aerosol backscatter in the transition zone from the ML to the free atmosphere.

Even though airborne lidar can provide the spatial and temporal depiction of ML height, its use can have limitations. High backscatter signals received from cloud tops are often mistaken as the top of the ML, which creates a positive bias in the ML depth. Also, lidar data has limited ability to detect the ML height when there is weak turbulence,

a lack of aerosols sources, or when there is not a distinct contrast between the aerosol backscatter in the free troposphere and the mixed layer (Senff et al. 2002). This makes determining ML depth difficult during nighttime hours and over water (Seibert et al. 2000; Coulter 1979). Other errors can result when an internal boundary layer is present, and the lidar measures the top of a residual layer as opposed to the current surface mixed layer. Residual layers occur after the convective PBL collapses in the afternoon and contain properties of the past ML air that is unrepresentative of the present ML.

Past research has included comparisons between lidar and wind profilers, and lidar and other instruments. In most cases, the lidar was ground-based; however, White et al. (1999) used an airborne DIAL lidar along with four wind profilers to measure the convective ML depth around Nashville, Tennessee. According to White et al (1999), the ML heights determined by both instruments were well correlated for the total 87 samples, but there was significant scatter and a bias of 69m with the lidar measuring higher heights than the wind profiler. To explain the scatter and bias, the effects of clouds were investigated by using daily cloud-fraction measurements provided by a ceilometer and the data was divided into cloudy and clear sky conditions. The largest difference in the estimated heights by the separate instruments dropped from 146m in cloudy conditions to just 37m for the mostly clear data. Also, for the mostly clear sky conditions, there was an increase in the correlation coefficient of 0.87 to 0.94, and a reduction in the RMSE scatter from 169m to146m. The results of this analysis indicated that the airborne lidar estimates of the ML height were higher than the wind profiler, especially in cloudy conditions, because of the misleading gradient in aerosol backscatter that

occurred near cloud tops. Based on the CBL evaluated in this study, it was concluded that the wind profilers measured the correct ML height for air pollution applications.

Several studies have used ground-based lidars to evaluate ML heights. Both Cohn and Angevine (2000) and Marsik et al. (1995) used ground based lidars to compared ML height estimates with estimates made by wind profilers. Cohn and Angevine (2000) used the ML heights determined by a high-resolution Doppler lidar (HRDL) and a staring/scanning aerosol backscatter lidar (SABL) for comparison with the ML heights determined by wind profilers during convective conditions over Champaign – Urbana, Illinois. Each lidar used a different algorithm for the comparison. The agreement was considered to be very good between the different estimates with high correlation coefficients found between both lidars and the wind profiler. The comparison between both lidars had a 0.99 correlation for 73 samples; the wind profiler and HRDL comparison had a correlation coefficient of 0.95 for 37 samples; and the wind profiler and the SABL comparison had a correlation of 0.87 for 52 samples.

There was a slight division between the estimated heights, even though there was good agreement between the instruments. The HRDL measured higher ML heights than either the profiler or the SABL when there was a shallow ML during the morning hours. This was blamed on the different characteristics of the instruments and the differences in the algorithm used for each lidar. There was also large scatter between the lidars and the profiler at higher ML height values. This scatter was related to the presence of clouds as in the study by White et al. (1999) and the variable nature of the PBL top in convective conditions.

Marsik et al. (1995) used the ML height measurements made by two ground-based lidars for comparison with the ML estimates by wind profilers and a rawinsonde system. The comparisons between all these instruments showed that there was often considerable spread in estimates of the ML heights. The spread was greatest during the early morning hours with a peak standard deviation among estimates of nearly 800m at 0800 EDT. This spread was blamed on the range resolution of wind profilers for shallow mixing layers and was greatly reduced by midday with an average standard deviation of approximately 300m at 1200 EDT. After this time, estimates deviated once again, with average standard deviations increasing to between 400 and 450 m.

The comparison between only the rawinsonde and the lidar had a significantly smaller deviation of estimated ML heights during the early morning. The standard deviation in this case was below 200m. The better agreement between lidar and rawinsondes is because the lidar systems had the ability to detect the shallow, developing mixed layers during the early morning hours. The ML height was within the lidar's range of detection throughout the day, and the lidar and the rawinsondes were better collocated for this study. Overall, the lidar systems usually produced the lowest estimates of the three systems, which meant that the aerosols being measured may not have been mixed vertically through the entire depth of the ML as deduced from rawinsonde and wind profiler measurements.

Other studies focused on the comparison of ML height estimates by lidars and radiosondes. Of these, Cooper and Eichinger (1994), Van Pul et al. (1994), Hooper and Eloranta (1986), and Kaimal et al. (1982) found strong correlations between the ML

heights measured by both instruments. Although Cooper and Eichinger (1994) and Van Pul et al. (1994) found radiosondes and lidar to be in good agreement, the ML estimates by the radiosondes data were generally higher than the ML height estimates by lidar. In Mexico City, these two instruments were in excellent agreement with ML height differences mostly within 100 to 300m of each other (Cooper and Eichinger 1994). The radiosonde estimates were larger than backscatter lidar estimates; this was blamed on the different time resolution of the separate instruments.

In a similar study that compared noontime ML height estimates by both radiosondes and lidar, the correlation between the two heights was good with a 0.93 correlation coefficient (Van Pul et al. 1994). However, in 10% of the cases, the lidar heights were significantly lower than the radiosonde with differences greater than 400m. This large difference was blamed on the conditions when there was rapid growth of the PBL around the time of the measurement, a large entrainment zone present, or large errors of 100 to 200m created because of systematically determining the ML height from radiosonde data using the method described by Holzworth (1964) (see radiosonde background section). Generally, no significant differences were found from the influence of clouds indicating that the lidar's performance was not affected by clouds. This was in opposition to the studies by White et al. (1999) and Marsik et al. (1995) which found that clouds caused a much greater bias in a lidar and wind profiler comparison.

Hooper and Eloranta (1986) also found good agreement between instruments and uncertainty in the radiosonde estimates. When compared over Weldon, Illinois, the

lidar measurements had a 99% correlation with the radiosonde profiles. The heights measured by the separate instruments were within 50m. The boundary layer depth was considered accurately measured by lidar and most differences were caused by the sample errors of a single radiosonde measuring the depth of a complicated mixed layer

Kaimal et al. (1982) found a good agreement between lidar and radiosondes, however more instruments were involved in the study and the good agreement was limited to the cases when a well-defined inversion was present. More variability was present in the comparison when the stratification was weaker. For this study, measurements were made in Boulder, Colorado by a rawinsonde system, two other in-situ methods (tower sensors, instrumented aircraft), a ruby lidar, and four other remote sensing techniques (x-band radar, acoustic sounder, FM-CW radar, TPQ-11 radar). All systems were capable of locating the inversion base within 10% of each other. The only outliers were blamed on the physical limitations of the individual instruments.

Several other studies have also used acoustic sounders (also called sodar) along with other instruments to measure ML heights for comparison with ML height estimates by lidar. Both Beyrich (1997) and Coulter (1979) found that the ML heights estimated by lidar were generally higher than the ML heights measured by sodar. Beyrich (1997) reviewed several comparisons of ML heights determined by sodar, radiosondes, and lidar, and found that ML height values derived from lidar measurements were slightly but systematically higher than values derived from sodar or temperature profiles. This is in opposition to the studies by Cooper and Eichinger (1994) and Van Pul et al. (1994) which found the radiosondes to estimate higher ML heights were than the lidar. Higher

lidar ML heights were blamed on the conditions when convective plumes penetrated into the inversion layer and caused aerosols to be transported higher than the mean height of the stable-layer base. These pollutants trapped within the stable capping inversion or free atmosphere caused a systematic overestimation of the MH values from lidar observations.

Coulter (1979) also compared ML height estimates from sodar, lidar, and temperature profiles measured by an ANL WHAT system (a double theodolite balloon-tracking system). This study was for Manilla, Indiana and the determined values agreed fairly well, but there were significant differences consisting of consistently higher lidar-derived values compared to the sodar, and consistently lower temperature profile values compared to the sodar. In the cases of temperature profiles, the differences did not have well-defined height dependence. On the other hand, the lidar differences appeared to be greater at larger and smaller heights. The lidar and sodar comparison showed the best agreement usually occurring near midday, with larger differences in the morning and afternoon. Some of the largest differences between lidar and sodar occurred near the lowest levels. Lidar was found to be the true measurement due to its direct sensitivity of passive particles and the height that they mix. However, at certain times (early morning, late afternoon) it appeared that this height may have been the height at which particles were mixed in the past, rather than the height at which they were mixed at the present time which led to discrepancies of as much as 150m in the data.

As opposed to the study by Coulter (1979), Russell et al. (1974) found sodar to be a better instrument for determining the ML height over St. Louis, Missouri. In this

study, the comparison between ML height estimates from an acoustic echo sounder and a monostatic lidar was divided into three stages to develop a picture of the diurnal cycle of the PBL. The first stage was in the early morning when the lidar and the acoustic sounder generally defined the depth of the ML equally as well. The second stage was the period of strong convective activity. Both remote sensors indicated the change from conditions of stable stratification to those of vertical activity; however, the lidar depicted this activity throughout its full vertical extent, whereas the acoustic sounder indicated only the minimum extent of vertical mixing. The third stage was the time of surface layer re-formation or subsidence aloft, in which there was no optical contrast between neighboring air masses. The acoustic sounder immediately detected the temperature structure associated with these phenomena, but lidar detection was delayed until sufficient new particles were trapped below the inversion. Overall, the sodar was considered a better instrument than the lidar for routine determination of the ML depth and subsidence in air pollution programs.

Lidar measurements have also been directly compared to in-situ data. Olsson et al. (1974) compared lidar measurements with temperature and aerosol concentrations obtained from aircraft to determine the ML height over western Oregon. The heights compared fairly well with each other and were typically (but not always) found above the base of the inversion. Usually, when both heights were within the inversion and the region of mixing ratio decrease, the agreement between the lidar and particle count descriptions of ML was quite good, within 50 m of each other. However, during periods

of good mixing, it was more difficult to specify a particular height from the lidar data and the agreements were not as good.

2. METHOD

The lidar used in this research was an airborne instrument and therefore provided mobile measurements which needed to be compared to the wind profilers whose measurements were more abundant than the radiosondes. Comparisons were made between the ML heights measured by airborne lidar and ML heights measured by the five wind profilers. The airborne lidar data was supplied by Christoff Senff and the ML heights were determined by the maximum gradient in the lidar backscattering signal, which was associated with the decrease in aerosol backscatter found in the entrainment zone from the mixed layer to the free atmosphere. The vertical resolution was approximately 15m.

Due to the fact the lidar measures in both space and time and the profiler was confined to one place but measures in time, the lidar data was manipulated to be easily compared with the profiler data. This was done by first organizing the time of the lidar measurements into time periods to match the profiler data. A time period consisted of the fifteen minutes before the profiler measurement to fourteen minutes after the profiler measurement. For example, a profiler measurement at 1700 UTC was compared to lidar measurements from 1645 to 1714 UTC.

To deal with the changing position of the lidar, all the usable ML height measurements within a specified radius of a profiler were averaged for the given time periods and compared to the corresponding profiler. For this, the RMSE difference

between lidar and wind profiler observations was computed separately for maximum lidar distances of 16.38km (distance between the closest two profilers), 14km, 10km, and 8km to find the optimal radius. The best agreement was used for the comparison.

The results of the comparisons between the airborne lidar and the wind profiles were found by statistical analysis performed on the differences between the heights determined by these two instruments in the form of bias, standard deviation, and RMSE. This was done for a variety of situations including comparisons of all the heights from both instruments regardless of the quality flag and comparisons focusing on the separate quality flags.

The statistics for the high quality flag wind profiler comparisons were then evaluated to determine their significance for application in other situations. This was done using a two-tailed, one-sample t test performed on the difference in heights between the wind profiler and the airborne lidar at a significance level of 0.05. The null hypothesis was a statement that the two instruments determined the ML to be at the same height so that the bias was equal to zero. The alternate hypothesis was a statement that the two instruments determined the ML to be at different heights so that the bias was nonzero. The corresponding p-value was also calculated to determine the probability of rejecting the null hypothesis when it was actually true. For a significance level of 0.05, the null hypothesis was not rejected when the calculated t statistical value was between -1.96 and 1.96 ($-1.96 \leq t \leq 1.96$) and the p-value was greater than 0.05. A p-value close to 1.00 represented high confidence in the null hypothesis while a p-value close to 0.00 represented low confidence in the null hypothesis.

3. RESULTS

For comparisons between the airborne lidar and the wind profilers, the best agreement between these two instruments was found with a radius of 10km. This was because there were not enough times when the lidar was within 8km of the wind profilers to average over the turbulent variations in individual height estimates, and when the lidar was farther than 14km away from the wind profilers, the height estimates had geographical influences unrepresentative of the wind profiler locations. The number of estimated heights for the comparisons between these two instruments was much less than the comparisons between the other instruments due to the limited times when the airborne lidar was within 10km of the wind profilers. Because of this, the wind profiler sites farther inland (HSW, WH, and LB) were combined into one group (inland sites) and the wind profiler sites near Galveston Bay (LM and EL) were combined into a separate group (coastal sites) to obtain better-quality results.

The comparison between the lidar ML heights and the wind profiler ML heights using the optimal radius of 10km is displayed in Table 5 and Figure 11. The bias, standard deviation, and RMSE were found by taking the difference in heights so that the wind profiler heights were subtracted from the lidar heights. The table is broken down into sections to show the comparisons of all the heights from both instruments and only the high quality profiler heights.

Table 5: Comparison of the difference in ML height estimates between the wind profilers and airborne lidar.

	All Heights			All lidar Heights and High Quality Profiler Heights		
Site	inland	Coastal	All	inland	coastal	All
Standard Deviation	0.19	0.31	0.30	0.20	0.27	0.25
Bias	-0.05	0.24	0.11	-0.06	0.16	0.02
RMSE	0.20	0.39	0.32	0.21	0.32	0.25
Sample Size	16	21	37	13	7	20

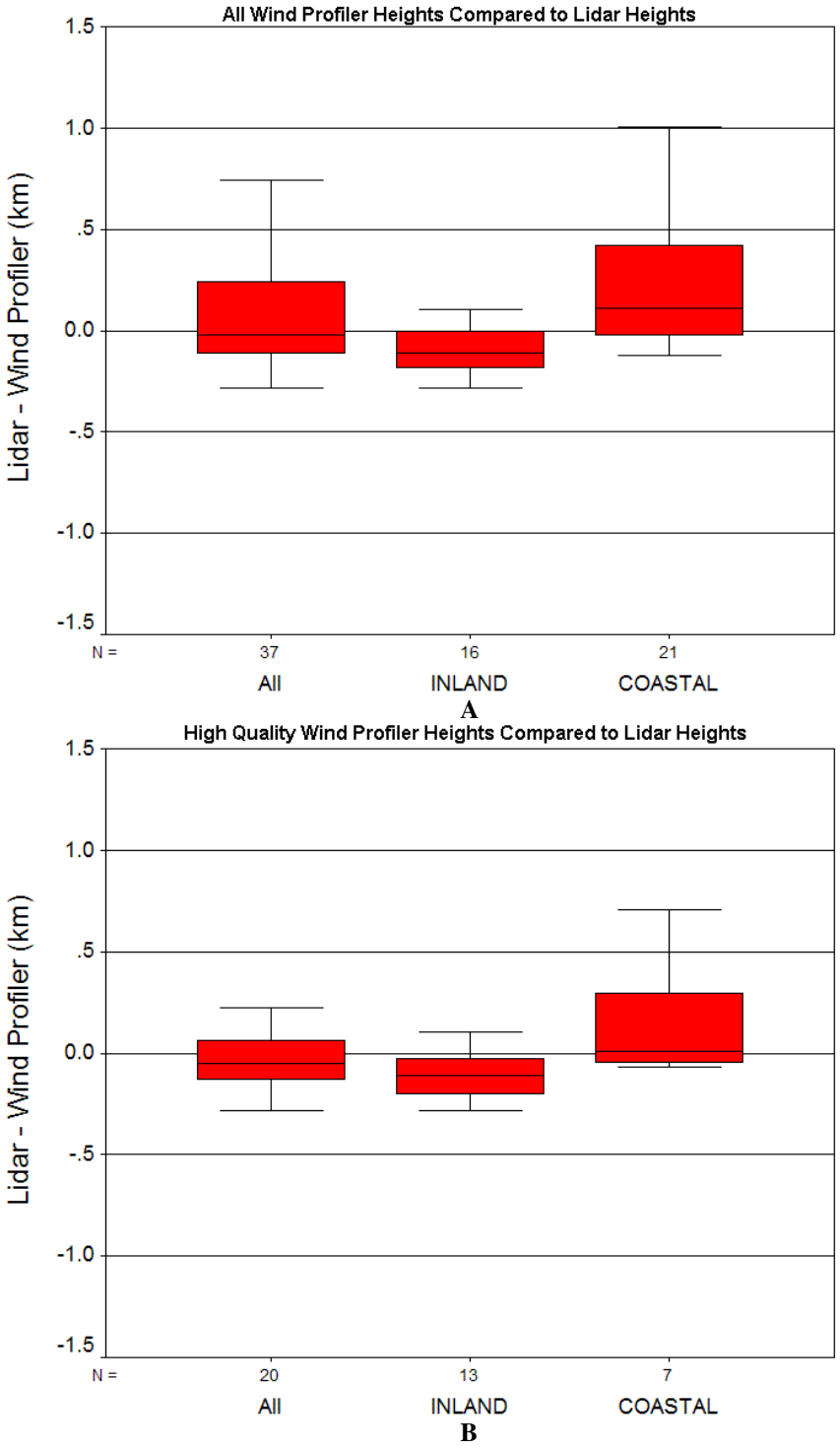

Fig.11: Box and Whiskers plots of the comparisons between the lidar ML heights and the wind profiler ML heights separated by the different quality flag of the wind profiler.
A: All wind profiler heights compared to lidar heights. B: High quality wind profiler height compared to lidar heights. N represents number of heights available for the comparisons and the solid black lines represent the median.

The standard deviation and RMSE values found for the comparison between the wind profiler and lidar were comparable to the values found for the comparison between the wind profiler and the benchmark method. For all the sites combined, the overall standard deviation values were slightly better for the comparison when all the wind profiler heights were used than the comparison when only the high quality heights were used from the wind profilers. Evaluating the individual sites, the standard deviation and RMSE values were higher for the coastal sites.

There was relatively small negative bias found between lidar and the wind profilers for the inland sites and much larger positive bias found between the lidar and wind profilers for the coastal sites. At the coastal sites, the lidar measured higher heights than the wind profiler by more than 200m for the comparison of all the heights, and 160m for the comparison of the high quality wind profiler heights.

The comparisons between the wind profilers and the lidar were fairly consistent over a range of heights (represented in Figure 12), showing a good agreement between these two instruments. However, there were some outliers for lidar-estimated mixing layers approximately 1km and above. In these cases the ML heights estimated using the lidar data were much higher than the ML heights estimated using the wind profiler data by as much as 1km. For mixing layers approximately between 1km and 1.50km, the ML heights estimated by both instruments were within a few meters of each other with a slight bias towards the wind profilers estimating higher heights.

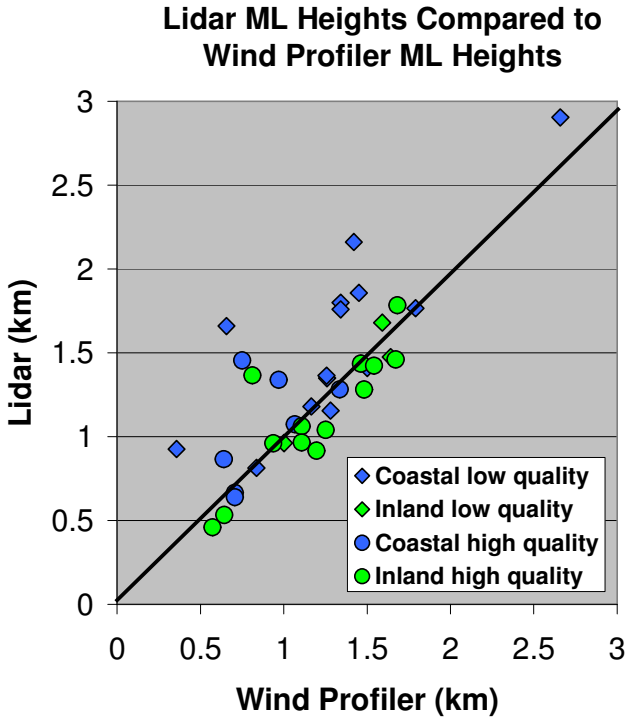

Fig. 12: Scatter plot of wind profiler and lidar ML heights.

The t statistic determined for the combined high quality flag inland and coastal wind profiler comparison was 0.337 with a p-value of 0.740. The t statistic for the high quality flag inland comparison was -0.996 with a p-value of 0.339, and the t statistic for the high quality coastal comparison was 1.502 with a p-value of 0.184. For all the comparisons, the t statistic was between -1.96 and 1.96 and the p-value was greater than 0.00. Therefore, the null hypothesis was not rejected and the ML height estimated by both instruments was determined as not significantly different.

4. DISCUSSION

Overall, the ML heights measured by the wind profilers were in good agreement with the ML heights measured by the airborne lidar. The results between the wind

profiler and the lidar were comparable to the results between the radiosonde and wind profiler, illustrating that error might be associated with the benchmark method in regards to turbulence in which the lidar can average over.

The greatest standard deviation and RMSE values were found at the coastal site, which confirms that separating the inland and coastal sites was worthwhile. The high values for the coastal sites was due to the varying flight tracks and whether the lidar was on the side of the wind profiler sites closer to the ocean or farther inland. When the lidar had a flight track that was farther inland from the wind profiler, or went from farther inland to closer to the coast or vise versa, the estimated ML heights from the lidar data were much higher and more variable than the wind profiler heights. This was because wind profiler data reflected the influence of the marine air and caused resulting estimated ML heights to be much lower than the lidar heights. For all the sites combined, there was less error and a lower bias when only the unambiguous wind profiler heights were used for the comparisons. This bias was mainly influenced by the coastal sites.

The lidar and the wind profilers were practically unbiased with respect to each other for the inland sites. However, the bias for the coastal sites was much higher; this can be blamed on both instruments measuring a low aerosol count or the variable boundary layer found near the coast. For the inland sites, the statistics were mostly independent of the wind profiler quality. This supports the wind profiler and benchmark results that there is equal confidence in the wind profiler performance when the ML heights measured were clear as opposed to unclear.

The comparisons between the wind profilers and the airborne lidar were consistent over a range of heights with some outliers where the lidar measured much higher heights than the wind profilers. This may have been caused by the lidar measuring a high backscatter signal received from cloud tops which is often mistaken as the top of the ML. Also, the errors may have resulted from an internal boundary layer being present and the lidar measuring the top of the residual layer as opposed to the current surface mixed layer. Aside from these errors, the ML height measured by both instruments was within a few meters of each other with a slight bias towards higher ML heights estimated from the wind profiler data. Higher wind profiler estimates may have been caused by weak turbulence or a lack of aerosols in the atmosphere resulting in lower estimates from the lidar data.

d. Airborne MTP

1. BACKGROUND

The MTP is a passive scanning instrument placed on an aircraft to measure the thermal emissions and absorption from oxygen molecules in the atmosphere at various elevation angles and frequencies both above and below the aircraft (Denning et al. 1989). The signals detected from the oxygen molecules are converted to a vertical temperature profile by data analysis and a retrieval technique (Mahoney 2002). In simple form, the retrieval technique statistically relates the observed signals to a reference temperature profile that was determined by actual data from radiosonde measurements (Mahoney 2002).

The MTP system was placed on the NCAR Electra aircraft during the Texas 2000 Air Quality Study to make vertical profiles of temperature along a flight track from which the ML height was deduced as a function of space and time. The retrieval techniques used to determine the temperature profiles were modified to include variable nature of the PBL throughout the day and low-level inversions such as the sea breeze inversions (Mahoney 2002). By modifying the retrieval techniques, the MTP was considered equally proficient over land and water.

As with other instruments, an objective or subjective technique is needed for relating the temperature profile to ML heights. Even though the MTP is capable of providing ML estimates for a range of topography, difficulties can occur when using this instrument. In particular, problems can occur when trying to identify the top of the ML in temperature profiles using the normal techniques based on changes in stratification of the atmosphere, because the retrieval temperatures obtained by the MTP have relatively coarse vertical resolution.

2. METHOD

Comparisons were made between the ML heights inferred by the airborne MTP and measured by the five wind profilers. The MTP raw data was supplied by MJ Mahoney. This was the first time the MTP was used for estimating ML heights. The same manipulations applied to the lidar data were also applied to the MTP to compensate for the fact the MTP measured in both space and time and the wind profiler was fixed in space but measured in time. Also, as with the lidar and wind profiler comparison, the wind profiler sites farther inland (HSW, WH, and LB) were combined

into one group (inland sites) and the wind profiler sites near Galveston Bay (LM and EL) were combined into a separate group (coastal sites).

Candidate methods for estimating the ML heights from MTP data were developed by Dr. John Nielsen-Gammon. Preprocessors interpolate the raw potential temperatures to 100m surfaces and perform a (9-point) smoother on the constant altitude data. A separate program uses these potential temperature values and computes the ML heights by 30 algorithms. Algorithms 1-24 find the ML heights by determining the adjoining lapse rate (the lapse rate between the current level and the next level above) and the minimum lapse rate (the smallest lapse rate between the current level and any level above) and comparing these two lapse rates to criteria based on arbitrary lapse rates and different fractions of the ambient lapse rate. The ambient lapse rate in this case is found between the 2000m and the 3500m levels. The vertical resolution of the ML heights was approximately 50m.

Algorithms 1-6 are based on criteria that determine the point in the atmosphere where the *adjoining* lapse rate is greater than a potential temperature increase of 1.50°/km, 1.75°/km, 2.00°/km, 2.25°/km, 2.50°/km, and 3.00°/km. Algorithms 7-12 are slightly different in that they are based on criteria that determine the point where the *minimum* lapse rate is larger than a potential temperature increase of 1.50°/km, 1.75°/km, 2.00°/km, 2.25°/km, 2.50°/km, and 3.00°/km. Algorithms 13-18 are based on criteria that determines the point where the *adjoining* lapse rate is 0.2, 0.3, 0.4, 0.5, and 0.6 the fraction of the ambient lapse rate and algorithms 19-24 are based on criteria that determines the point where the *minimum* lapse rate is 0.2, 0.3, 0.4, 0.5, and 0.6 the

fraction of the ambient lapse rate. These methods are analogous to the T Base and T Lapse Rate Methods for soundings described in the Radiosonde section.

Algorithms 25-30 determined the ML heights by finding the level of the minimum temperature and evaluating upwards from this level to determine where the difference in temperature is greater than a surplus temperature criterion. These algorithms are based on criteria that determine the height where the potential temperature is 1.00°, 1.25°, 1.50°, 1.75°, 2.00°, and 2.25° warmer than the minimum temperature. This method is analogous to the method described in Marsik et al. (1995) and the θ Increase Method described in the Radiosonde section.

The results of the comparisons between the MTP and the wind profiles were found by statistical analysis performed on the differences between the heights determined by these two instruments in the form of bias, standard deviation, and RMSE. This was done for a variety of situations including comparisons of all the heights from both instruments regardless of the quality flag and comparisons focusing on the separate quality flags.

The statistics for the high quality flag wind profiler comparisons were then evaluated to determine their significance for application in other situations. This was done using a two-tailed, one-sample t test performed on the difference in heights between the wind profilers and the MTP at a significance level of 0.05. The null hypothesis was a statement that the two instruments determined the ML to be at the same height so that the bias was equal to zero. The alternate hypothesis was a statement that the two instruments determined the ML to be at different heights so that the bias was

nonzero. The corresponding p-value was also calculated to determine the probability of rejecting the null hypothesis when it was actually true. For a significance level of 0.05, the null hypothesis was not rejected when the calculated t statistical value was between -1.96 and 1.96 ($-1.96 \leq t \leq 1.96$) and the p-value was greater than 0.05. A p-value close to 1.00 represented high confidence in the null hypothesis while a p-value close to 0.00 represented low confidence in the null hypothesis.

3. RESULTS

The standard deviations found between the ML heights computed by the separate MTP algorithms and the wind profiler ML heights are displayed in Figure 13. This figure shows the comparisons for all the sites combined, which was found by taking the difference in heights so that the wind profiler heights were subtracted from the MTP algorithm heights. Overall, the MTP data was in reasonably good agreement with the wind profilers, with only a few algorithms having standard deviation values greater than 500m. These were algorithms 4, 5, 6, 11, 12, and 24. For the all the sites combined, the standard deviation was lower when only the high quality heights were used from the wind profilers. This was true for all of the comparisons except for those with algorithms 11, 12, and 24.

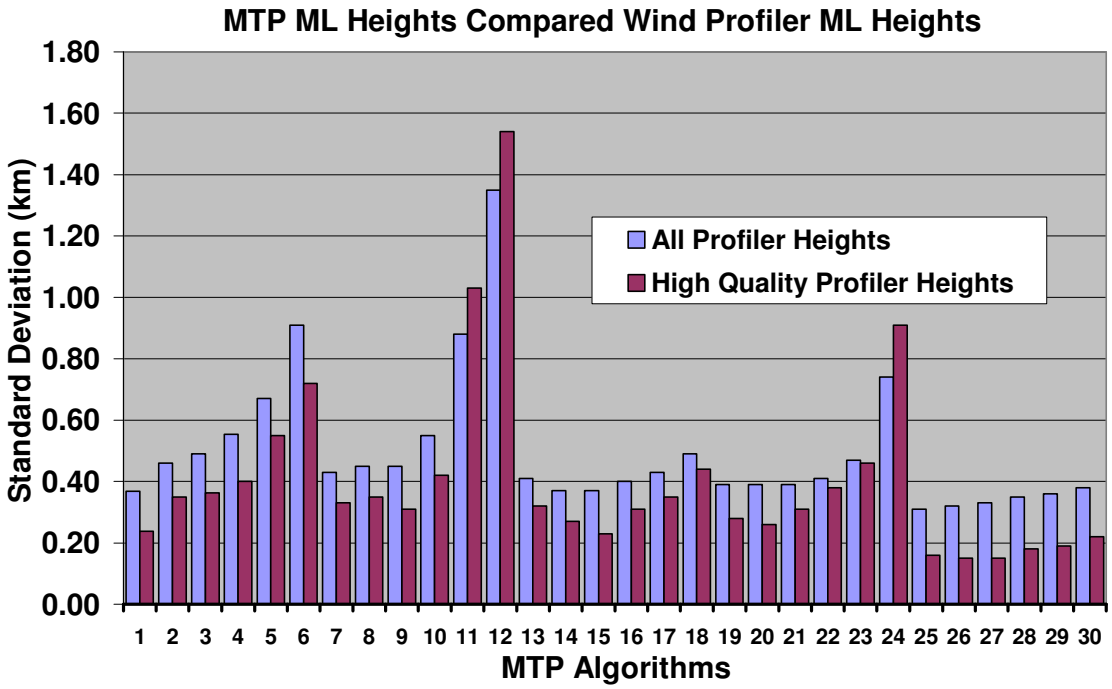

Fig. 13: Standard Deviation between the MTP algorithm ML heights and wind profiler ML heights for all the sites combined.

Algorithms 25-30 had the lowest standard deviations values. Because the results were nearly equivalent in terms of bias and standard deviation between algorithms 25-30, algorithm 27 was chosen arbitrarily for a more detailed evaluation of these comparisons. Algorithm 27 determines the ML heights by finding the level of the minimum potential temperature and evaluating upwards from this level to determine where the difference in potential temperature is greater than 1.50° (the surplus temperature criteria). The bias, standard deviation, and RMSE between algorithm 27 and the wind profilers are found in Table 6 and Figure 14. The table is broken down into sections to show the comparisons of all the heights from both instruments and only the high quality profiler heights.

Table 6: Comparison of the difference in ML height estimates between the wind profilers and MTP algorithm 27.

	All Heights			All MTP Heights and High Quality Profiler Heights		
Site	Inland	coastal	All	Inland	Coastal	All
Standard Deviation	0.31	0.34	0.33	0.10	0.17	0.15
Bias	0.10	0.10	0.10	-0.07	-0.07	-0.07
RMSE	0.33	0.35	0.35	0.12	0.19	0.17
Sample Size	12	19	31	6	11	17

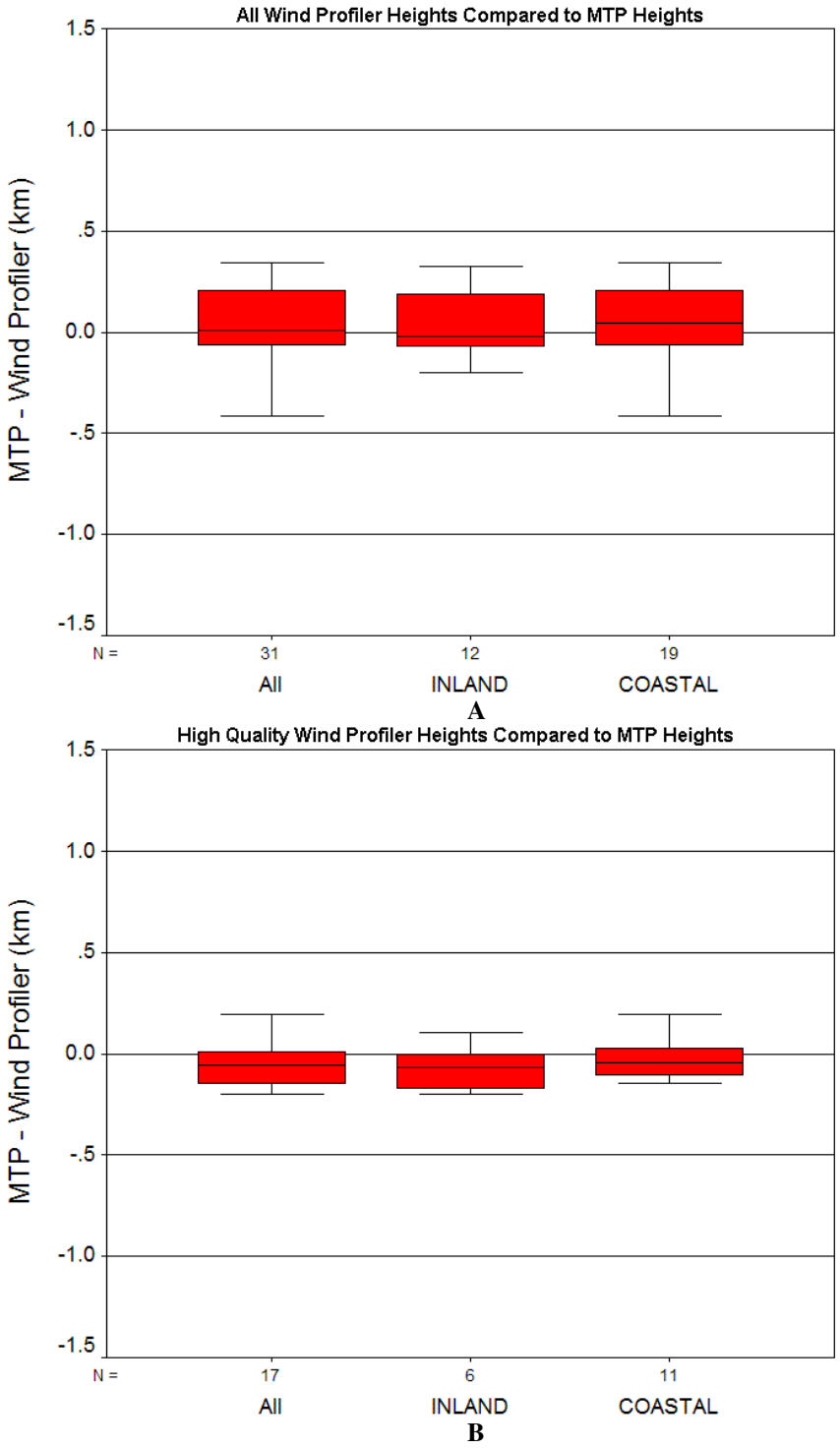

Fig. 14: Box and Whiskers plots of the comparisons between the MTP algorithm 27 ML heights and the wind profiler ML heights separated by the different quality flag of the wind profiler.
A: All wind profiler heights compared to MTP heights, B: High quality wind profiler height compared to the MTP heights. N represents number of heights available for the comparisons and the solid black lines represent the median.

The standard deviation and RMSE were comparable to the results found from comparisons between the wind profilers and airborne lidar, and the wind profilers and benchmark method. Although the standard deviation values were slightly better for the inland wind profiler sites, overall, there was not a considerable separation between the statistics found for the inland as opposed to the coastal sites. There was a separation between the cases when all the heights were used and when only the high quality wind profile heights were used. Here, the standard deviation values were much less for the comparison using only high quality wind profiler heights.

The comparison between algorithm 27 and the wind profilers had equal bias for the inland and coastal wind profiler sites for both the comparison of all heights and the comparison of the high quality wind profiler heights. However, the bias was positive for the comparison of all the heights and was negative for the comparison of only the high quality wind profiler heights.

The comparisons between the wind profilers and the MTP algorithm 27 were consistent over a range of heights (represented in Figure 15). This showed a good agreement between these two instruments. However, there were some outliers primarily for mixing layers above 2km. In these cases, algorithm 27 measured much higher heights than the wind profilers by as much as 1km. Most of these outliers were on 8/30/00 after 2100 UTC. Removing the ML heights estimated on 8/30/00 after 2100 UTC lowers the bias and standard deviation for both the inland and coastal sites. These values are displayed in Table 7. For mixing layers around 1km and below, the ML height measured by both instruments was within a few meters of each other. There was

a larger spread between the ML heights for mixing layers between 1km and 2km with the bias consistent towards both instruments.

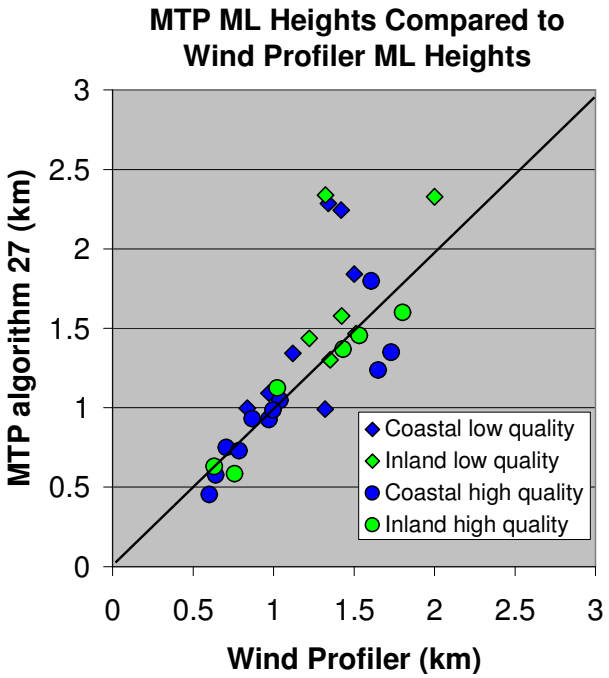

Fig. 15: Scatter plot of wind profiler and MTP algorithm 27 ML heights.

Table 7: Comparison of the difference in ML height estimates between the wind profilers and MTP algorithm 27 without estimates from 8/30/00 after 2100 UTC.

	All Heights			All MTP Heights and High Quality Profiler Heights		
Site	inland	coastal	All	inland	Coastal	All
Standard Deviation	0.13	0.21	0.18	0.10	0.17	0.15
Bias	-0.01	-0.02	-0.02	-0.07	-0.07	-0.07
RMSE	0.13	0.21	0.18	0.12	0.19	0.17
Sample Size	10	16	26	6	11	17

The t statistic determined for the combined high quality flag inland and coastal wind profiler comparison was -1.885 with a p-value of 0.780. The t statistic for the high quality flag inland comparison was -0.504 with a p-value of 0.193, and the t statistic for the high quality flag coastal comparison was -1.338 with a p-value of 0.211. For all the comparisons, the t statistic was between -1.96 and 1.96 and the p-value was greater than 0.00. Therefore, the null hypothesis was not rejected and the ML height estimated by both instruments was determined as not significantly different.

4. DISCUSSION

The ML heights determined from the MTP data by the 30 algorithms were comparable to the ML heights measured by the wind profilers. The only case when the standard deviation was greater than 500m was when the ML height was determined from the MTP data by comparing the adjoining lapse rate (the lapse rate between the current level and the next level above) and the minimum lapse rate (the smallest lapse rate between the current level and any level above) to criteria based on arbitrary lapse rates and different fractions of the ambient lapse rate. There was a better agreement when only the unambiguous wind profiler heights were used, except for the comparison with three of the MTP algorithms. These three algorithms were three of the algorithms that had standard deviations greater than 500m, and can be considered unreliable to determine the ML heights. The smallest errors were found using algorithms 25-30, in which the ML height was found by locating the level of the minimum temperature and evaluating upwards from this level to determine where the difference in temperature was greater than surplus temperature criteria.

Using algorithm 27, the bias was the same at the inland and coastal sites for both the comparison when all the wind profiler heights were used and when only the high quality wind profiler heights were used. This shows that the modified retrieval algorithms were successful in producing equally proficient temperature profiles over both land and near the water. As with the lidar comparison, the standard deviation values were slightly larger for the coastal sites than for the wind profiler sites. The cause of this bias can be blamed on the variable nature of the PBL found near the coast and the differences in techniques of both instruments for analyzing the PBL.

The bias changed significantly depending on the quality flag of the wind profilers. The bias was positive for the comparisons using all the wind profiler heights, showing that the wind profiler measured lower heights than algorithm 27 and the bias was negative for the comparison using only the unambiguous wind profiler heights; meaning, in this case, the wind profiler heights measured higher heights than algorithm 27. This is different from the results between the other instruments in that the comparisons were usually independent of the quality flag of the wind profilers. This can be attributed to the three cases when the MTP heights were higher than the wind profiler heights by almost 1km when the wind profiler heights were low quality (Figure 15).

The low quality wind profiler heights were all estimated on August 30th after 2100 UTC. At this time in the afternoon, there is usually a decrease in the heating at surface by solar radiation, which might have caused turbulence to weaken while the temperature profile remained constant. In this case, the wind profilers may have measured the weaker turbulence resulting in lower estimated ML heights. There were

no other days when the comparisons were made after 21 UCT which makes it is difficult to determine if the time of the day was the reason for the lower wind profiler heights. Eliminating these points from the dataset (Table 7) provides more consistent results with the other comparisons in that wind profiler heights can be trusted regardless of the ambiguity of the wind profiler data.

The comparisons between the wind profilers and the MTP algorithm 27 were consistent over a range of heights, which showed good agreement between these two instruments. For deeper mixing layers, there were a few cases where algorithm 27 measured much higher heights than the wind profilers. This may have been caused by the relatively coarse vertical resolution of the retrieval temperatures obtained by the MTP. The ML height could have been determined at a higher height because of the changes in the temperature stratification of the atmosphere. Otherwise, the bias was consistent towards both instruments. At times, there was a fairly large spread between the ML heights measured by algorithm 27 and the wind profilers; this can be attributed to the different methods used for determining the ML heights by the separate instruments. The different methods that are based on different atmospheric phenomena did not allow the depth of the ML to be determined at the same height.

e. In-situ Aircraft Data

1. BACKGROUND

In-situ instruments on aircraft often make measurements of temperature, humidity, wind speed, wind direction, and concentrations of various species. These

measurements can illustrate the PBL structure. Deducing vertical profiles of temperature and dewpoint from flight patterns can reveal the inversion base and lead to the determination of the ML height. The ML height determined from these profiles is related to a particular position and time which is similar to measurements made by radiosondes. Because these measurements are not spatially and temporally averaged, ML height estimates made by in-site aircraft data may be misleading in that they are unrepresentative of the entire PBL (Kaimal et al. 1982).

There has been past research where in-situ measurements were used to estimate the ML height for comparisons with ML height estimates from other instruments. Generally, the results of the comparisons between the different estimates were in good agreement with each other (Martin et al. 1988; Russell and Uthe 1978; Olsson et al. 1974) with the same errors that result with use of radiosondes.

Martin et al. (1988) studied the ML over the rain forest of central Amazonia by comparing measurements made by tethered balloon, rawinsonde and aircraft. The frequency and vertical height resolution of the tethered balloon and rawinsonde measurements used together provided the best local measurement of the depth of the ML. The ML growth pattern determined by aircraft was very similar to the mean ML heights determined by the tethered balloon and rawinsonde measurements at a fixed point.

Russell and Uthe (1978) compared sodar-inferred ML depth to those inferred from simultaneous measurements of temperature and humidity profiles from aircraft for the San Francisco Bay area. The overall agreement between the airplane and sodar mixing depths was reasonably good with little or no systematic differences evident.

However, there was large scatter in the data set in certain cases, mostly caused by uncertainty in airplane-inferred mixing depths. When the comparison consisted of heights obtained mainly in the late afternoon, evening, and nighttime hours, the temperature and humidity profiles were quite ambiguous to interpret in terms of ML depth. Therefore, the direct profile measurements made at these times were not remarkably better than the sodar measurements for determining ML height. During daytime in the Bay area, both sodar measurements and temperature profiles were easier to interpret. The daytime comparisons were less ambiguous with good agreement between sodar and temperature-inferred mixing depths.

2. METHOD

Comparisons were made between the ML heights inferred from the MTP data using algorithm 27 and ML heights determined by in-situ Electra aircraft data using temperature and dewpoint profiles. The MTP was located aboard the Electra so that the purpose of these comparisons was to check the accuracy of using the MTP data for estimating ML heights. Algorithm 27 determines the ML heights by finding the level of the minimum temperature and evaluating upwards from this level to determine where the difference in temperature is greater than 1.50° (the surplus temperature criteria). The aircraft data was collected using the Electra during selected days of the Texas 2000 Air Quality Study and evaluated to exclude the times when the Electra was over Galveston Bay and the Gulf of Mexico.

Since both the MTP and the Electra made measurements as a function of space and time, the data collected from the Electra was manipulated to be easily compared

with the ML heights calculated by algorithm 27. This was accomplished by first finding the times when the Electra was ascending or descending. During each appropriate ascent or descent, the ML height was determined by the benchmark method (the combination of the mid-point of the moisture transition layer with the base of the temperature inversion with the mid-point of the moisture transition layer taken as the preferred height) which was also used for the radiosonde comparisons.

The ML height determined from the Electra data was related to a particular position and time and compared to the closest algorithm 27 ML height by three different stipulations. First, the time of the Electra heights was compared to the closest time of the MTP heights, regardless of the distance between them. Second, the time of the Electra heights were compared to the closest time of the MTP heights for a distance less than 16.38km (the distance between the closest to wind profilers) between the two estimates. Third, the time of the Electra heights was compared to the closest time of the MTP heights for a distance less than 10km (the optimal radius between the MTP and profilers) between the two estimates. In past research, ambiguous temperature and dewpoint profiles caused uncertainty in the airplane-inferred mixing depths (Russell and Uthe 1978). Because of this (and to determine the outcome of the separate components of the benchmark method) the comparisons were also performed using ML heights determined from the Electra data using only the base of the inversion layer (T Base Method) in the temperature profile, and using only the mid point of the transition layer (q Mid Method) in the dewpoint profile.

The results of the comparisons between the Electra and the MTP algorithm 27 were found by statistical analysis performed on the differences between the heights determined by these two instruments in the form of bias, standard deviation, and RMSE. This was done for a variety of situations, including comparisons of all the heights from both instruments regardless of the quality flag and comparisons focusing on the separate quality flags.

The statistics were then evaluated to determine their significance for application in other situations. This was done using a two-tailed, one-sample t test performed on the difference in heights between the Electra data and the MTP at a significance level of 0.05. The null hypothesis was a statement that the two instruments determined the ML to be at the same height so that the bias was equal to zero. The alternate hypothesis was a statement that the two instruments determined the ML to be at different heights so that the bias was nonzero. The corresponding p-value was also calculated to determine the probability of rejecting the null hypothesis when it was actually true. For a significance level of 0.05, the null hypothesis was not rejected when the calculated t statistical value was between -1.96 and 1.96 ($-1.96 \leq t \leq 1.96$) and the p-value was greater than 0.05. A p-value close to 1.00 represented high confidence in the null hypothesis while a p-value close to 0.00 represented low confidence in the null hypothesis.

3. RESULTS

The comparison between the ML heights inferred from the airborne MTP using algorithm 27 and ML heights determined by in-situ aircraft data using temperature and dewpoint profiles is displayed in Table 8a, Table 8b, and Figure 16. The bias, standard

deviation, and RMSE were found by taking the difference in heights so that the Electra heights were subtracted from the algorithm 27 heights. The table is broken down into sections to show the comparisons of the varying distances between the estimates and the comparisons of the separate components of the benchmark method.

There were small standard deviation and RMSE values found between algorithm 27 and the Electra. Overall, these results were smallest out of all the comparisons between the separate instruments. These standard deviation and RMSE values decreased with decreasing distance between the two instruments. Also, the values were higher for the case using only the dewpoint component (q Mid Method). The results found between algorithm 27 and the ML heights inferred using the benchmark method from the Electra data were very similar, if not the same, as the results found using only the temperature component (T Base Method) of the benchmark method.

There was relatively small positive bias between the two estimates for all the distances. The bias was almost double when the q Mid Method was used to find the ML heights from the Electra data, as opposed to when the T Base Method and the benchmark method were used for the comparison of all the distances and the distance of 16.38km. The T Base Method and the benchmark method had practically the same bias when compared to the algorithm 27.

Table 8a: Comparison of the difference in ML height estimates between the Electra and MTP algorithm 27for all distances between instruments.

	All Distances		
Site	Benchmark Method	T Base Method	q Mid Method
Standard Deviation	0.23	0.26	0.34
Bias	0. 04	0.03	0.12
RMSE	0.23	0.26	0.36
Sample Size	25	25	25

Table 8b: Comparison of the difference in ML height estimates between the Electra and MTP algorithm 27 for distances of 16.38km and 10km between instruments.

	Distances within 16.38km			Distances within 10.0km		
Site	Benchmark Method	T Base Method	q Mid Method	Benchmark Method	T Base Method	q Mid Method
Standard Deviation	0.16	0.16	0.25	0.13	0.13	0.25
Bias	0.01	0.02	0.10	0.06	0.06	0.17
RMSE	0.16	0.16	0.27	0.14	0.14	0.30
Sample Size	14	13	14	7	7	7

The comparisons between the in-situ Electra data and algorithm 27 were consistent over a range of heights (represented in Figure 16). This showed a good agreement between these two instruments. The ML height measured by both instruments was for the most part within a few meters of each other with bias consistent for both instruments. For mixing layers above 1.5km, there was the largest spread with ML determined by each instrument still within 500m of each other.

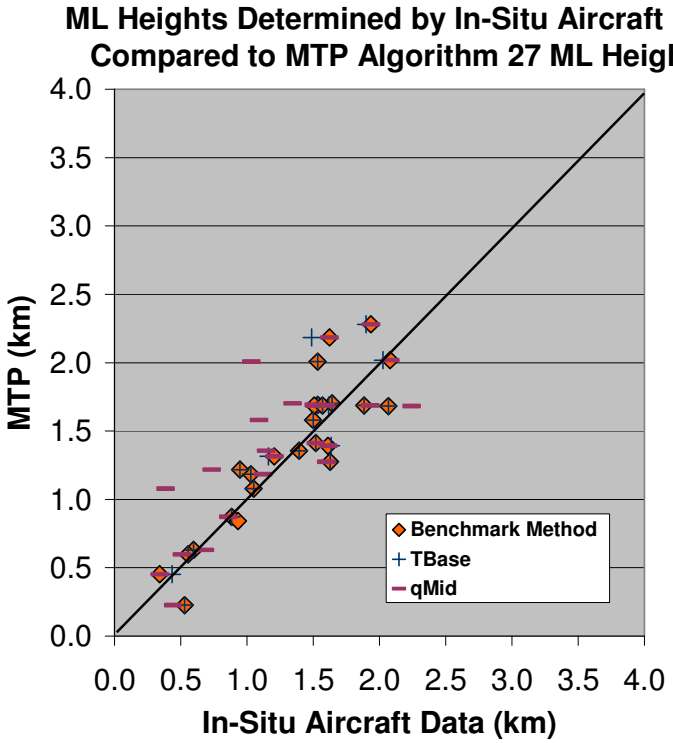

Fig. 16: Scatter plot of MTP algorithm 27 and Electra aircraft ML heights for all distances between estimates.

The t statistic determined for the comparison regardless the distance between the instruments was 0.829 with a p-value of 0.415. The t statistic for the comparison when the instruments were within 16km of each other was 0.268 with a p-value of 0.793, and the t statistic for the comparison when the instruments were within 10km of each other was 1.127 with a p-value of 0.303. For all the comparisons, the t statistic was between -1.96 and 1.96 and the p-value was greater than 0.00. Therefore, the null hypothesis was not rejected and the ML height estimated by both instruments was determined as not significantly different.

4. DISCUSSION

The statistics found for the Electra data were practically identical for the comparisons using the benchmark method as with using only the temperature component of the benchmark method. Larger errors occurred in the statistics for the comparison using only the moisture component of the benchmark method. A possible reason for this could have been an instrument error caused by the response time of the different instruments. However, the statistics were not sensitive to whether the aircraft was ascending or descending, and a difference in bias would have been evident if it was an instrument error. Another possibility is the fact the MTP measured the temperature structure. If the temperature structure from the Electra data clearly determined the ML height at a certain level and the moisture structure from the Electra data determined the ML height at another level, the MTP was more likely to better agree with the temperature structure.

The comparisons between algorithm 27 and the Electra data showed good agreement, which supports the argument for using multiple methods for ML height comparisons. Their comparisons were consistent over a range of heights, supporting the use for using MTP data to infer ML heights. The largest discrepancies occurred when the ML heights were estimated by the q Mid Method from the Electra data. This leads to problems when using the benchmark method to determine ML heights from aircraft data. In the future, an intercomparison of methods for using in-situ aircraft data would be useful.

f. Overall Comparisons

Overall, the ML heights estimated by the different instruments were in good agreement. Because the instruments were not exactly compared to each other, this agreement was based on the results compared with the wind profilers. For the high quality flag comparisons, the ML heights estimated by the different instruments were determined as not significantly different by the t test.

The good agreement between instruments was limited to co-located comparison, which was found through the wind profiler and radiosonde comparison. The fact that Houston is a major city located near the coast causes variations in the PBL structure and ML depth across a short distance. The good agreement may also be restricted to times when the evolution of the PBL was fairly static. During times when the ML was growing or decaying, there may have been discrepancies between the estimates inferred from the different instruments. This occurred in the MTP and wind profiler comparisons, which showed higher ML heights measured by the MTP on August 30th after 2100 UTC. There is still uncertainty as to the cause of this, because the discrepancy was only limited to one day and only in the MTP and lidar comparison.

Comparisons between the benchmark method and wind profilers were mostly independent of the quality flag of the wind profiler estimates. This means that a wind profiler estimated with a low quality flag can still be used with confidence. However, the benchmark method can not be used with confidence at all times. The discrepancies between the estimates increased with the lower quality flags. This shows that there might be error associated with the different aspects of the benchmark method. When

considering only high quality benchmark method heights, these heights were within 10m below the wind profiler heights. However, when considering all benchmark method heights, the separation increased to within 60m below the wind profiler heights.

Comparisons between the lidar and wind profilers depended on the location of the lidar in respect to the coast. For the inland sites, the comparisons were mostly independent of the quality of the wind profilers as in the benchmark comparison. When comparing airborne lidar to inland wind profilers, the lidar measured lower heights on average by 50 or 60m. When comparing lidar to coastal sites, there were more discrepancies which depended on whether the lidar was on the side of the wind profiler closer to the coast or farther inland. In these cases, the lidar measured higher heights than the wind profilers on average by 240m compared to all wind profiler heights, and higher heights on average by 160m compared only to high quality wind profiler heights.

Comparisons between the MTP and wind profiler were less dependant on the topography and more dependant on the quality flag of the wind profiler. However, when the outliers that caused this dependence were excluded, the comparisons were similar to the other instruments. In this case, the MTP measured lower heights on average by 10m for the inland sites and 20m for the coastal sites. When compared to the high quality wind profiler heights, the MTP measured lower heights on average by 70m at both inland and coastal sites.

Combining the inland and coastal sites compared to high quality wind profiler heights, the lidar measured higher heights on average by 20m and the MTP measured lower heights on average by 70m. Combining the inland and coastal sites compared to

all the wind profiler heights, the lidar measured higher heights on average by 110m and the MTP measured lower heights on average by 20m. Overall, the lidar measured the highest heights and the MTP measured the lowest heights.

Using the bias and standard deviation values found by comparing the different instruments, the relationship between the true ML height and the ML heights determined by the individual instruments was found for the high quality inland ML height estimates. The true ML height was defined as the depth that a passive tracer was mixed which corresponded to the midpoint of the moisture transition layer. This allowed for the inland high quality benchmark method ML heights to be considered unbiased. Using this information, and adding the bias found by the comparison with the inland high quality wind profiler heights, the bias found between the wind profiler heights and the true ML heights was negative 20m. Similarly, the bias found between the lidar heights and the true ML heights was negative 70m and the bias found between the MTP heights and the true ML heights was negative 80m. Using the bias found between the true ML heights and the MTP heights, the bias found between the in-situ data (for all the ML heights compared when the instruments were within a distance of 10km of each other) and the true ML heights was negative 20m.

Estimates of the upper and lower bounds on the total standard deviation due to random process as opposed to systematic biases were found for each instrument using the available data. The estimates were based on the agreement between the instruments and the assumption that the source of errors associated with each instrument was independent of one another. Starting with the inland high quality comparison between

the MTP heights and the wind profiler heights, the standard deviation found between the true ML heights and the MTP heights was less than or equal to 100m. Likewise, the standard deviation found between the true ML heights and the wind profiler heights was less than or equal to 100m as well. Using this information, the standard deviation found between the true ML heights and the lidar heights was in the range of 0 to 100m, and the standard deviation found between the benchmark method heights and the true ML heights was in the range of 0 to 140m.

CHAPTER V

ML HEIGHT DISTRIBUTION – SEPTEMBER 1, 2000

a. Method

The second objective of this paper was to determine as completely as possible the horizontal distribution of mixing depths as a function of space and time on September 1, 2000 of the Texas 2000 Air Quality Study. This builds on the work of Christoph Senff and collaborators which involves the use of airborne lidar, wind profiler, and radiosondes to determine the spatial and temporal variation of the ML height in Houston during the ozone episode of the Texas 2000 Air Quality Study. For this paper, the available ML height data from the radiosonde systems, wind profilers, airborne lidar, airborne MTP, and in-situ aircraft data were analyzed both spatially and temporally. The results from the intercomparison part of this paper were used to account for the bias between instruments along with both space and time interpolations between height measurements so that the horizontal ML height distribution could be plotted and described as accurately as possible. September 1, 2000 was chosen for this analysis because there were measurements available from all the instruments, and the ML height evolution was fairly straightforward.

The ML height analysis is from 1600 UTC to 2100 UTC. From 1600UTC to 1900UTC, the wind was mainly from the west at 10knots across most of Houston and shifted slightly to the southwest around 1900 UTC. At 2000 UTC, locations near the coast, including the LM wind profiler site, experienced a southerly wind at 10knots and as high as 30knots right along the coast.

Throughout most of the day, there was an increase in temperature with values slightly warmer to the north of Houston. At 1600 UTC the temperature ranged from 32°C close to Galveston Bay and near the HSW, EL, and LM wind profiler sites to 36°C north of the Houston and near the WH and LB sites. By 1800 UTC, the temperature had increased with values of 38°C and above far north of Houston and 33°C close to Galveston Bay. By 1900 UTC, the temperature values around downtown Houston were mostly near 38°C which included the HSW site. The temperature around the WH site was above 38°C and near the EL and LB sites, the temperature readings were just below 38°C. At the LM site, the temperature was close to 35°C. By 2000 UTC, the temperature had increased to above 38°C around all of the Houston area except south of the city near the coast where there was a southerly wind. At the WH, LB, EL, and HSW sites, the temperature values were a few degrees above 38°C. Farther north of the city, closer to the WH site, the temperature was warmer with values as much as 42°C. By 2100 UTC, there was a slight increase in temperature around Houston downtown. At the individual sites, the temperature change was variable. At most, there was only an increase of a degree. Near the WH, HSW, and LM sites the temperature decreased one degree.

A general sense of how the ML varied throughout the day was needed in order to determine the ML distribution across the Houston area as a function of space and time. As a starting point, the high quality wind profiler estimates were used to determine the hourly variation of the ML heights. The wind profiler estimates were used because the wind profiler was the only instrument compared directly to the other instruments, and

the wind profiler estimates were available at half hour intervals which made them more abundant than the radiosonde estimates. Only the high quality estimates were chosen because of the results from the intercomparison section of this paper. Using the t test statistics, the high quality ML height estimates determined by the separate instruments were determined as not significantly different. Also, for the coastal comparisons, both the bias and standard deviation values were less when the high quality wind profiler estimates were compared to the lidar and MTP estimates. The lower quality estimates caused more outliers in the comparisons which were unrepresentative of the dataset as a whole. By using only the high quality wind profiler heights, these outliers were eliminated and a more confident hourly distribution of the ML height evolution was established.

The ML estimates at each wind profiler location were plotted as a function of time to establish the hourly variation which is displayed in Figure 17. The ML height evolution inferred by the wind profilers was similar for the separate sites. In general, the ML height increased until about 1530 UTC or 1630 UTC depending on the individual sites, leveled off until about 1630 UTC or 1730 UTC, and then rapidly increased again. There were slight variations in the exact progression of the ML height for the separate wind profilers mainly around the time when the ML height leveled off.

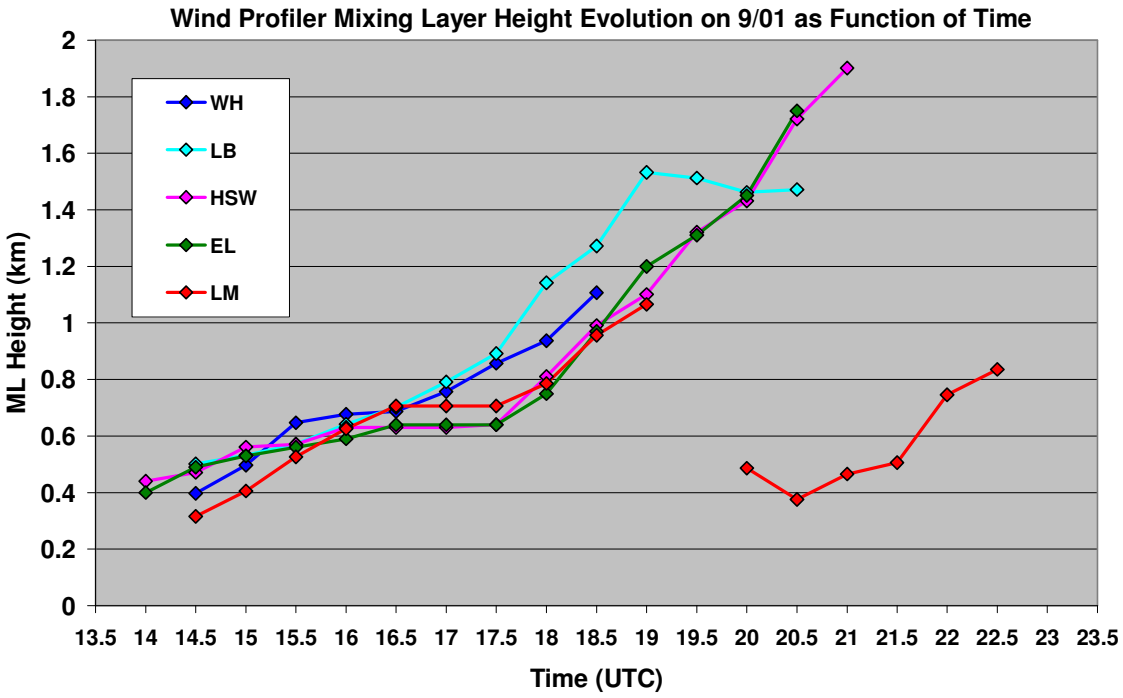

Fig. 17: Evolution of ML heights as a function of time on 9/01/00 inferred by wind profilers at the Wharton (WH), Liberty (LB), Houston Southwest (HSW), Ellington (EL), and LaMarque (LM) sites.

The ML at the WH site was the first to reach the point where the ML leveled off. This was at 1530 UTC and the ML was just below 700m. There was gradual growth to 700m at 1700 UTC from which the ML grew rapidly. At the LB site, there was a steady increase to about 800m at 1730 UTC followed by a rapid increase. The ML evolution at the HSW, EL, and LM sites was all similar in that the ML height grew rapidly after 1730 UTC. The differences between these sites were in the time period where the ML leveled off. The ML at the HSW site reached just over 600m, the height where the ML leveled off, at 1600 UTC which was a half hour earlier than the EL and LM sites. The ML at the EL site and LM site both leveled off at 1630 UTC however, the ML at the LM site was approximately 100m deeper than it was at EL and LM sites.

The reason the ML height did not grow between 1630 UTC and 1730 UTC, depending on the individual sites, was the result of a temperature inversion. Figure 18 is a Skew-T from WH data at 1100UTC showing that a nearly neutral layer was present above the inversion. The temperatures aloft remained constant and the ML did not grow until the surface temperature reached approximately 36°C and the ML reached close to 700m. After the ML reached approximately 700m and broke through the inversion, there was rapid growth as more heat was added to surface from solar energy. The location of the wind profiler sites determined when the ML broke through the inversion. The ML at the more northerly sites (WH and LB) reached 800m before the ML at the sites farther south (EL, LM, and HSW), which corresponds to the warmer surface temperatures in the northern locations. An inversion was barely evident in the LB heights where the surface temperatures were the warmest.

After the ML broke through the inversion, large deviations were found at the LB and LM sites. At the LB site, the ML rapidly increased until between 1830 and 1900 UTC where there was a leveling off followed by slight decrease. At the LM site, the ML height increased until 1900 UTC at which there was missing data. The next data point had the ML height much lower. The reason for these discrepancies could not be determined without knowledge of the spatial evolution of the ML.

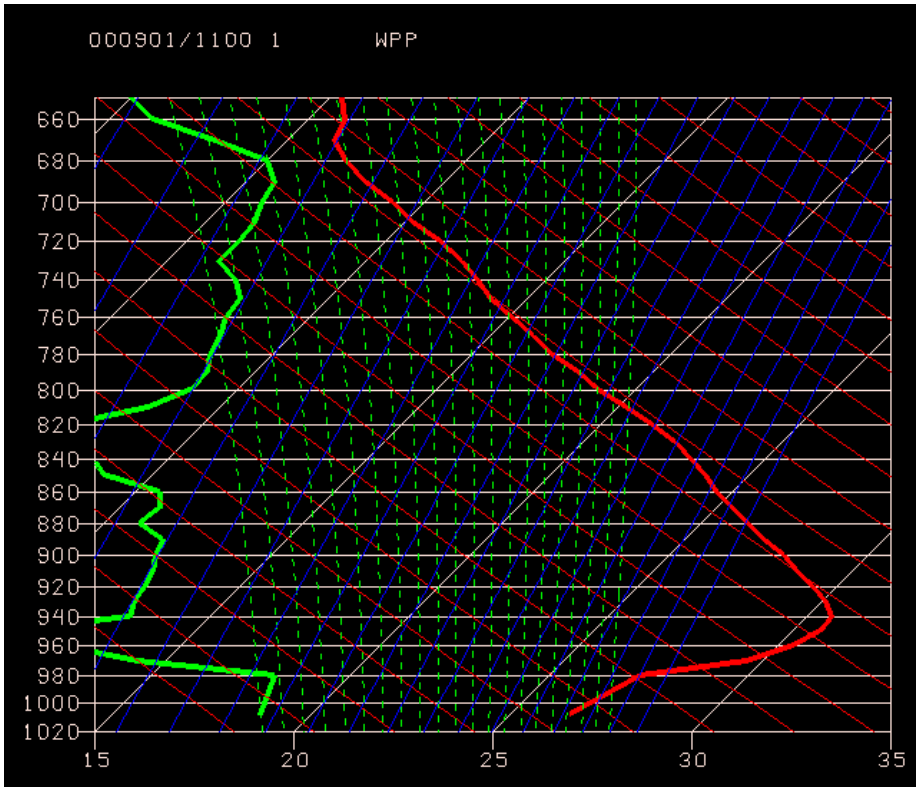

Fig. 18: Skew-T of WH radiosonde data at 1100 UTC. Red line represents temperature and green line represents dewpoint temperature.

The WH radiosonde data at 2251 was evaluated to determine why the ML leveled off at 1830 UTC and then slightly decreased. This was the closest data available for the LB location and time of day. Figure 19 shows a Skew-T of this data. From Figure 19, it is evident that the LB ML heights were inconsistent with the WH sounding which showed an extremely deep ML with an almost completely dry adiabatic temperature increase. From this, the ML height should have deepened as long as the temperature increased. Although there was a disagreement between the sounding and LB wind profiler, the two instruments were located almost 100km apart and the ML height leveling off and decrease in the afternoon at the LB profiler may have been the result of local thunderstorms later in the day evident in surface data that did not

influence the WH sounding or the wind profiler. The thunderstorms may have cast a shadow that did not allow adequate ground heating.

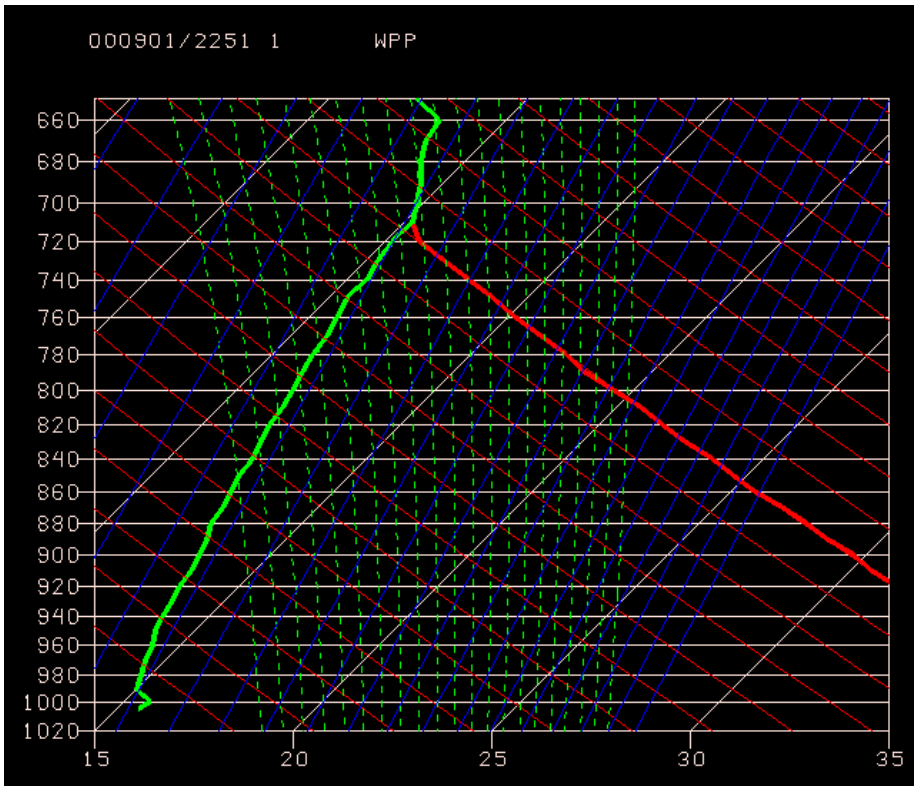

Fig. 19: Skew-T of WH radiosonde data at 2251 UTC. Red line represents temperature and green line represents dewpoint temperature.

At the LM site, the ML height increased until 1900 UTC at which time there was missing data. The next data point had the ML height much lower. Because the LM site was near the coast and surface data showed the winds from the south at this time, the shallow ML heights was related to the advection of Gulf of Mexico air as found by Senff et al. 2002.

After the actual ML height evolution was determined for each wind profiler site (Figure 17), an average temporal evolution was found by averaging the rate of change

each half hour between major inflection points in the time series and is represented in Figure 20. The airborne lidar and MTP estimates were used to determine the spatial evolution of the ML height. For these estimates to be appropriate at a particular time, the data was reduced using the wind profiler average rate of change, as explained below.

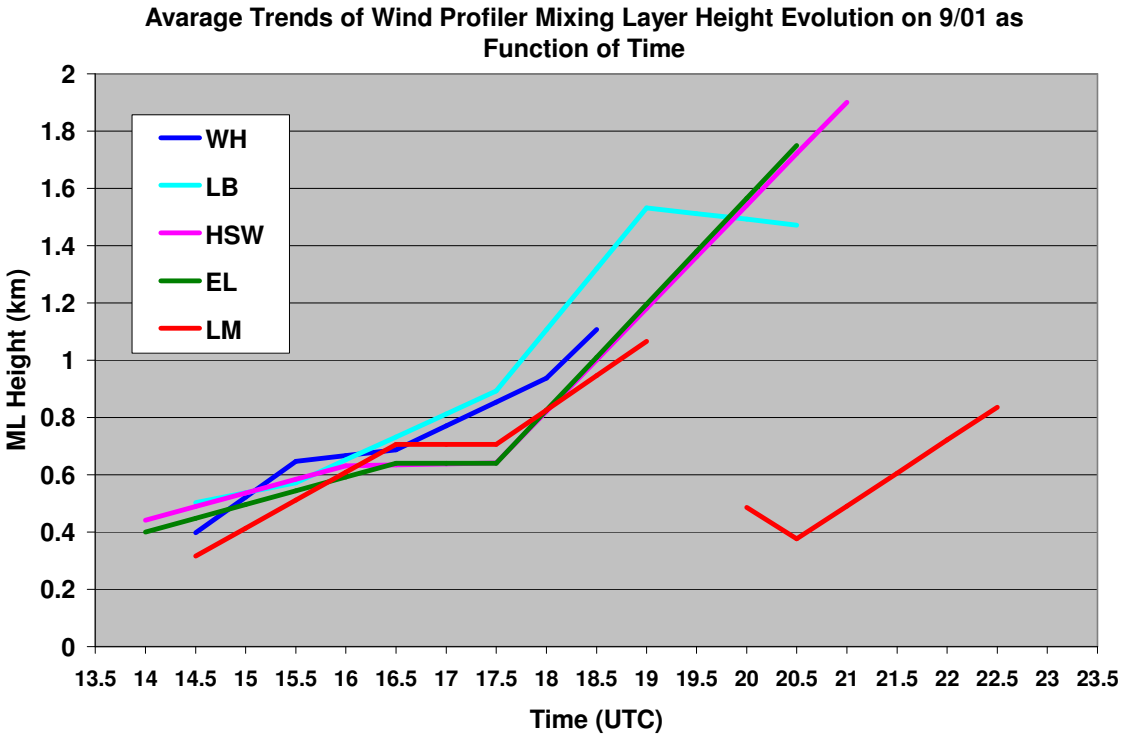

Fig. 20: Average trend of the evolution of ML heights as a function of time on 9/01/00 inferred by wind profilers at the Wharton (WH), Liberty (LB), Houston Southwest (HSW), Ellington (EL), and LaMarque (LM) sites.

Due to the fact the lidar and MTP measure not only in space, but in time as well, their data was manipulated to be easily plotted with the profiler data for each hour analysis. This was done by organizing the time of the measurements into hourly time periods. A time period consists of the thirty minutes before the hour of analysis to

twenty-nine minutes after the hour of analysis. For example, an analysis at 1700 UTC uses lidar and MTP measurements taken from 1630 to 1729 UTC.

To deal with the changing position of the lidar and MTP, all the usable ML height measurements within each hourly time period were averaged every 10km (the optimal radius in the comparison study). The averaged height was then assigned a time value and latitude and longitude positions based on the corresponding median values of each 10km data set. The latitude and longitude positions were compared to each wind profiler to determine the closest wind profiler. Depending on the location and the closest wind profiler, the average ML height was adjusted in time to correspond to the hour of analysis. If the average height was not located so that it would be influenced by the marine air during the time of the interval, the ML height was adjusted by the average rate of change (Figure 20) of the closest profiler. This was repeated for each average height and the heights were plotted for each hour of analysis.

b. Results

The ML height evolution determined using the wind profilers, airborne lidar, and airborne MTP are displayed in Figures 21, 22, 23, 24, 25 and 26. These figures were created to show the ML height evolution around the city of Houston by using contour lines that connect ML heights of equal value. By hourly analysis of the airborne lidar and MTP in respect to these figures, three main features were evident in the ML height distribution. These features include the ML height around Galveston Bay, the ML height north of Houston, and the ML height south of Houston.

1600 UTC

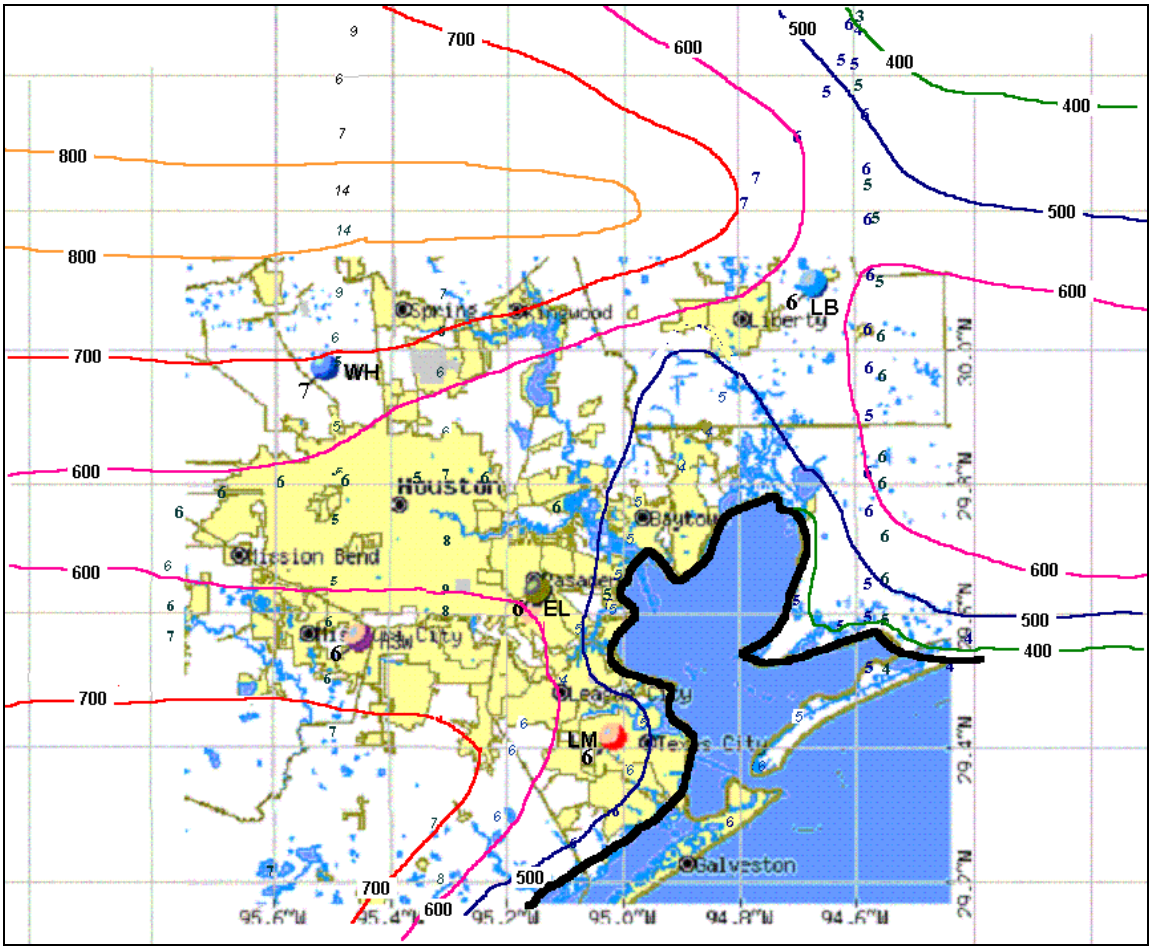

Fig. 21: The ML height distribution at 1600 UTC around the city of Houston. The contours are for every 100m. The ML heights at the wind profiler locations are black, the MTP heights are green, and the lidar heights are blue. The values represent the ML height divided by 100m. The larger numbers are the ML heights inferred for the current time period, the smaller bold numbers represent the ML heights inferred for the previous time period, and the italic numbers represent the ML heights inferred for the following time period.

1700 UTC

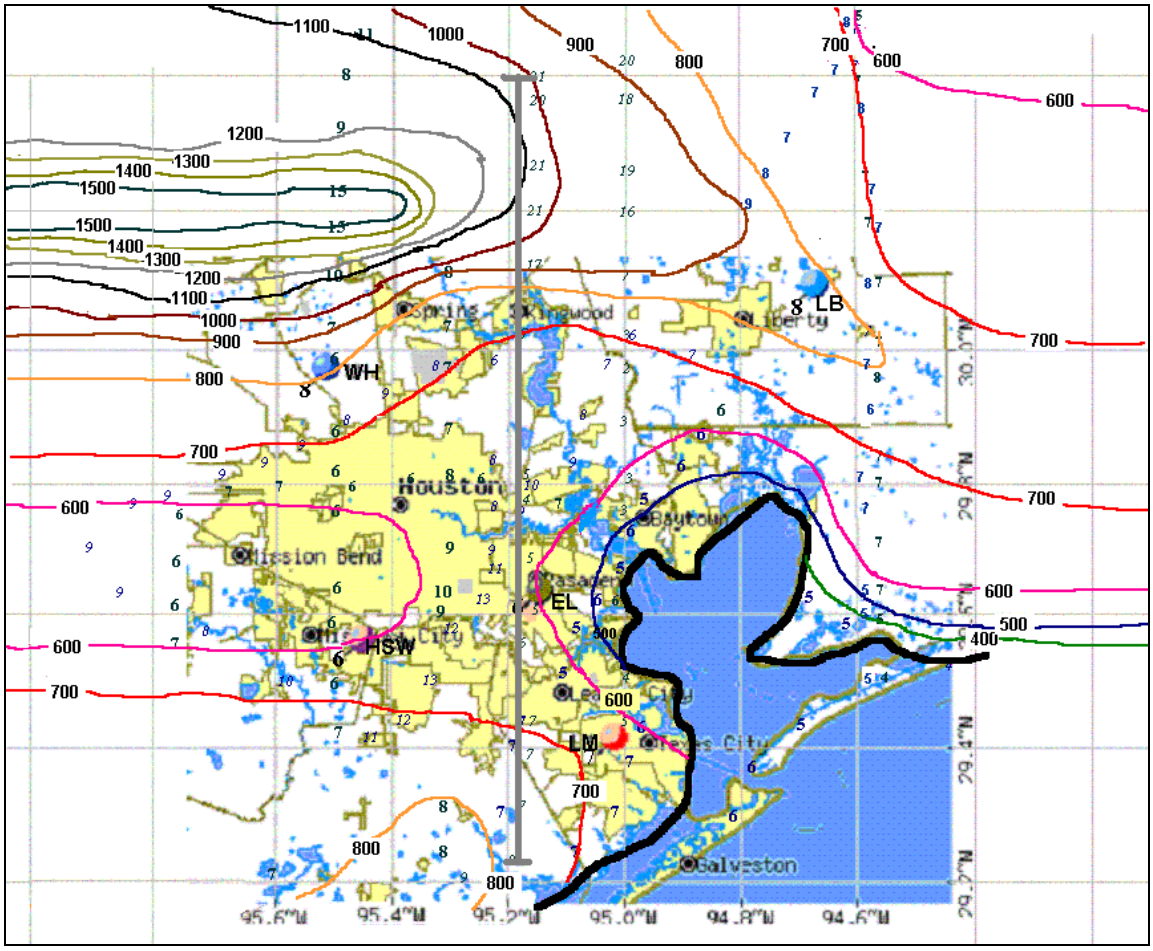

Fig. 22: The ML height distribution at 1700 UTC around the city of Houston. The contours are for every 100m. The ML heights at the wind profiler locations are black, the MTP heights are green, and the lidar heights are blue. The values represent the ML height divided by 100m. The larger numbers are the ML heights inferred for the current time period, the smaller bold numbers represent the ML heights inferred for the previous time period, and the italic numbers represent the ML heights inferred for the following time period. The solid grey line represents the flight track corresponding used for a vertical cross-section of potential temperature.

1800 UTC

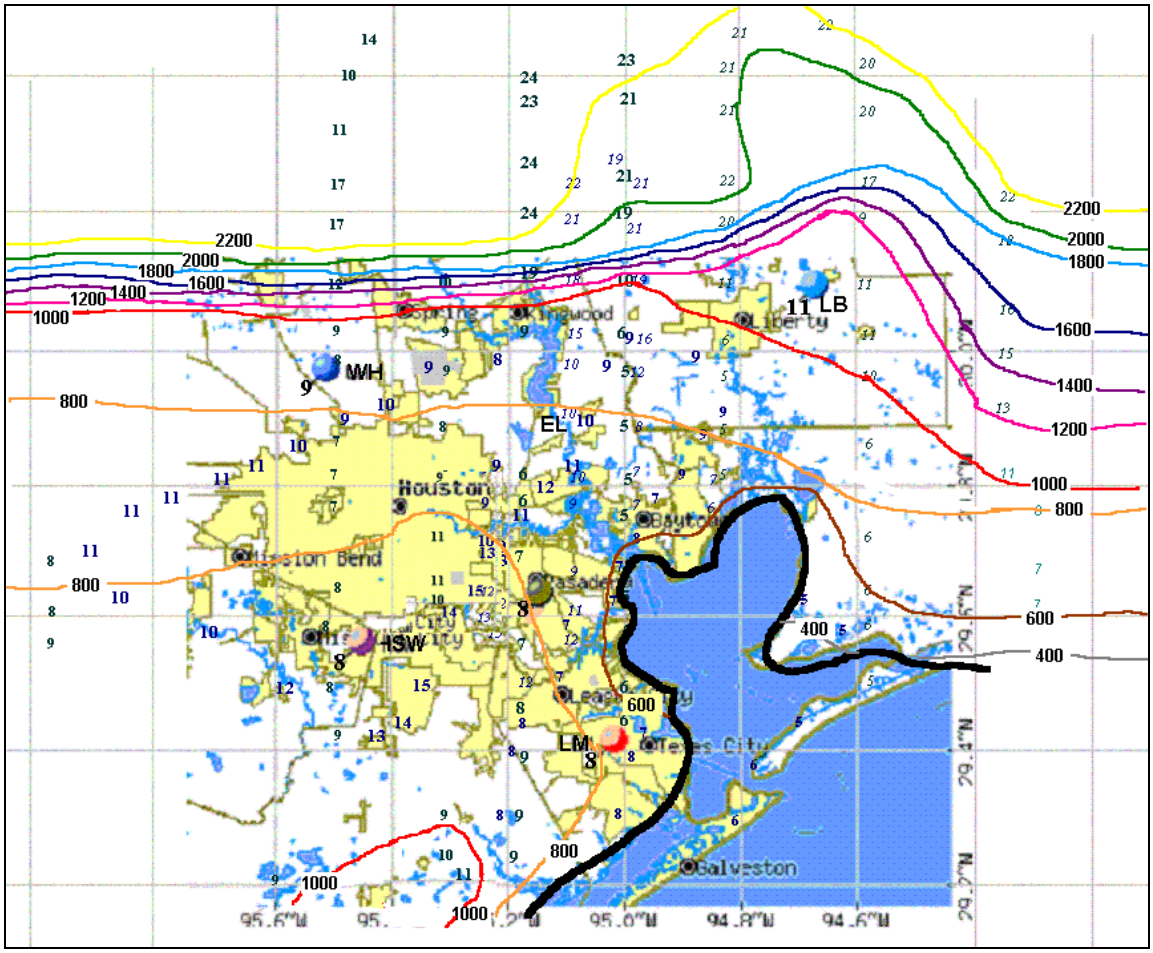

Fig. 23: The ML height distribution at 1800 UTC around the city of Houston. The contours are for every 200m. The ML heights at the wind profiler locations are black, the MTP heights are green, and the lidar heights are blue. The values represent the ML height divided by 100m. The larger numbers are the ML heights inferred for the current time period, the smaller bold numbers represent the ML heights inferred for the previous time period, and the italic numbers represent the ML heights inferred for the following time period.

1900 UTC

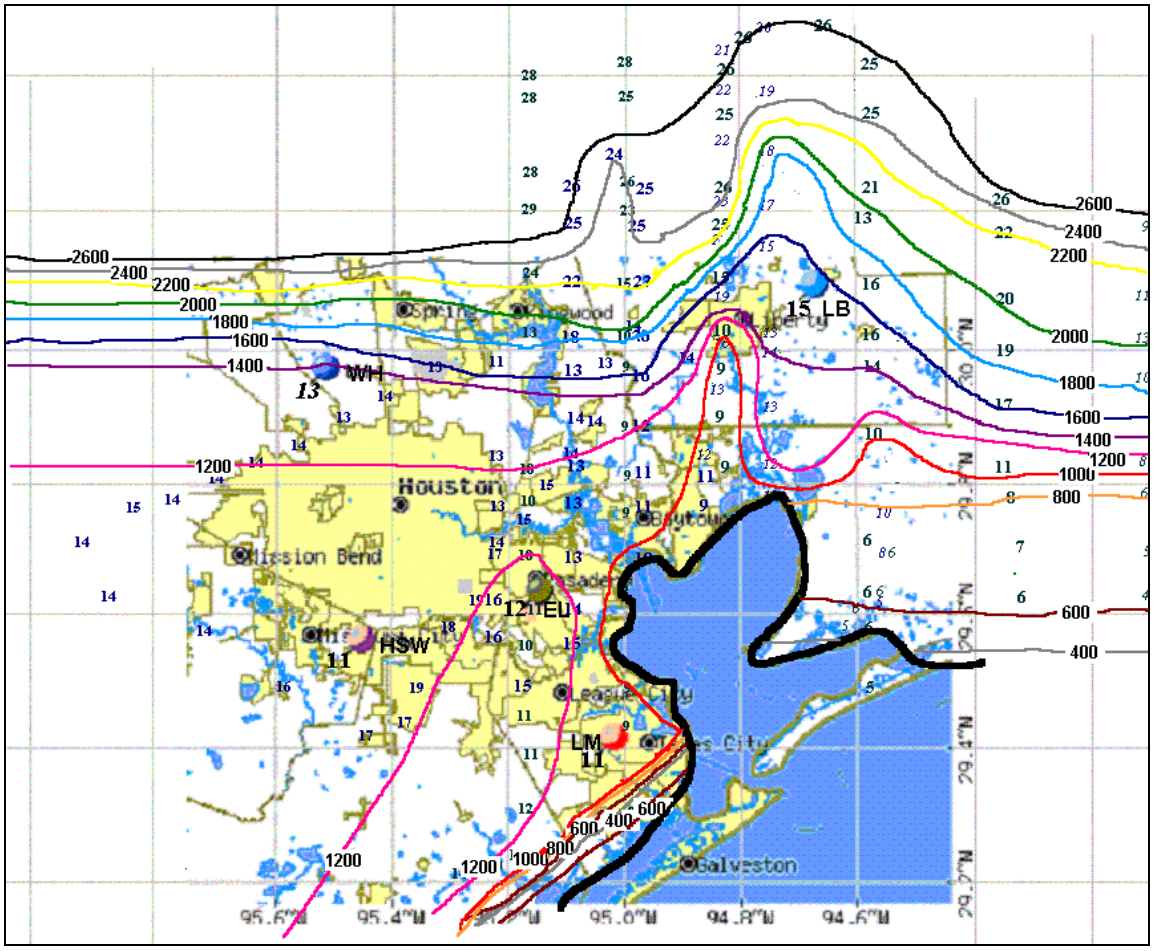

Fig. 24: ML height distribution at 1900 UTC around the city of Houston. The contours are for every 200m. The ML heights at the wind profiler locations are black, the MTP heights are green, and the lidar heights are blue. The values represent the ML height divided by 100m. The larger numbers are the ML heights inferred for the current time period, the smaller bold numbers represent the ML heights inferred for the previous time period, and the italic numbers represent the ML heights inferred for the following time period.

2000 UTC

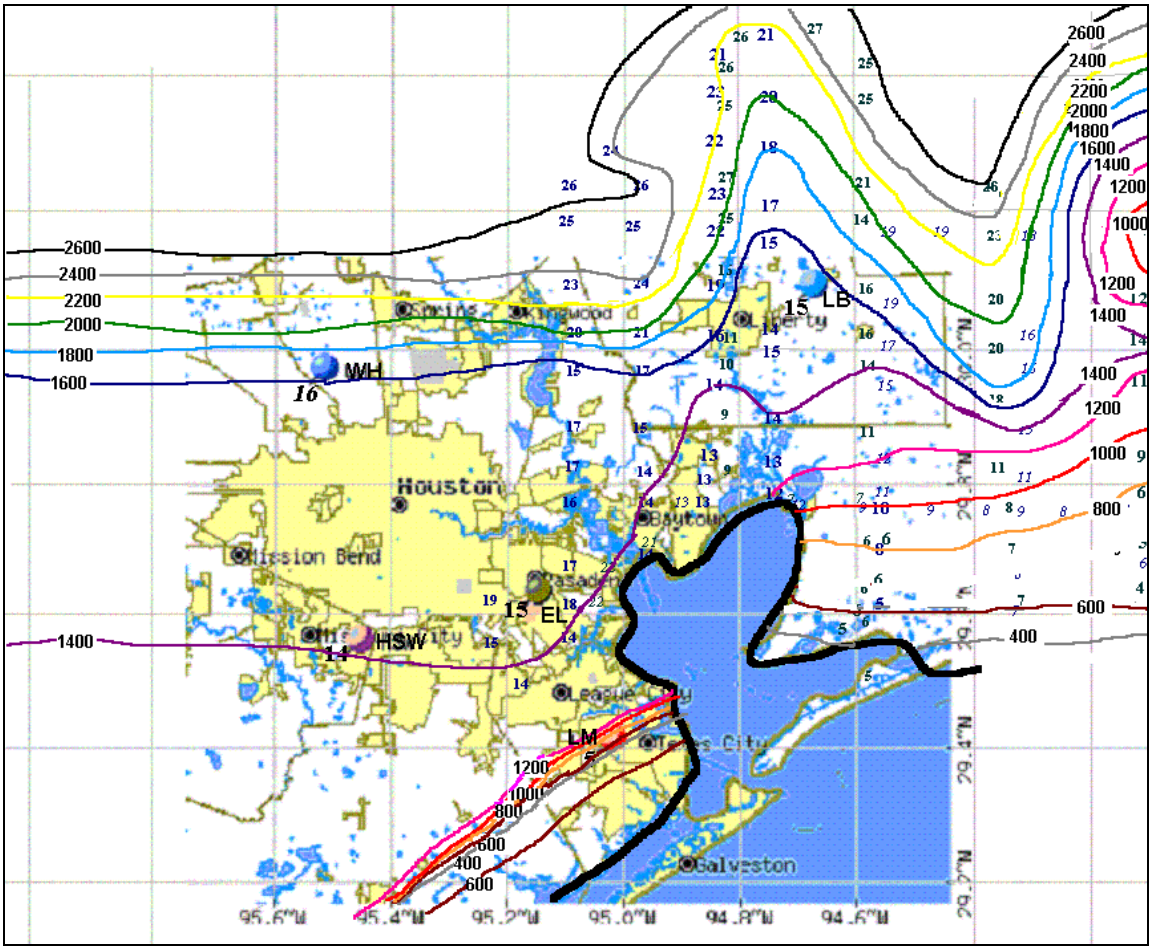

Fig. 25: ML height distribution at 2000 UTC around the city of Houston. The contours are for every 200m. The ML heights at the wind profiler locations are black, the MTP heights are green, and the lidar heights are blue. The values represent the ML height divided by 100m. The larger numbers are the ML heights inferred for the current time period, the smaller bold numbers represent the ML heights inferred for the previous time period, and the italic numbers represent the ML heights inferred for the following time period.

2100 UTC

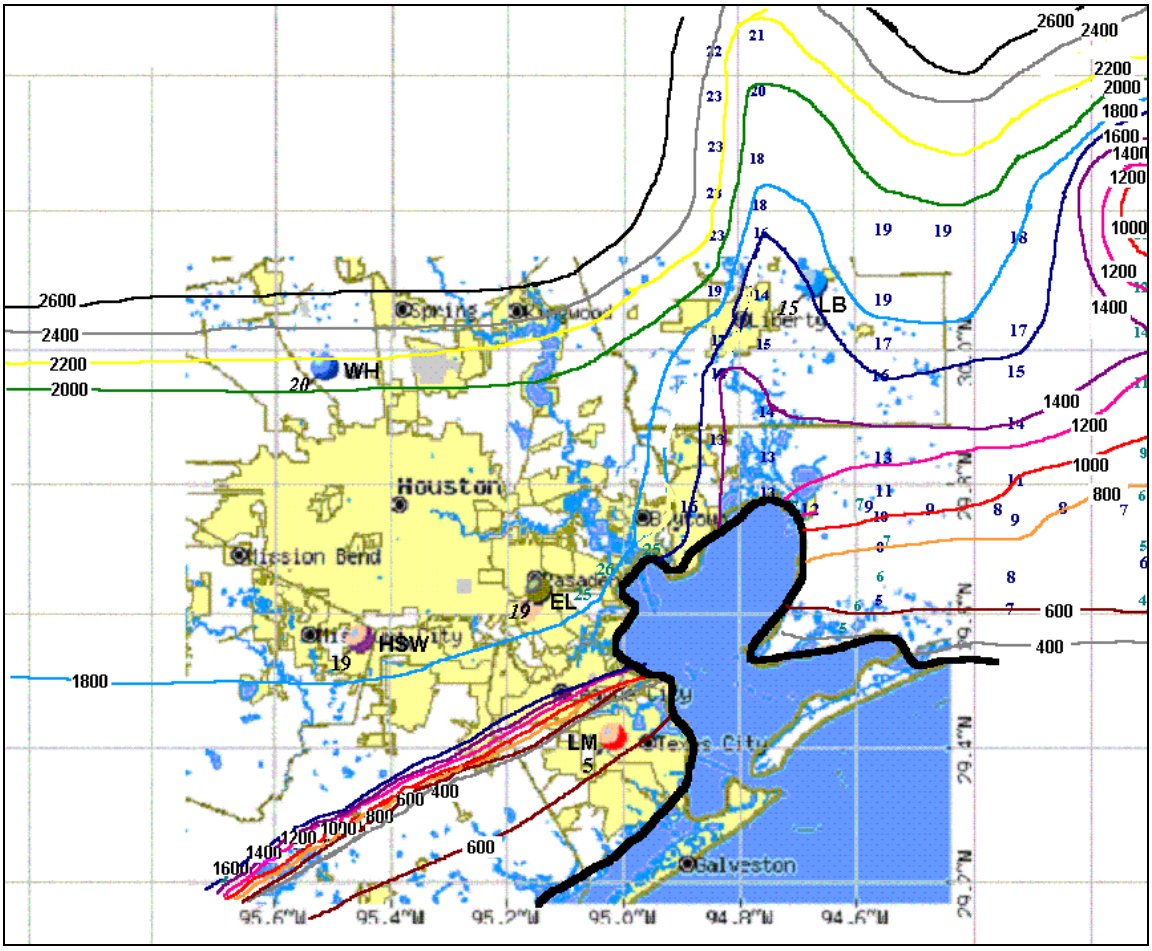

Fig. 26: ML height distribution at 2100 UTC around the city of Houston. The contours are for every 200m. The ML heights at the wind profiler locations are black, the MTP heights are green, and the lidar heights are blue. The values represent the ML height divided by 100m. The larger numbers are the ML heights inferred for the current time period, the smaller bold numbers represent the ML heights inferred for the previous time period, and the italic numbers represent the ML heights inferred for the following time period.

The first feature evident in both the MTP and lidar data was the ML height around Galveston Bay. The ML height around Galveston Bay was shallow along the coast and increased with increasing distance from the coast. Throughout the analysis period, the contour lines were parallel to the coastline. According to both the lidar and MTP data at 1600 UTC, the ML height was less than 500m around Galveston Bay to

distance of approximately 15km away from the coast and as much as 40km north of Galveston Bay. At 1700 UTC there was a more defined ML height gradient with the lidar data showing values of 600m closer to the coastline. At 1800 UTC there was not lidar or MTP data for the exact hour of analysis, but interpolation combined with the LM wind profiler data showed the ML had deepened around Galveston Bay, with higher heights and a stronger gradient to the west and a weaker gradient and lower heights to the east.

At 1900UTC the surface data showed that a sea breeze front had developed west of Galveston Bay near the coast. The ML height ahead of the front was above 1km, and the ML height along the front was below 400. Behind the front, there was a gradual increase in ML height with distance from the front. By 2000 UTC the wind had shifted to the south farther inland, which was evident by the LM wind profiler height and in the surface data near the coast. Ahead of the sea breeze front, the ML heights were above 1200m. At 2100 UTC, the sea breeze front was farther inland with heights above 1600m ahead of the front and still a gradual increase behind the front.

The second feature was the ML height distribution north of Houston. Starting at 1600 UTC, the MTP data at the time of the analysis showed a minimum of ML heights less than 400m in the far eastern corner of the analysis and the interpolated lidar data from 1700 UTC showed a maximum to the west with ML heights greater than 800m. Combining both data produced a gradient in ML heights from west to east with greater ML heights values found to the west. This gradient was also evident in the wind profiler

data where the ML height at the LB site (more easterly site) was 600m and the ML height at the WH site (more westerly site) was 700m.

At 1700 UTC, both the lidar and MTP data showed that north of Houston there was still a gradient in ML heights from west to east with higher ML height values to the west. The maximum of ML heights was greater than 1500m but did not cover as large an area. The gradient around this maximum strengthened with the height to the south reaching values of 800m within 50km.

By 1800 UTC, the maximum that was located to the west in the previous analysis was replaced by a strong gradient of increasing ML heights to the north according to both the lidar and MTP data. The gradient was stronger to the west than it was to the east. To interpret the ML height gradient north of Houston, the vertical cross-section of potential temperature was plotted as a function of latitude for the time period between 1730 UTC and 1800 UTC using the MTP data (Figure 27). The flight track for this cross-section is represented as the solid gray line in Figure 22.

The gradient in ML heights found between 30° N and 30.2°N was in the same location as the large transition in the potential temperature as seen in Figure 27. There were large variations in the vertical structure of potential temperature from 29.2° N to just above 30°N which corresponded to the plane was flying near the inversion. Below the base of the inversion, the potential temperature was more uniform which corresponded to the ML. Just above 30°N, the potential temperature was more uniform and an inversion was no longer evident. The inversion extended to a higher altitude in the atmosphere farther south than farther north.

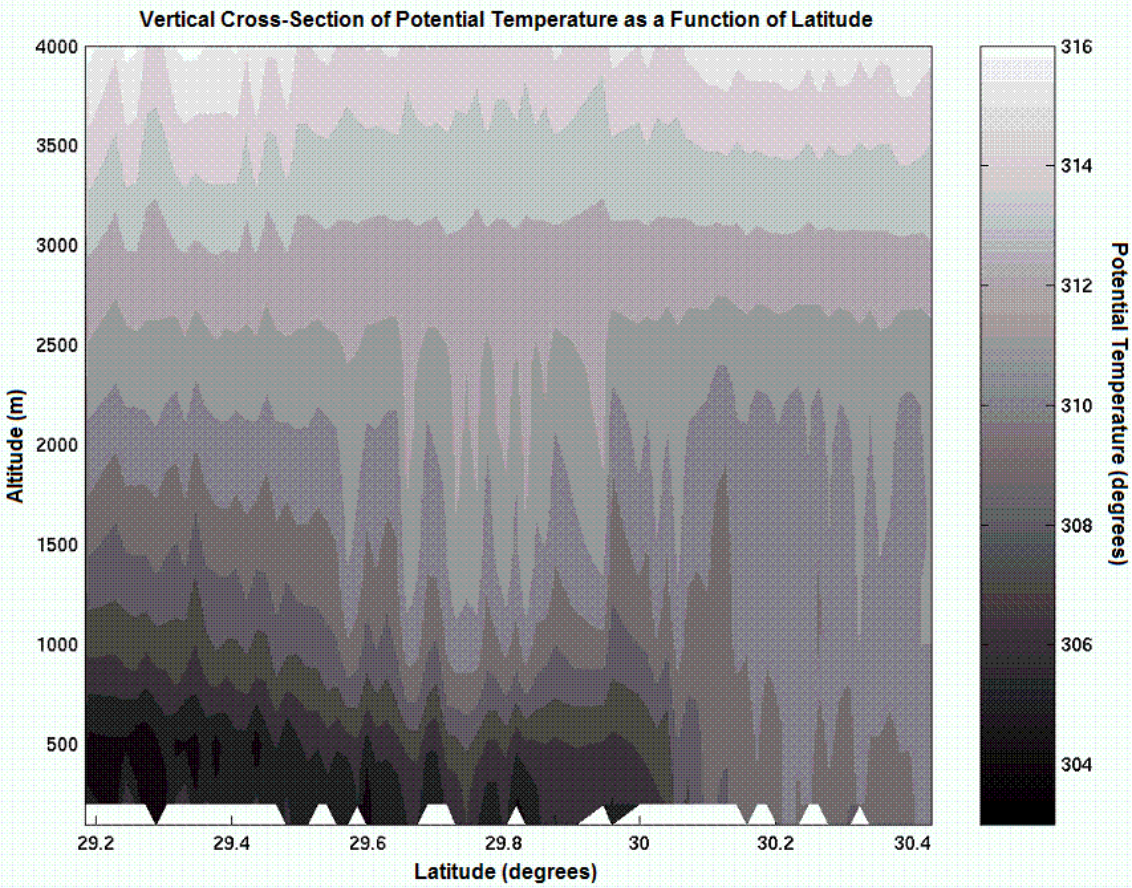

Fig. 27: A vertical cross-section of potential temperature as a function of latitude at -95.17° longitude between 1730 UTC and 1800 UTC on September 1, 2000.

At 1800 UTC, around the LB wind profiler site and just north of Galveston Bay, the MTP data showed a ridge in the gradient with a large area of ML height values between 1000m and 1200m. This caused the ML heights to be lower in value farther east than west at the same latitude. At 1900 UTC, north of Houston, the MTP and lidar data still showed a strong gradient in ML height values with the gradient stronger to the west. Around the LB wind profiler site and just north of Galveston Bay, the ridge in the gradient was more defined.

By 2000 UTC there was still an ML height gradient north of Houston according to the lidar and MTP data, but overall, the gradient had weakened. The gradient was still stronger to the west, and around the LB wind profiler site and just north of Galveston Bay there was still a ridge in the gradient. Data from the LB wind profiler, lidar, and MTP all showed that the ML height around the LB wind profiler site and within the ridge remained fairly constant from the previous analysis. During this same analysis, an ML height minimum had developed northeast of Houston and Galveston Bay from the MTP data with ML height values less than 1000m.

By the last analysis at 2100 UTC, most of the ML height distribution was inferred from the previous analysis period. North of Houston, there was still a gradient in ML heights that was stronger to the west. Around the LB wind profiler site and just north of Galveston Bay, there was still a ridge in the gradient. By interpolating the MTP data from the previous analysis, there was still an ML height minimum located northeast of Houston and Galveston Bay with ML height values less than 1000m. A stronger gradient had developed around this minimum.

The third feature was an ML height maximum located south of Houston. This maximum was evident in the MTP data at 1700 UTC with ML heights greater than 800m. By interpolating the data, the maximum was also evident at 1600 UTC with a large area where the ML heights were greater than 700m. The maximum remained until 1800 UTC with ML heights greater than 1000m. By 1900 UTC, the ML height maximum located south of Houston was replaced by a large area of ML height values approximately 1200m and less.

c. Discussion

There were systematic variations in the ML height from north to south according to the wind profiler data. The sites farther inland and more northerly broke through the inversion earlier and reached higher ML values earlier in the day. There was barely an inversion evident in the LB evolution. The LB wind profiler was the most northerly wind profiler and located where more surface heating and a weaker inversion was present and allowed for steady growth during the morning hours. The sites near the coast, EL and LM, along with the most southerly inland site, HSE, all followed nearly the same evolution at which between 1700 UTC and 1730 UTC the ML height broke through the inversion and then experienced rapid growth.

Using the MTP potential temperature data, the inversion early in the day was found to extend from the coast, where it was higher in the atmosphere, to approximately 30°N, where it was shallower. Because of this, the inversion was related to the remnants of the sea breeze front from the previous day, resembling a residual layer. The colder marine air from the coast remained until there was enough heating at the surface for the ML to break through the inversion.

Combining the wind profiler ML height evolution with the modified airborne MTP and lidar ML heights allowed for the ML height evolution across the Houston area to be analyzed according to the main features evident in the ML height distribution. These features included the ML height around Galveston Bay, center of Houston, and north of Houston.

The ML height around Galveston Bay was dependent on the wind direction. The wind was out of the west until approximately 2000 UTC, at which the onset of the sea breeze began. The west wind caused locations west of Galveston Bay to have ML heights mainly influenced by local mixing from heating at the surface. Locations east of Galveston Bay were influenced by the marine air and the west wind meant that the air was cooled as it traveled over the Bay. Downwind of Galveston Bay, the ML height was mainly a function of distance from the Bay.

As evident in the lidar and MTP data, the ML height exactly along the coast and east of Galveston Bay was a few tens of meters and increased rapidly with increasing distance from the water to about 500m or 600m which was consistent with the data from Senff et al. 2002. From this, the ML heights gradually increased. Higher values were reached later in the day when the air became well-mixed from adequate warming at the surface. At 2000 UTC, the winds shifted to the south and caused the advection of Gulf of Mexico air inland. This was evident in the surface data especially for the western side of Galveston Bay and near the LM wind profiler. The ML height deepened as time passed and the marine air advanced farther inland.

There was a ML height gradient located to the north of Houston throughout the whole day. During the morning, there was a maximum to the west with values decreasing to the north and south, determined by combing the lidar and the MTP data for 1600 UTC and 1700 UTC. This may have been caused by the west wind which means that the air flowed from west to east so that this major feature moved from west to east without being forced by something at the surface. The temperature may have been

higher in the area of the ML height maximum which would have allowed the ML to grow deeper as well.

By 1800 UTC, there was no longer a maximum, but a sharp gradient where the ML heights decreased to the north. At this time a ridge of minimum ML heights developed in the gradient around the LB site north of Galveston Bay. Around this ridge the ML heights decreased to the north. This feature can not be explained because of the lack of data, although it is evident in the wind profiler, lidar, and MTP estimates.

The ML height gradient north of Houston was caused by the variation in the depth of the inversion. The inversion was lower in the atmosphere north of Houston than south of Houston near the coast. Less energy was required to break through the inversion allowing the ML to grow more rapidly earlier in the day in the northern areas than the areas farther south.

At 2000 UTC, an ML height minimum was determined from the MTP to be located northeast of Houston and Galveston Bay with ML heights less than 1000m. The ML heights gradually increased in all directions. This feature remained through 2100 UTC by interpolation of the MTP data. The lower values may have been the result of convection taking place and the formation of a gust front. The cool air associated with the gust front may have suppressed the mixing and caused the ML to be much lower.

Early in the day, there were higher ML heights located southeast of downtown Houston. The higher heights were identified by the MTP data at 1700 UTC and were interpolated to remain from 1600 UTC to approximately 1900 UTC. The lidar data at this time was untrustworthy by comparison with the wind profilers and therefore

disregarded. The flight track during the time of the higher heights was more than 600m higher than the flight tracks during the rest of the analysis. Because this was the only source of data, the higher heights were related to the different altitudes of the flight tracks and disregarded for the analysis.

Early in the day, there was an ML height maximum located south of Houston. The maximum started out greater than 700m at 1600 UTC and remained until 1900 UTC where it was replaced by a large area of ML heights greater than 1200m. After 2000 UTC, the ML height became more homogenous around the Houston area.

The reason there were higher ML height values south of Houston early in the day was related to the inversion higher in the atmosphere farther south. Since the ML extended to the base of the inversion, the ML was at a higher height near the coast than farther north. The ML height maximum remained until the ML had broken through the inversion across the Houston area, allowing for a more homogenous ML height distribution.

CHAPTER V1

CONCLUSION

In the first part of this paper, new techniques were used to determined ML heights. These included a benchmark method which was developed from radiosonde data and new algorithms to determine ML heights from MTP data which was the first time MTP has been used in this manner. As a part of this research, the significance of using the base of an inversion layer as opposed to the midpoint of the inversion layer was quantified using radiosonde data and the issue of comparing co-located instruments versus instruments that were not co-located was addressed. In the second part of this paper, the horizontal ML height distribution was determined as a function of space and time using real data from several instruments.

The midpoint of the inversion layer in the moisture profiler was found to be an average of 110m above the base of the inversion layer in the moisture profile by evaluation of radiosonde data. Also by evaluating radiosonde data, the midpoint of the inversion layer in the moisture profile compared best with the base of the inversion layer in the temperature profile from which the benchmark method was created. The comparisons between the benchmark method and the wind profilers were independent of the quality flag of the wind profiler and more influenced by the flag of the benchmark method heights. There were smaller bias and standard deviation values when only the high quality benchmark method heights were used for the comparisons.

Overall, there was a relatively good relationship between the ML determined by the separate instruments with respect to the bias, standard deviations, and RMSE of the

difference in the heights. However, this good agreement was limited to comparisons between co-located instruments. Comparisons between instruments that were not co-located had more discrepancy in their estimates. This was especially true for the comparisons between coastal and inland instruments. In this paper, the largest standard deviation and bias values were found for the comparisons between the EL coastal wind profiler and inland HDT radiosonde and the combined EL and LM coastal wind profilers and airborne lidar that had flight tracks on the side of the wind profiler farther inland.

The smallest standard deviation and bias values between the airborne lidar and wind profilers occurred for the comparisons using the inland profilers. Even so, the statistics for coastal sites were similar to the comparisons between the benchmark method and wind profilers which suggest these instruments can be used to determine the ML heights in a coastal megacity, such as Houston, where there is variability in the aerosol content. This also suggests that even with the development of the benchmark method, there was error in the radiosonde estimates due to the lack of representation of the entire PBL in which the radiosondes were subject to turbulent variations in the local height of the PBL.

The comparisons between the MTP algorithms and the wind profiler show that MTP can be used for determining ML heights and can give fairly accurate estimates. These results were comparable with the results found between the other instruments and better in that the statistics were similar for the both the inland and coastal wind profilers. The results between algorithm 27 and the Electra data provided additional support for the use of MTP for determining ML heights. The good agreement between these two

instruments validated the need for multiple methods for a complete set of ML height comparisons.

The comparisons and resulting good agreement between the separate instruments allowed for the determination of the ML height distribution across the Houston area on September 1, 2000. The combination of the inland and coastal wind profilers with the airborne instruments provided adequate information for the spatial and temporal evolution of the ML height to be determined. By analyzing the distribution of the ML height throughout the day, major features were evident. These features included the shallow ML heights associated with Galveston Bay and the Gulf of Mexico and the sharp gradient of increasing ML heights north of Houston associated with the variation in the inversion depth found in the same area.

There will be future work that builds on the results of this paper which includes determining as completely as possible the horizontal distribution of ML heights during other selected days of the Texas 2000 Air Quality Study and establishing the proper combination of instruments for measuring the ML height in future field programs. The conclusions gathered from this paper can be used for ML height research in other cities and can aid in the improvement of air pollution prediction and modeling.

REFERENCES

Angevine, W.M, A.B. White, and S.K. Avery, 1994: Boundary-Layer Depth and Entrainment Zone Characterization with a Boundary-Layer Profiler, *Boundary-Layer Meteor.*, **68**, 375-385.

Baxter, R., 1991: Determination of Mixing Heights from Data Collected during the 1985 SCCCAMP Field Program, *J. Appl. Meteor.*, **30**, 598-606.

Beyrich, F., U. Gorsdorf, 1995: Composing the Diurnal Cycle of Mixing Height from Simultaneous SODAR and Wind Profiler Measurements, *Boundary-Layer Meteor.*, **76**, 387-394.

_____, F., 1997: Mixing Height Estimation from SODAR Data – A Critical Discussion, *Atmos. Environ.*, **31**, 3941-3953.

Cohn, S.A, and W.M Angevine, 2000: Boundary Layer Height and Entrainment Zone Thickness Measured by Lidar and Wind-Profiling Radars, *J. Appl. Meteor.*, **39**, 1233-1247.

Cooper, D.I., and W.E. Eichinger, 1994: Structure of the Atmosphere in an Urban Planetary Boundary Layer from Lidar and Radiosonde Observations, *J. Geophys. Res.*, **99**, 22937-22948.

Coulter, R. L., 1979: A Comparison of Three Methods for Measuring Mixing-Layer Height, *J. Appl. Meteor.*, **18**, 1495-1499.

Dayan, U., R. Shenhave, and M. Graber, 1988: The Spatial and Temporal Behavior of the Mixed Layer in Israel, *J. Appl. Meteor.*, **27**, 1382-1394.

_____, B. Lifshitz-Goldreich, K. Pick, 2002: Spatial and Structural Variation of the Atmospheric Boundary Layer during Summer in Israel – Profiler and Rawinsonde Measurements, *J. Appl. Meteor.*, **41**, 447-457.

Denning, R.F., S.L. Guidero, G.S. Parks, and B.L. Gary, 1989: Instrument Description of the Airborne Microwave Temperature Profiler, *J. Geophys. Res.*, **94**, 16,757-16, 765.

Dupont, E., L. Menut, B. Carissimo, J. Pelon, P. Flamant, 1999: Comparison Between the Atmospheric Boundary Layer in Paris and Its Rural Suburbs during the ECLAP Experiment, *Atmos. Environ.*, **33**, 979-994.

Garrett, A.J., 1981: Comparison of Observed Mixed-Layer Depths to Model Estimates Using Observed Temperature and Winds, and MOS Forecasts, *J. Appl. Meteor.*, **20**, 1277-1283.

Glickman, T.S., 2000: *Glossary of Meteorology*. American Meteorological Society, 855 pp.

Grimsdell, A.W., and W.M. Angevine, 1998: Convective Boundary Layer Height Measurement with Wind Profilers and Comparison to Cloud Base, *J. Atmos. Oceanic Technol.*,**15**, 1331-1338.

Heffter, J.L., 1980: Air Resources Laboratories Atmospheric Transport and Dispersion Model. NOAA Tech. Memo. ERL ARL-81, 24 pp.

Holzworth, G.C, 1964: Estimates of Mean Maximum Mixing Depths in the Contiguous United States*, Mon. Weather Review*, **92**, 235-242.

_____, G.C, 1967: Mixing Depths, Wind Speeds and Air Pollution Potential for Selected Locations in the United States*, J. Appl. Meteor.*, **6**, 1039-1044.

Hooper W.P., E.W. Eloranta, 1986: Lidar Measurements of Wind in the Planetary Boundary Layer: The Method, Accuracy and Results from Joint Measurements with Radiosonde and Kytoon, *J. Climate Appl. Meteor.*, **25**, 990-1001.

Kaimal, J.C., N.L. Abshire, R.B. Chadwick, M.T. Decker, W.H. Hooke, R.A Kropfli, W.E. Neff, F. Pasqualucci, and P.H. Hildebrand, 1982: Estimating the Depth of the Daytime Convective Boundary Layer, *J. Appl, Meteor.*, **21**, 1123-1129.

Kalthoff, N., H.J. Binder, M. Kossmann, R. Vogtlin, U. Corsmeier, F. Fiedler, H. Schlager, 1998: Temporal Evolution and Spatial Variation of the Boundary Layer Over Complex Terrrain, *Atmos. Environ.*, **32**, 1179-1194.

Mahoney M.J., 2002: TAMU Final Report, http://mtp.jpl.nasa.gov/missions/texaqs/science/TAMU_Report.htm.

Marsik, F. J., K.W. Fischer, T.D. McDonald, and P.J. Sampson, 1995: Comparison of Methods for Estimating Mixing Height Used during the 1992 Atlanta Field Intensive, *J. Appl. Meteor.*, **34**, 1802-1814.

Martin, C.L., D. Fitzjarrald, M. Garstang, A.P. Oliveira, S. Greco, E. Browell, 1988, Structure and Growth of the Mixed Layer Over the Amazonian Rain Forest, *J. Geophys. Res.*, **93**, 1361-1375.

McElroy, J.L, and T.B Smith, 1991: Lidar Descriptions of Mixing-Layer Thickness Characteristics in a Complex Terrain/Coastal Environment, *J. Appl. Meteor*, **30**, 585-597.

Miller, M.E., 1967: Forecasting Afternoon Mixing Depths and Transport Wind Speeds, *Mon. Weather Review*, **95**, 35-44.

Olsson, L. E., M.P. McCormick, W.P. Elliot, S.H. Melfi, 1974: An Observational Study of the Mixing Layer in Western Oregon, *Atmos. Environ*., **8**, 241-252.

Russell, P.B, E.E Uthe, F.L Ludwig, N.A. Shaw, 1974: A Comparison of Atmospheric Structures as Observed With Monostatic Acoustic Sounder and Lidar Techniques, *J. Geophys. Res*., **79**, 5555-5566.

_____, _____, 1978: Regional Patterns of Mixing Depth and Stability: Sodar Network Measurements for Input to Air Quality Models, *Bull. Amer, Meteor. Soc.*, **59**, 1275-1287.

Seibert, P., F. Beyrich, S.E. Gryning, S. Joffre, A. Rasmussen, and P. Tercier, 2000: Review and Intercomparison of Operational Methods for the Determination of the Mixing Height, A*tmos. Environ*., **34**, 1001-1027.

Senff, S., R. Banta, L. Darby, W. Andesine, A. White, C. Berkowitz, and C. Doran, 2002: Spatial and Temporal Variations in Mixing Height in Houston. TNRCC Project F-20, 58 pp.

Stull, R.B., 1988: *An Introduction to Boundary Layer Meteorology*. Kluwer, 666pp.

Van Pul, W.A.J, A.A.M Holtslag, and D.P.J. Swart, 1994: A Comparison of ABL Heights Inferred Routinely from Lidar and Radiosondes at Noontime, *Boundary-Layer Meteor*., **68**, 173-191.

White, A.B., C.J. Senff, and R.M Banta, 1999: A Comparison of Mixing Depths Observed by Ground-Based Wind Profilers and an Airborne Lidar, *J. Atmos. Oceanic Technol.*, **16**, 584-590.

VITA

Christina Lynn Smith was born and spent most of her life in southeast Ohio. In June 2002, she graduated from Ohio University with a B.S. degree in Meteorology and minors in Mathematics and Physics. Christina moved to College Station, Texas to earn her Masters degree in Atmospheric Sciences at Texas A&M University under the instruction of Dr. John Nielsen-Gammon. During this time she enjoyed participation in Texas A&M Mobile Severe Storms Data Acquisition (TAMMSSDA). Upon graduation from Texas A&M University in May 2005, Christina plans on continuing her education in Environmental Sciences back in Ohio. During the summer of 2006 she will be married to Jeffrey Powell, a fellow graduate of Ohio University. Christina can be reached at the following address:

Christina Lynn Smith
2303 Twp Rd 126
New Lexington, Ohio 43764